NOVEL DESIGN INTEGRATION FOR ADVANCED NUCLEAR HEAT-PIPE SYSTEMS

A Dissertation

by

COLE M. MUELLER

Submitted to the Graduate and Professional School of
Texas A&M University
in partial fulfillment of the requirements for the degree of

DOCTOR OF PHILOSOPHY

Chair of Committee,	Pavel V. Tsvetkov
Committee Members,	Mark Kimber
	Sunil S. Chirayath
	Michael Pate
Head of Department,	Michael Nastasi

December 2022

Major Subject: Nuclear Engineering

ABSTRACT

The research performed here is focused on heat-pipe modeling and simulation and performance predictions. Heat-pipes are analyzed with axisymmetric assumptions that limit the validity towards geometries that cannot be reduced to these geometries. This reduces confidence from engineers designing these products when the geometry is more novel or exotic. The research investigated the prevailing limits for a novel design configuration for a heat-pipe cooled fuel-element. This includes a more general formulation for the prevailing limits within heat-pipes. A review was performed of prior heat-pipe modeling and simulation efforts investigating the cost and benefits of various heat-pipe models. Using that review, a new method capable of quickly solving full core heat-pipe simulations with reasonable accuracy is developed.

More general characteristic limits that show dependence on geometric properties such as that described in the novel design are developed. The design is analyzed showing an increase in fuel density of 17% when comparing to a specific design present in the literature. Compared to that design the novel integration approach did not significantly harm maximum performance of the heat pipe and provided support that non-standard heat-pipe geometries could provide boosts to performance that are being missed because the analytic tools are not present or are not rapid. The merits of a 3D conduction model for approximating heat-pipe solutions in a transient scenario were briefly investigated. Conduction models tend to perform well if the thermal capacity of the whole system is adequately accounted for.

A review of the current modeling and simulation approaches for heat-pipes is performed. This explores the benefits and associated costs of each modeling paradigm so that readers can better inform their analytic approach. Recommendations are included to inform the use cases of these models to ensure efficient analysis. Some models miss valuable information that when each and every bit of performance is desired can cause a designer or analyst to improperly select a design or improperly evaluate safety criteria. For example, in conduction models sonic limiting behavior and capillary limiting behavior is missed because flow is entirely ignored. In standard operating

regimes this may be desirable but in casualty events these limits may become important to the operation of the reactor. Some models are simply too slow to use in certain scenarios, such as design studies. Rapid design iterations require fast solutions so that many designs can be evaluated in short order. A modeling scheme was developed that could bridge the gap between speed and accuracy. Using this research a development effort resulted in a new model that can obtain accurate results for full core heat-pipe configurations quickly.

A network analysis method for obtaining 3D full core temperature solutions from a simple linear system of equations is developed. The theory and performance of the method are discussed and bench marked against OpenFOAM solutions of the conduction problem. The method creates a linear system of equations based on a unit-cell configuration which allows the network approach to work. Then resistances between the points of interest and the interfaces of the neighbors are generated. Then the conservation laws are applied which are discussed in detail. These geometries being a standard cylindrical geometry from literature and the second being similar to the novel geometry described in this dissertation. What was shown is that this method provides accurate solutions and for certain geometries comes within 1% of the high-fidelity solution but in general was shown that this solution is within about 7% of the high-fidelity simulation. This is acceptable because standard experimental uncertainties are of larger order than that for thermal-hydraulic phenomena. This is for steady-state analysis but in literature, network based approaches have been shown to perform well in transients and to add transient behavior would be simple.

The completion of these objectives gives a new set of possibilities for heat-pipe design in nuclear systems. Novel geometries with fast approximate simulation methods will accelerate the creation of better, more cost effective nuclear systems to compete with existing technologies. It will give additional confidence and flexibility to designers that analyze these systems.

DEDICATION

I would like to dedicate my dissertation to my family. I would like to thank my parents specifically, Janice and Mike, for the encouragement and support they have given me throughout my life and education. There are no words to describe the the appreciation I have for my wife, Kelsey, for being so loving and supporting throughout my career and always being there.

ACKNOWLEDGMENTS

I would like to acknowledge, and thank, the Department of Energy and their Integrated University Program Graduate Fellowship for supporting this work. This material is based upon work supported under an Integrated University Program Graduate Fellowship. Any opinions, findings, conclusions or recommendations expressed in this publication are those of the authors and do not necessarily reflect the views of the Department of Energy Office of Nuclear Energy.

CONTRIBUTORS AND FUNDING SOURCES

Contributors

This work was supported by a dissertation committee consisting of, my advisor, Professor Pavel V. Tsvetkov, Professor Mark Kimber, Professor Sunil S. Chirayath and the Department of Nuclear Engineering and Professor Michael Pate of the Department of Mechanical Engineering.

Funding Sources

Graduate study was supported by Texas A&M university. I would like to acknowledge, and thank, the Department of Energy and their Integrated University Program Graduate Fellowship for supporting this work. This material is based upon work supported under an Integrated University Program Graduate Fellowship. Any opinions, findings, conclusions or recommendations expressed in this publication are those of the authors and do not necessarily reflect the views of the Department of Energy Office of Nuclear Energy.

Annals of Nuclear Energy Article Use Disclosure

Three articles were published in the "Annals of Nuclear Energy" that have been used in this dissertation. Those articles are [1], [2], and [3]. "Annals of Nuclear Energy" give rights to use published work in dissertations as well as in any work for the university at which the work was performed as laid out in `https://www.elsevier.com/about/policies/copyright`.

Bibliography

[1] Cole Mueller and Pavel Tsvetkov. Novel design integration for advanced nuclear heat-pipe systems. *Annals of Nuclear Energy*, 141:107324, 2020. ISSN 0306-4549. doi: https://doi.org/10.1016/j.anucene.2020.107324. URL https://www.sciencedirect.com/science/article/pii/S0306454920300220.

[2] Cole Mueller and Pavel Tsvetkov. A review of heat-pipe modeling and simulation approaches in nuclear systems design and analysis. *Annals of Nuclear Energy*, 160:108393, 2021. ISSN 0306-4549. doi: https://doi.org/10.1016/j.anucene.2021.108393. URL https://www.sciencedirect.com/science/article/pii/S0306454921002693.

[3] Cole Mueller and Pavel Tsvetkov. A network approach to full core temperature analysis in advanced nuclear heat-pipe systems. *Annals of Nuclear Energy*, 160:108354, 2021. ISSN 0306-4549. doi: https://doi.org/10.1016/j.anucene.2021.108354. URL https://www.sciencedirect.com/science/article/pii/S0306454921002309.

TABLE OF CONTENTS

Page

LIST OF FIGURES

FIGURE Page

LIST OF TABLES

TABLE Page

1. INTRODUCTION

The ability to build a walk away safe reactor is something that will make the nuclear industry safer and more reliable. There are various ways to approach this, passive cooling technologies, accident tolerant fuel, the plant infrastructure, the design and construction of a reactor considers all of these to create a safe and profitable plant. There are technologies becoming popular within the commercial nuclear community because they were designed to be passive as well as light weight. These are heat-pipes and are passive self contained heat transport and heat spreading technologies. They are popular because they were designed for space exploration and power production, and naturally create system redundancy that improves reliability and safety in the application.

Heat-pipes are promising because they are passive in nature and can work effectively in a wide assortment of geometries and orientations. They have been used for temperature control in electronics to maintain milliKelvin temperature accuracy [1] as well as for thermal management on spacecraft and in laptop computers. The nuclear industry is investigating heat-pipe technology for use in nuclear reactors as not only emergency passive heat transport units but also as primary heat removal systems, specifically for small nuclear reactors that need to operate for long periods of time without fail. These are reactors that the military is interested in, as are small communities with limited to no access to developed infrastructure. Examples include villages in remote Alaskan regions or permanent research posts in inaccessible regions. The expected customers have significant access restrictions and need power solutions that can operate in harsh conditions.

1.1 Heat-Pipe Technology

The principle of a heat-pipe is not new and has an interesting history. In 1831, A.M. Perkins took out a patent on a "Hermetic Boiler Tube" which resembles a heat-pipe but was a simplified version of the modern heat-pipe [2]. Later, a descendent of A.M. Perkins, Jacob Perkins, applied for a patent on what would be called the "Perkins Tube" that resembles a modern two phase thermosyphon [2]. In 1944 the modern description of a heat-pipe was patented by R. S. Gaugler of

General Motors Corporation, but it was never manufactured because other solutions were found in place of a heat pipe. It wasn't until 1963 George Grover realized that this could be used to move large amounts of energy from very small spaces passively. The latent heat of vaporization was known to be much larger than the heat capacity of the fluid. However, it was not conceived to use the surface tension present as a result of phase change to generate flow as a "Capillary Pump". The passive nature of heat-pipes makes them beneficial for use in nuclear cooling applications. Being highly scalable and able to transport large amounts of energy gave Grover the idea that this could be used on spacecraft reactors because they were extremely light weight and able to be fit to the application [3]. Currently heat-pipes are used all over the world and most notably in CPU cooling equipment, such as in laptops as heat spreaders. This has allowed much smaller and more powerful processing units to be used, bringing better capabilities to a portable platform. More than 124,000 heat-pipes are used in the Trans-Alaska pipeline to cool the oil and prevent permafrost melt [3]. The applications in nuclear have been limited to space and as a result no nuclear reactor has been built with heat-pipes. There is an increase in the number of concepts using heat-pipes but no designs are close to commercial or military deployment. The challenging issue to address here is why? Are there technical or economic significant reasons that this hasn't occurred, or is it simply the speed at which the nuclear industry has been advancing holding these new technologies back?

Figure 1.1 shows a basic heat-pipe. They operate on the large heat of vaporization rather than heat capacity. So, for similar power transfer requirements, flow rates are much lower and are easier to establish naturally without active pumping mechanisms.

The fundamental properties of a heat-pipe, as seen in Figure 1.1, show that it is mostly vapor. The components in Figure 1 are exaggerated in size for description purposes, from [4] the heat-pipe used experimentally had tube internal diameter of 1.73 cm and a liquid-wick thickness assumed to be 0.75 mm and [5] specifies a wick and liquid channel thickness of 0.13 cm with a tube internal diameter between 1.5 cm and 5 cm depending on the exact version. More importantly, the central cavity is permanently vapor and the liquid and vapor components will remain in their respective

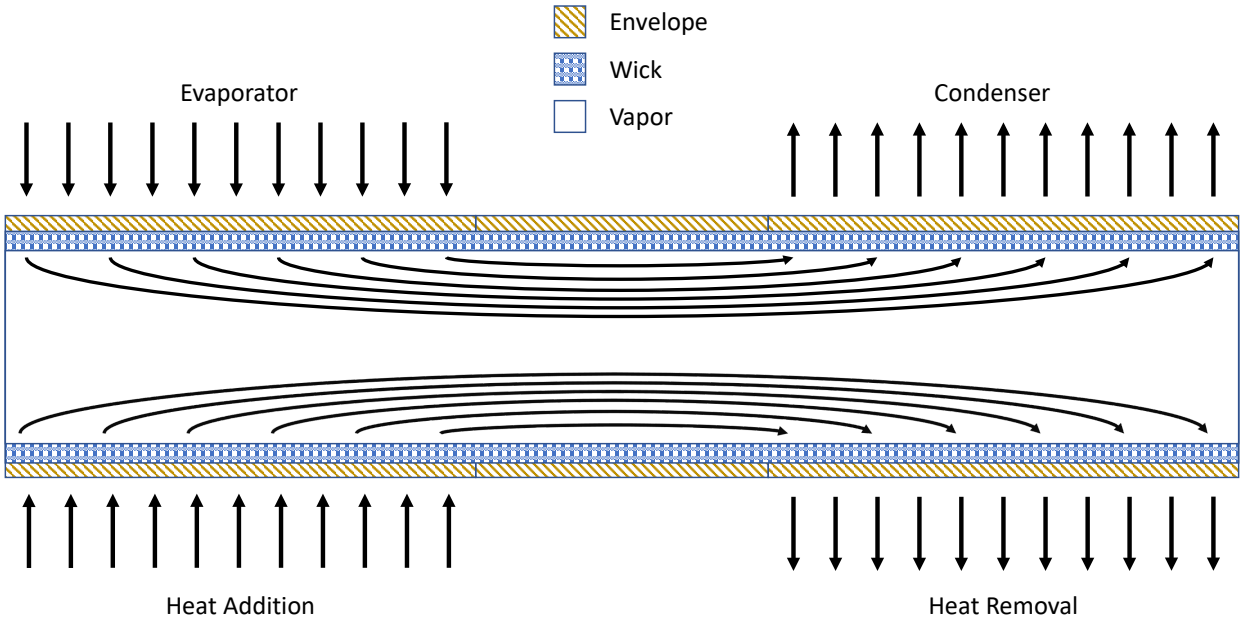

Figure 1.1: Diagram of a Heat-Pipe

regions. From a neutronic perspective this is essentially void. Void formation near the center of a liquid metal cooled reactor can yield large power increases because of positive void reactivity coefficients. This issue is addressed because there is very little liquid volume in the heat-pipe relative to the vapor or void region in the heat-pipe. This makes them a promising substitute for liquid metal coolants. You can achieve similar cooling capabilities as liquid metals without the negatives associated with them. There is a relative increase in manufacturing costs associated with a heat-pipe over liquid metals, but the much lower coolant mass may negate this. Neutronically, heat-pipes are very consistent across temperature and power ranges with only real changes occurring in the vapor density, which would likely lead to a negative feedback affect intuitively. The working fluid selection is extremely versatile.

The most attractive aspect of heat-pipes is the versatility and compatibility due to the method used to transport heat. Any fluid that has a vapor pressure can be used as a working fluid re-

gardless of its atmospheric boiling point. This means that there is likely a fluid that operates best in a temperature range that is ideal for the application considered. In reactor applications and power production applications this can be working fluids such as lithium, sodium, potassium, or even water depending on the specific part of the facility being considered and the temperature and powers required. There have been experimental studies with molten salt heat-pipes like in [6]. This means that the fluid region or the wick has the ability to be shaped or sized based on what properties are desired, or what properties need to be avoided. But there is a lack of capabilities in this region and typically geometries are approximated to cylindrical or planar and prototypes are constructed to verify. This approach works for cooling scenarios as simple as a laptop but this will not be sufficient for nuclear regulatory procedures and because of that heat-pipes are designed to be cylindrical, most commonly, or planar for the purpose of creating a geometry that can be accurately predicted.

The nuclear industry is investigating heat-pipes for passive solid core “Nuclear Batteries” [5] as the primary heat removal mechanism coupled to a Brayton cycle for energy conversion. This was based on the NASA reactor design called SAFE-300. The SAFE-300 had a solid core with fuel pins and heat-pipes in a hexagonal lattice configuration [7]. Conducting heat from the fuel to the coolant channels is a popular approach and has been used throughout this century when it comes to solid core reactor technology. From space reactors like the SAFE-300 to Chernobyl it is common to allow conduction from the fuel elements to the primary heat removal system. This research looks to develop an integral Fuel-Element Heat-Pipe (FEHP) to reduce the conduction resistances between the fuel and the heat removal system. A recent study at Idaho National Laboratory investigated core designs that reduced the conduction resistances from the fuel to the heat-pipe. The first design involved hexagonal fuel elements with a heat-pipe running down the center [8]. The second used a container of liquid sodium with heat-pipes and fuel elements submerged in the sodium conductively and convectively transporting energy from the fuel pins to the heat-pipes [8]. These two designs show attempts to remove some of these "thermal barriers" to allow higher heat throughput. This technology removes some of the conduction limitations and potentially allow for

higher thermal throughput than the traditional solid core approach. It isolates each fuel-element into its' own self-contained cooling system, so if other cells fail then the whole of the reactor is not jeopardized. In current concepts local heat-pipe failure could lead to core failure and fuel melt in a large region of the core. This particular event could be caused by a subpar batch of heat-pipes or random chance. This technology addresses this through its cell like nature; if one FEHP fails its neighbors will continue to operate and could potentially transfer a portion of the failed FEHP energy. A goal of this research is to help integrate the technology into a current solid core reactor design.

1.2 Objectives

The objectives of this research were in support of developing techniques for analyzing non-standard heat-pipe geometries such as the geometry described previously. There are many aspects to analysis depending on what the goals of the analysis are but it is important to understand the implications of the modeling decisions, such as simplifying assumptions. Using this a method can be developed to analyze full core behavior accurately.

The objectives of the research are:

1. Develop a method for the parametric analysis and optimization of the novel integration approach and use the developed method to design and characterize a Fuel-Element Heat-Pipe for integration into a nuclear battery design

2. Integrate the technology into an evaluation of a nuclear battery type reactor and quantify key performance characteristics that result such as power, temperatures, and mass using the developed method

The next steps in this research would be to apply the methods developed in an optimization and analysis work. Using the full core analysis tool to optimize the entire core's performance. The prevailing limits would be used as part of the constraints to the thermal system. The research performed in this dissertation demonstrate a method for parametric analysis and show an integration into a prior design. Design optimization is a substantial additional effort and would require some

form of neutronic coupling whether that is an assumed power profile or a tightly coupled solve where temperatures and and powers are dynamically solved in each direction.

1.3 Overview

This dissertation investigates a non-standard heat-pipe geometry. This is a novel geometry known as a fuel-element heat-pipe. Standard heat-pipe are typically analyzed as cylinders or plates, but can be extended to constant flow area devices. This results in little effort to investigate other geometries or even more general geometries in both a simulation type approach or characteristic limit approach. This leaves a gap in the capabilities of designers and analysts for accounting for these more complex geometric shapes.

The dissertation begins by describing the novel geometry and derives more general characteristic limits for it's operation. The derivations were presented clearly so that the same derivations could be applied to other geometries that have more exotic geometric descriptions. These characteristic limits allows operational envelopes to be created for the novel geometry such that confidence in analytic methods could be gained. The main purpose of this was to provide calculations that demonstrate the veracity of other geometries but also show that the change in performance could be substantial and the need to adequately determine operational behavior is present. With improved manufacturing procedures and methods, more complex geometries are possible and designs can become more specific to the application.

A needed review on the simulation methods used within the nuclear engineering community for analyzing heat-pipes is presented next. Many simulation methods have been developed for analyzing single heat-pipes in various configurations and various complexities but the majority of these methods are highly specific and have not been investigated for their applications in general geometries. With the plethora of general partial differential equation solvers that have been developed, such as OpenFOAM, a thorough review of these methods is warranted as well as a comparison of their strengths and weaknesses. Chapter 4 performs this review and compares three methods of varying complexity using OpenFOAM as a solver for the most complicated equation sets.

Finally, a low complexity method for the purpose of design optimization is developed and

compared to higher fidelity approaches. This method takes pseudo 1-D analytical solutions to the heat equation applies them locally to a 2-D network based mesh and then extends this into a pseudo 3-D solution to get peak fuel temperatures, heat-pipe vapor temperatures, and heat-pipe power throughput. A benchmark is performed in this chapter to compare the solution of this method to solutions generated in OpenFOAM to determine the accuracy of the method. This method is capable of getting temperature profiles for a whole core with 100's or 1000's of heat-pipes and fuel elements in fractions of the time as high fidelity solvers like OpenFOAM while maintaining accuracy within 10% for the worst case bench-marked and within 1% for the best case tested. This will allow much faster design iteration to be performed but could be used as an initial guess for high fidelity solvers and in multiphysics solvers where approximate material properties would like to be known before high fidelity simulations are performed.

1.4 Impact of Work

The impact of this work could be substantial. Improved performance predictions would improve designs directly through the design iteration process. Faster tools that provide good accuracy will allow more combinations of parameters to be analyzed and better designs to be obtained. This will impact safety analysis and operations as well. Safety analysis relies on understanding the behavior within the system and how that system responds to external stimulus. If the analysts can determine more quickly and with higher confidence then reactors designs will be able to more quickly approach maximum operational performance. These goals will be the same for operators as decisions are not made unless the safety of the plant is assured.

With the current stage of development for heat-pipe based reactors it is likely only designers and safety analysts that will see benefit from this work. However, the benefits in those areas will lead to operators obtaining better tools at the start and having a better understanding of the systems that they manage.

Bibliography

[1] Advanced Cooling Technologies. Pchps for precise temperature control, 2020. URL https://www.1-act.com/resources/heat-pipe-fundamentals/different-types-of-heat-pipes/pchps-for-precise-temperature-control/.

[2] AMS Energy. Heat pipe technology history. URL http://www.amsenergy.com/heat-pipe-technology-history/.

[3] Octavio Ramos Jr. Inspired heat-pipe technology, Sep 2009. URL https://www.lanl.gov/science/NSS/issue1_2011/story6full.shtml.

[4] J-M Tournier and MS El-Genk. A heat pipe transient analysis model. *International Journal of Heat and Mass Transfer*, 37(5):753–762, 1994.

[5] Ehud Greenspan. Solid-core heat-pipe nuclear battery type reactor. Technical report, University of California, 2008.

[6] Yaxuan Xiong, Li Bo, Meng Qiang, Yuting Wu, Xingxing Zhang, Peng Xu, and Chongfang Ma. A characteristic study on the start-up performance of molten-salt heat pipes: Experimental investigation. *Experimental Thermal and Fluid Science*, 82:433–438, 2017.

[7] Steven A Wright and Michael Houts. Coupled reactor kinetics and heat transfer model for heat pipe cooled reactors. In *AIP Conference Proceedings*, volume 552, pages 815–821. AIP, 2001.

[8] James W Sterbentz, James E Werner, Andrew J Hummel, John C Kennedy, Robert C O'Brien, Axel M Dion, Richard N Wright, and Krishnan P Ananth. Preliminary assessment of two alternative core design concepts for the special purpose reactor. Technical report, Idaho National Lab.(INL), Idaho Falls, ID (United States), 2017.

2. NOVEL DESIGN INTEGRATION FOR ADVANCED NUCLEAR HEAT-PIPE SYSTEMS

2.1 Overview

A new design integrating heat-pipes into a nuclear cooling system is presented. The heat-pipes are presented as the primary mode of heat transfer. Analyzing the prevailing limits to determine suitability for predicting the performance of the heat-pipe concept. When the limits are determined for the design integration, steady-state behavior needs to be quantified. A model that accounts for 3D behavior is evaluated for use. Using the limits to evaluate the design integration, with sodium, the operating regime would still remain below the predicted limits. With potassium the operating regime would exceed the capillary limit. This is caused by the increase in pressure drop. With the 3D model, a validation shows that conduction can give very good results for both transient and steady-state behavior for sodium. It shows that water has poor transient prediction but accurately predicts the steady-state behavior. Both solutions were close to the reported experimental results for steady-state.

2.2 Introduction

Compact Nuclear Reactors, sometimes known as Micro-Modular Reactors, are quickly gaining interest globally. They are being designed to be deployed rapidly, be walk away safe, and to be competitive with natural gas [1]. With communities rapidly becoming technology dependent, power becomes a real concern. Remote communities often have little access to power and rely on fuel shipments to keep essential services supplied to the people. In emergency scenarios power is essential to bring water and electricity to emergency responders as well as individuals potentially trapped; restoring communication channels are key to a quick recovery. Developing technologies that can reliably power these customers for long periods of time without a need to refuel have multiple benefits.

[0]Reprinted with permission from "Novel design integration for advanced nuclear heat-pipe systems" by Cole Mueller and Pavel V. Tsvetkov, 2020. Annals of Nuclear Energy, Volume 141, Copyright 2020 by Annals of Nuclear Energy

Several Reactors have been designed to meet these design goals [2, 3, 4, 5]. These have been designed for remote power needs, like Sundance, Wyoming or McMurdo Station, Antarctica [6]. Small Modular Reactors are already approaching these requirements and Micro Modular Reactors are being designed to meet these requirements. They are inherently modular, but are also safe and designed to provide long term power on a moments notice. Heat-pipes can be found in almost everything from electronics to vehicle engines [7]. Heat-pipes are a common cooling solution for electronics because of their simplicity and their reliability. They take on all shapes and sizes and allow for extremely efficient heat transfer over long distances or very simple heat spreading to improve the thermal characteristics of the product [7].

Heat-pipes are very popular passive heat transfer devices because of their ability to be applied to almost any situation. Heat-pipes fall under the classification of thermosyphon along with vapor-chambers. Thermosyphons do not have wicks, and can only operate assisted by gravity as a result. This is precisely the opposite when considering heat-pipes and vapor-chambers. Both of these rely on capillary pressure to generate the primary driving head rather than buoyancy. This characteristic allows the heat-pipe to take on various shapes such as a flat plate like in a vapor chamber.

The integration presented is a modification to the standard understanding of a heat-pipe. It is not strictly a long distance heat-transfer device nor is it a heat spreading device. The design integration is an integral fuel-element heat-pipe. The concept will be a single unit cell composing the fuel-element, and the cooling system which is the heat-pipe. There are several distinct advantages for this.

The design allows each individual element to be cooled directly greatly reducing conduction resistances from the fuel to the ultimate heat sink. This benefit is two-fold because it improves the margins for temperature limitations. It also allows a simplification in the manufacturing process. Current heat-pipe based reactor designs involve a monolithic core block with long holes machined into them for the heat-pipe and fuel elements to be inserted into. The required tolerances on these blocks are much smaller than is technologically possible [2]. The novel design integration involves production of a unit cell type assembly that can be replicated. The design may address a cascading

failure scenario but this analysis is not performed.

There are drawbacks to the design. The wick length could potentially be much longer than a traditional heat-pipe resulting in a lower power throughput. On the other hand, the wick structure could become large resulting in increased parasitic absorption, this issue comes down to manufacturing capabilities. This would result in a larger core, more fuel, or a higher enrichment required. There is also drawbacks on the ability to predict the operating performance of a heat-pipe in this configuration.

2.3 Fuel-Element Heat-Pipe Concept

There are several key differences between a Fuel-Element Heat-Pipe (FEHP) and standard approaches to heat-pipe cooling systems. A significant difference includes a variable flow area. Almost all heat-pipe systems, nuclear or not, rely on a constant cross-sectional area and in a significant number of cases a constant circular cross-section. Designing a reactor system with a coolable geometry involves some repetition in geometric properties. The typical approach involves organizing cylindrical fuel-elements and cylindrical heat-pipes in a hexagonal lattice. This requires large amount of structural material and thermal bonding materials. This is typically done simultaneously with conductive structural material like stainless steel. A fuel element with a central cavity for a heat-pipe has been considered [2, 8].

An FEHP involves containing the fuel within the heat-pipe. The fuel can be in any form but the simplest to visualize is a cylindrical fuel geometry within a hexagonal evaporator section. For simplicity the wicking structure will run along the walls of the heat-pipe envelope and up the surface of the fuel. This does not have to be the case, especially with advanced manufacturing quickly allowing more complex geometries to be manufactured. Containing fuel within a heat-pipe is not new, but the research is limited and was very focused. The only other instance found was as a control mechanism for nuclear thermal rockets which analyzed the feedback effect of UF_4 as a heat-pipe working fluid in the NERVA nuclear rocket [9]. The versatility of heat-pipes are demonstrated by this analysis. The geometry of the FEHP can be seen in Figure 2.1.

When viewing Figure 2.1, green is the wicking structure, the lighter shade is the vapor region,

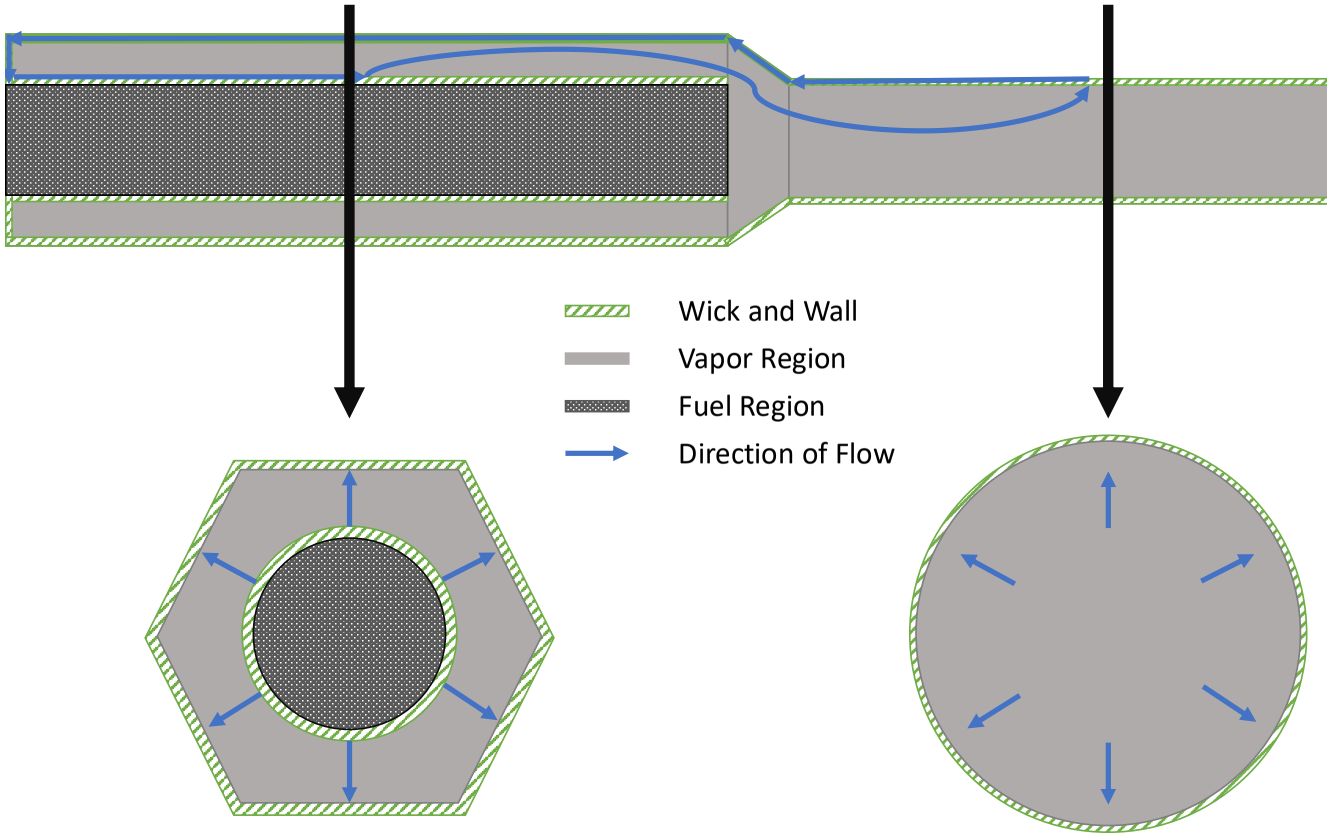

Figure 2.1: Fuel-Element Heat-Pipe Concept

the darker shaded region is the fuel region. The two large black arrows represent a cross-section with the normal parallel to the axis of the geometry and the corresponding cross-section displayed below. The lighter arrows represent the flow path from the surface of the fuel to the condenser through the vapor region and then from the condenser wick all the way to wick on the fuel travelling through the wick. In Figure 2.1 other flow paths can be envisioned. These flow paths include directly from the fuel to the heat-pipe wall. This is why the FEHP was referred as a mix between a vapor-chamber and a heat-pipe. If it is able to reject heat through all external surfaces then it will act as both a heat spreader and a heat transport device.

2.3.1 Advantages

The FEHP gives several advantages over traditional heat-pipe systems and in some cases over traditional cooling systems. It does not have as much conduction resistance between the fuel and the coolant. This is because the structural material separating the fuel from the heat-pipe are now removed. This shortens the conductive "journey" between the heat source, the fuel, and the heat sink, the condenser.

The FEHP allows neighbor to neighbor communication. This means that heat can easily flow from one heat-pipe to the next without be restricted by structural material. A substantial manufacturing improvement is made with the FEHP concept. Hundreds of individually drilled precision holes are not required and, instead, a single geometry is manufactured and produced at scale and assembled into the final product. This process gives much greater flexibility in delivery options and manufacturing and assembly options. There is also higher fuel densities associated with the FEHP concept. If the specifications described by [2] for the LANL MegaPower design are analyzed some interesting conclusions are made. First it is assumed that the cross-sectional flow areas, fuel areas, and structural areas are conserved on a per fuel element basis. This indicates that the 2 fuel elements per heat-pipe is reduced to one element per heat-pipe, which inherently increases redundancy, and it eliminates a lot of the structural material put in place to thermally couple the fuel-elements to the heat-pipes. Table 2.1 summarizes the calculations performed.

The Fuel Area Ratio is the ratio of the fuel area to the total area of a unit cell. The Improvement

	LANL	FEHP
Fuel Diameter	1.412 cm	1.412 cm
System Pitch	1.600 cm	1.813 cm
Approximate Fuel to HP Ratio	$\approx$ 2.000	1.000
HP Outside Diameter	1.775 cm	
HP Internal Diameter	1.575 cm	
HP Annular Gap Thickness	0.700 mm	
HP Wick Thickness	1.000 mm	
HP Vapor Area	1.198 cm^2	1.198 cm^2
HP Wick Area	0.419 cm^2	0.419 cm^2
HP Annular Gap Area	0.331 cm^2	0.331 cm^2
Minimum Wall/Web Thickness	0.100 cm	0.050 cm
Fuel Area Ratio	0.471	0.550
Improvement Factor	1.000	1.169

Table 2.1: Comparison of LANL MegaPower unit cell to the Proposed unit cell

Factor is the Fuel Area Ratio of the selected over the Fuel Area Ratio of the LANL MegaPower Fuel Area Ratio. As is shown in the Improvement factor in Table 2.1, there is almost a 17% increase in fuel density within the core. This is a substantial increase in fuel density and further investigation is justified. Some substantial difficulties are encountered because this is a non-standard geometry. The FEHP does not have a constant vapor flow area, it can have unequal vapor and fluid flow lengths, and it is not an entirely independent system from it's neighbor.

2.3.2 Disadvantages

As previously mentioned, there are several disadvantages associated with the FEHP. The more complicated wick geometry will result in higher pressure drops through the wick and a lower capillary limit. This will be seen later. Also, there are no readily available models that can quickly and accurately ascertain the quality of a design. A changing vapor flow area complicates the calculation of the sonic limit as area and mass addition can both choke the flow independently. Believing that only mass addition can choke the flow could result in an area choked flow at a heat transfer rate substantially below that of the sonic limit estimation. There are few models that can accurately handle heat-pipes with 3D geometries.

With the FEHP concept there is an estimated 17% increase in fuel relative to previous concepts. This leads to less structural material to hold energy in the event that there is an accident. This could be detrimental to operations and safety of the reactor. On the same hand there is much more fuel to hold and produce energy meaning the power density of the reactor can be brought down to increase lifetime and safety of the plant. These are some issues that need to be analyzed.

2.4 Characteristic Limits

As mentioned previously, the FEHP challenges the conventional characteristic limits when it comes to predicting the peak operational performance of it. Other heat-pipe designs that would have cross-sectional areas that are not constant with respect to axial location also would encounter difficulties. This is a problem for operational confidence. To handle this problem the characteristic limits are re-analyzed to account for a potential variable area.

There are four characteristic limits: entrainment limit, capillary limit, sonic limit, and boiling limit. These exist because heat-pipes transfer heat in a fundamentally different fashion when compared to solid conductors or pumped flow systems. In a conductor you are only limited by the gradient provided and in a pumped system if more heat needs to be moved a larger pump is obtained to do so. In a heat-pipe, however, the system may encounter or pass through regions of operation that will limit the throughput of the heat-pipe. For example, the sonic limit is typically encountered at low temperatures and can inhibit the startup of the heat-pipe [10]. This is why it is important to know roughly where these limits are.

2.4.1 Entrainment Limit

The Entrainment Limit exists because of the high gas velocity present within a heat-pipe. The high velocity causes a high shear stress on the wick surface. If that stress is large enough it can actually pick droplet of coolant out of the wick and carry them in the vapor. This has several detrimental effects. It can cause an increased pressure drop in the vapor region because of two-phase flow behavior. This entrainment can also reduce the liquid in the wick temporarily, potentially leading to wick dry-out and heat-pipe failure.

To derive the Entrainment Limit one starts with the definition of the Weber number

$$We(x) = \frac{\rho(x)v(x)^2 L(x)}{\sigma(x)} \tag{2.1}$$

where ρ is the density of the vapor, v is the average velocity of the vapor, L is the characteristic dimension of the wick, and σ is the surface tension. These are all functions of the axial position of the heat-pipe and thus the true limit is not simply evaluated at the location of the peak velocity. If the assumption is made where the vapor region is approximately isothermal and isobaric, which is saturation conditions typically, then the density and the surface tension become independent of axial location. With advanced manufacturing techniques it is easy to imagine a wick with characteristic dimensions non-constant axially. Typically the characteristic dimension, L, of the wick is either the wire diameter of the wick or the effective pore radius.

The heat transported through is then defined as

$$Q = \dot{m} \cdot h_{fg} \tag{2.2}$$

where $\dot{m}$ is defined at the evaporator exit. If the assumption is made that the evaporator section is always adding heat, and the characteristic dimension of the wick does not change, then the limit can be defined as

$$Q_{entr} = \sqrt{\frac{We \cdot \rho \cdot \sigma}{L}} \cdot h_{fg} \cdot A_v \tag{2.3}$$

Where A_v is the smallest area between the evaporator exit and condenser inlet if the evaporator section is constant area. In most cases We is equal to unity but this will depend on what the critical We number is for the system. If the characteristic dimension is allowed to change then more information is needed to determine the limit. The extra information is the shape of the power input or heat flux axially. The vapor area also needs to be known as a function of length if it is assumed to change between the evaporator beginning and end. The general form of this limit can be derived simply. Start with

$$Q(x) = \int_0^x q"(x)dA \tag{2.4}$$

dA is the differential heat transfer area for the heat-pipe. $q"(x)dA$ represents the differential heat addition for that axial location in the heat-pipe. This simply defines the total power throughput at any point in the heat-pipe. Now it will be useful to define this as a shape function multiplied by a constant. This constant will be the total power throughput which in this case is the entrainment limit. To do this we modify the previous

$$Q(x) = Q_{entr} \cdot SH(x) \tag{2.5}$$

$$SH(x) = \frac{\int_0^x q"(x)dA}{\int_0^{L_e} q"(x)dA} \tag{2.6}$$

$SH(x)$ is a shape function describing the shape of the heat flux into the heat-pipe. Inherently, the denominator is equivalent to the limit. The 0 indicates the beginning of the evaporator section and x is following the vapor region not the wick region. From here, the limit can be defined similarly to before with minor changes.

$$Q_{entr} = h_{fg}\sqrt{\frac{We(x) \cdot \rho \cdot \sigma}{L(x)}} \cdot \frac{A_v(x)}{SH(x)} \tag{2.7}$$

Leaving We as a function of axial location makes this a constant, but that would require knowing everything before evaluating. By setting We to the critical value everywhere the limit becomes a function of axial location. To correct for this the minimum value is selected for those properties and the true limit becomes.

$$Q_{entr} = \min_x \left(h_{fg}\sqrt{\frac{We \cdot \rho \cdot \sigma}{L(x)}} \cdot \frac{A_v(x)}{SH(x)} \right) \tag{2.8}$$

Because of the way the shape function was defined this is valid for the entire length of the heat-pipe but the proper characteristic dimension needs to be selected. It is also worth noting the

typical critical value for We is unity but, in this evaluation, can also be variable depending on the local conditions. Because of the $\min_x$, the limit becomes a function of state properties alone.

2.4.2 Capillary Limit

The Capillary Limit is a pressure drop related limit. It states that the flow induced pressure drops cannot exceed the maximum supply pressure. This supply pressure is the capillary pressure generated by the wick. This limit is always geometry dependent and must be evaluated for each individual geometry. It is very simple and represented by the following relation

$$\Delta P_{capmax} \geq \Sigma \Delta P_i \tag{2.9}$$

The pressure drop of each section to be summed is based on the best correlation or theory that is available for those situations. There is sometimes a fifth limit that is called the viscous limit or the vapor pressure limit that states the system pressure should never be negative. This is important at relatively low temperatures where the vapor pressure could be around the same size as the pressure drop in the vapor section or the whole system. This could result in a negative pressure which is physically unrealistic. To account for this, the maximum generated capillary pressure is selected based on the minimum of the two values given in the following equation

$$\Delta P_{capmax} = \min\left(\frac{2\sigma}{R_{eff}}, P_{Vapor}(T)\right) \tag{2.10}$$

The first value being the pressure differential caused by wick capillary pressure derived from the Young-Laplace equation [11] assuming a wet point in the condenser and the evaporator having an effective radius of curvature equal to the effective pore radius, and the second value being the vapor pressure at a specific temperature. This is only dependent on temperature so evaluation of the limit is assumed to be with material properties specified at a specific temperature throughout. This ensures both limits are accurately captured as well. The viscous limit is not as important because operation in that regime is almost always because of improper working fluid selection.

2.4.3 Sonic Limit

The Sonic Limit is a heat transport limit caused a choked flow condition. This means the flow velocity has reached the sonic velocity somewhere in the heat-pipe. This does not prevent increased mass flow rate but increased flow will cause the vapor region to depart from the traditional isothermal assumption. Increased heat transport capacity comes at the expense of effective conductivity of the heat-pipe. There are multiple derivations of the sonic limit. There is an approach that accounts for the changing velocity profile through the vapor region assuming incompressible flow [12]. This approach is the most conservative but does not apply to non-cylindrical geometries. Another common approach is to assume 1-D compressible flow with constant area and mass addition [13]. This is similar to the approach taken when deriving the limit for a variable area heat-pipe. Starting with conservation equations and the equation of state.

$$\frac{d}{dz}(\rho V A) = d\dot{m} \tag{2.11}$$

$$\frac{dp}{dz} = -\frac{d}{dz}(\rho V^2) \tag{2.12}$$

$$\rho V A \cdot \left(\frac{dh}{dz} + \frac{d\left(\frac{V^2}{2}\right)}{dz}\right) = -d\dot{m} \cdot \left(\frac{V^2}{2} - \frac{V_n^2}{2} + h - h_g\right) \tag{2.13}$$

$$V_n = \frac{d\dot{m}}{A_n \rho_g} \tag{2.14}$$

$$Q_e = d\dot{m} \cdot \left(h_{fg} + \frac{V_n^2}{2}\right) \tag{2.15}$$

These equations are very similar to [13] except the area is assumed to be variable instead of constant. Now assuming an ideal gas equation of state the following two relations are incorporated.

$$\frac{dp}{p} = \frac{d\rho}{\rho} + \frac{dT}{T} \tag{2.16}$$

$$\frac{dM^2}{M^2} = \frac{dV^2}{V^2} - \frac{dT}{T} \tag{2.17}$$

Combining these equations and making several assumptions, a relation between Mach number,

M, cross sectional vapor flow area, A, and mass flow rate, $\dot{m}$, can be made.

$$\frac{dM^2}{M^2} \cdot \frac{M^2 - 1}{\gamma M^2 + 1} = \frac{dA}{A} - \frac{d\dot{m}}{\dot{m}} \cdot (2 + (\gamma - 1)M^2) \tag{2.18}$$

Several important concepts are shown with this equation. With variable area and mass addition both can cause the flow to choke. This equation is non separable so both geometry and the mass flow rate needs to be known within the pipe to determine the mach number distribution. If area is assumed constant then the original sonic limitation formulation is obtained. It can also be assumed that as long as the area doesn't decrease throughout the heat-pipe the standard sonic limit evaluation will give a conservative estimate for that geometry. If the area decreases then the area could easily choke the flow and is not accounted for by the traditional sonic limit evaluation.

$$Q_{sonic} = \frac{\rho \cdot A_v \cdot V_{sonic}}{\sqrt{2(\gamma + 1)}} \cdot h_{fg} = \sqrt{\frac{\gamma \rho P}{2(\gamma + 1)}} \cdot h_{fg} A_v \tag{2.19}$$

There are feasible heat-pipe geometries, especially with advanced manufacturing techniques improving, that could result in choking conditions occurring in locations other than the evaporator exit.

2.4.4 Boiling Limit

This limit is described very simply as the point where boiling begins. If a bubble forms in the wick of a heat-pipe it will block a portion of the flow path in the wick leading to increased pressure drop. This is also a positive feed-back situation where the bubble forms on a heated surface thus insulating that part of the surface from the coolant resulting in a growing bubble and more pressure drop. This is a potentially destructive scenario in a heat-pipe and could quickly result in heat-pipe failure. It is because of this that a limit for the heat transport capacity of a heat-pipe needs to be determined. To start this derivation it is easy to jump directly to nucleate boiling theory and apply this to the derivation. [14] was the first to do this and was then referenced in [2]. This will be the basis for the derivation with one small change. Starting with the required super-heat to create boiling.

$$\Delta T_{boil} = \frac{2 \cdot \sigma \cdot T_v}{h_{gf} \rho_v} \cdot \left(\frac{1}{r_b} - \frac{1}{r_{eff}} \right) \tag{2.20}$$

This is then used in conjunction with Fourier's law to develop the boiling limit.

$$q"_{boil} = k \frac{dT}{dr} \tag{2.21}$$

This is a heat flux limitation and so the temperature difference between the wick surface and the heated surface must be less than the required super-heat defined earlier. If the heat flux is assumed constant and the surface area is defined by a cylinder this can be combined to get.

$$Q_{boil} = 2\pi r L_e k \frac{dT}{dr} \tag{2.22}$$

This can then be integrated from the heated surface to the vapor interface giving the following relation.

$$Q_{boil} = \frac{2\pi L_e k \Delta T_{boil}}{ln\left(\frac{r_{vapor}}{r_{heat}}\right)} \tag{2.23}$$

Which is precisely the opposite for a standard heat-pipe limit as indicated by [2]. It is worth describing in more detail that these limits are really identical. The difference occurs because the gradient is with respect to increasing radius and not decreasing radius. This negative sign is absorbed into the logarithm causing it to flip making it the opposite. Realistically this would be evaluated similarly to the way critical heat flux is evaluated because boiling is a heat flux phenomena and not related to total power. Severe peaking problems could lead to boiling at a lower overall power than a uniform heat flux. If a heat flux is defined that represents the flux required to cause nucleate boiling then a ratio of the critical heat flux to the predicted heat flux allows for a factor of safety to be generated to the boiling phenomena and would align more appropriately with prior reactor analysis. But with approximately constant heat flux axially then there is no difference between this limit and a critical heat flux based approach.

2.5 Modeling

Heat-pipe modeling has been thoroughly investigated for standard cylindrical geometries. There have been 2D direct numerical models using kinetic gas theory to account for them as well as compressible equations for the vapor region [15, 16]. Simpler models have been developed using lumped capacitance approaches as well as 1D simulation approaches that do very well in predicting the transient behavior of the heat-pipes [17]. The biggest problem with any approach to heat-pipe modeling and simulation is that the equations end up extremely stiff. With heat-pipe simulations, reducing the computational complexity of the model for faster computations is ideal. In [16] this was done with a 2D simplification and axisymmetric assumptions. [17] simplified the models through a lumped capacitance model and then using a method of lines solution to solve the resultant equations. The equations were also approximated as a pseudo 2D problem where heat transfer in the evaporator and condenser was assumed only to have radial conduction and the adiabatic region had only axial conduction. A further simplification said the vapor region was negligible resistance thermally and so the evaporator and the condenser could be coupled directly with their respective equations.

The main issues with prior modeling and simulation is that important 2D and 3D phenomena is ignored making the models most appropriately used with heat-pipes that can be reduced to an accurate 2D representation. With 3D geometries that are interacting with surrounding heat-pipes, knowledge of the 3D effects is necessary to obtain accurate safety and operational information.

The model developed in [17] will help with understanding the approach taken here. It is an electrical resistance network that treats portions of the heat-pipe like resistors and organizes them such that there is only radial conduction in the condenser and evaporator and only axial conduction in the adiabatic region. Figure 2.2 shows a drawing of the network including the vapor region.

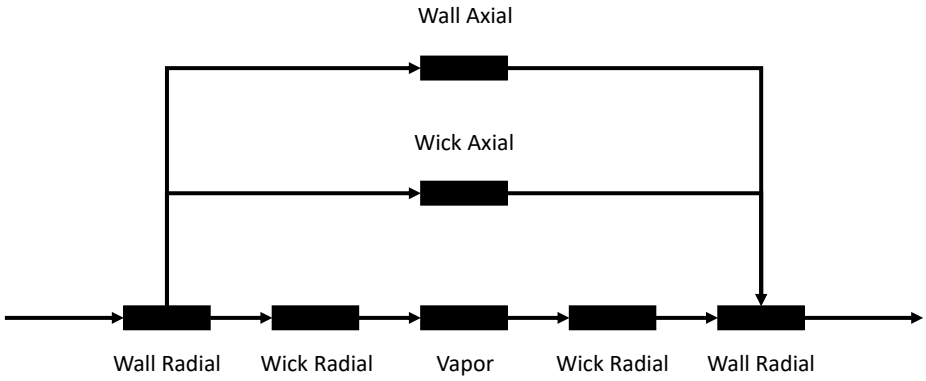

Figure 2.2: Electrical Resistance Network as represented in [17]

As drawn, there are seven total resistors representing theradial wall and wick resistance of the evaporator and condenser, adiabatic region axial wall and wick resistance, and vapor region resistance. There are potentially two more resistors in this depending on the boundaries. These additional resistors are for convective boundaries or contact resistance. The most common uses will be convective boundary conditions on the condenser outer surface. This model at it's core is a lumped parameter model. There are more complicated lumped capacitance models such as [18] that account for flow in the system but these are not great for describing the developed model. With this being a lumped parameter model the resistors need to be defined as well as how they interact with their neighbors in a transient situation. The derivation starts with Fourier's law of conduction

$$Q_{i,1} = 2k_i A_i \frac{T_{i,1} - T_i}{\lambda_i}, \quad Q_{i,2} = 2k_i A_i \frac{T_i - T_{i,2}}{\lambda_i} \tag{2.24}$$

In this equation i represents the lumped element and the subscripts of one and two are the respective surfaces that heat can flow into or out of that element. From this it can then be substituted into the transient portion to capture time varying affects.

$$\rho_i A_i \lambda_i C_{p,i} \frac{dT}{dt} = Q_{i,1} - Q_{i,2} \tag{2.25}$$

In these equations k_i is the thermal conductivity, A_i is the area that heat is flowing through, λ_i is the thickness of the element, $C_{p,i}$ is the heat capacity of the element, and ρ_i is the density of the element. Substituting the known heat flows from the first set of equations into the second a general form of the resistance equations can be obtained for the network.

$$\frac{dT}{dt} = \frac{2k_i}{\rho_i C_{p,i} \lambda_i^2}(T_{i,1} - 2T_i + T_{i,2}) \tag{2.26}$$

It can be easily seen from this equation that this is a finite difference approximation of the heat equation. There is a factor of two difference but this is due to the approximation of Q at the element boundary. From this the equations for the wall and the wick can be derived assuming the resistance of vapor is negligible. These then become a system of first order ODE's and can be

solved as a method of lines implementation. This work can be followed to completion in [17].

Knowing this a model can be formulated using a heat equation approximation. There are many general purpose solvers for the heat equation so creating a new one will not be the goal. Instead, a finite volume code, OpenFOAM, will be used. There is an issue that needs to be addressed. This is the zero thermal resistance of the vapor. Most sources treat it as simply a zero capacitance region [19]. This, being the industry standard, works very well because the capacitance of the vapor is low. To capture this a small capacitance is assumed for ease of computation and numerical stability. This is the implementation used to simulate the 3D heat-pipes. To obtain a small capacitance a small mass is used with a small heat capacity. This allows for a zero resistance to exist with very small thermal inertia.

2.6 Results

The results demonstrate the heat transport limits of the novel concept as compared to sodium and potassium versions [2]. The derived limits were used to generate the prevailing limits values and compare them. A comparison of the sodium designs prevailing limits can be seen in Figure 2.3.

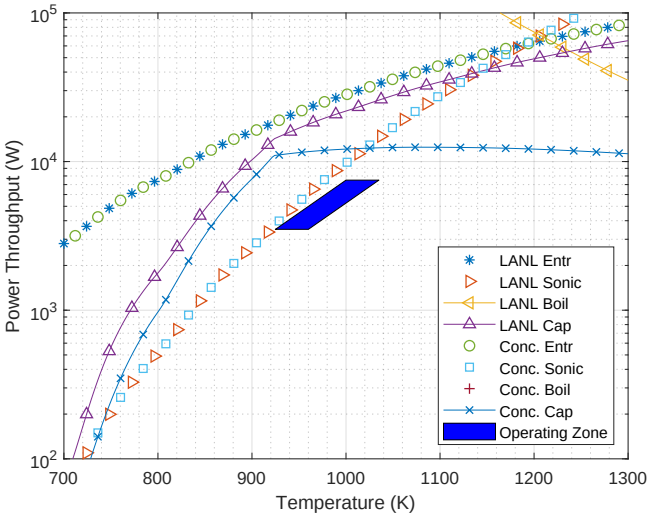

Figure 2.3: Sodium working fluid LANL design [2] compared to the FEHP design

What can be immediately seen in the plot is that the capillary limit is reduced. This is due to the longer wick structure and more associated pressure drops. This region is also flattened significantly meaning operating near here could give much more temperature sensitive behavior. There is room to improve the wick to give better performance. With improved wick design, lower pressure drop will occur improving the benefits of the integral design. The plot also doesn't indicate a boiling limit for the FEHP. This is only because it does not appear on the plot and is much higher, which is an expected result of the new geometry. The sonic and entrainment limit remain unchanged because they are not explicitly geometry based. Figure 2.4 shows the comparison of the same design except with potassium as the working fluid instead of sodium.

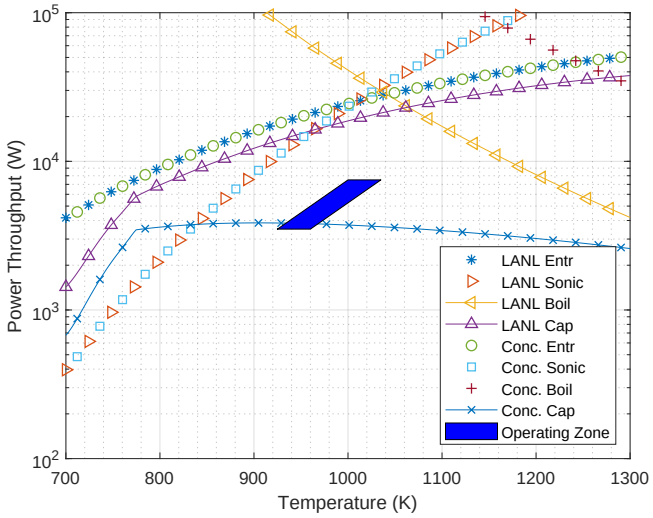

Figure 2.4: Potassium working fluid LANL design [2] compared to the FEHP design

Similar to the sodium work fluid, the potassium has a reduced capillary limit. In this case though, it is reduced substantially more than in the sodium case. This is caused by increased viscosity and decreased surface tension which is generally why sodium is selected over potassium. However, at low temperatures the sonic limit hinders sodium's performance and as a result potassium was selected. What made potassium the leading choice is the increased sonic limit giving a larger margin for operational uncertainty. But with the FEHP, it is reduced too far to be useful or ideal. This could likely be rectified with an improved wick geometry to give better flow but the current design prevents potassium from being ideal as a working fluid. The boiling limit is also reduced from sodium allowing it to be seen but the temperature range where this becomes an issue is well above the expected operating temperature of the heat-pipe system.

The goal is to now verify OpenFOAM's ability to determine the operating characteristics of a heat-pipe with 3D geometry. To do this experimental data was used from [20] and then benchmark data was used from [17]. Comparing these to the conduction model described confidence can be gained in simulations for the FEHP.

The first comparison is a water heat-pipe experiment described in [20]. This is a copper water heat-pipe with a 170 mm long condenser section and 393 mm long evaporator section. The total length was 610 mm long with an outside diameter of 19.1 mm and inside diameter of 17.3 mm. The wick consists of a 2 layer copper mesh of 150 mesh. For the simulation the condenser boundary was a convective boundary with an average temperature of 320 K and a heat transfer coefficient of 1063 $Wm^{-2}K^{-1}$. This fits with a flowing water cooling jacket but is also simplified. This does not account for the time varying temperature of the cooling waters temperature and may be partly responsible for the discrepancy in the transient. The adiabatic section is perfectly adiabatic and produces no losses which is another difference from the experiment. The heater section boundary condition is a heat addition condition of 570 W which in OpenFOAM translates to a uniform heat flux condition on the surface. The wick internal boundary is held as a constant temperature for the whole heat-pipe. To do this a lumped mass condition is used with small mass and small heat capacity to ensure that it remains a small portion of the thermal inertia. Figure 2.5 shows the

comparison of the experimental data and the simulation.

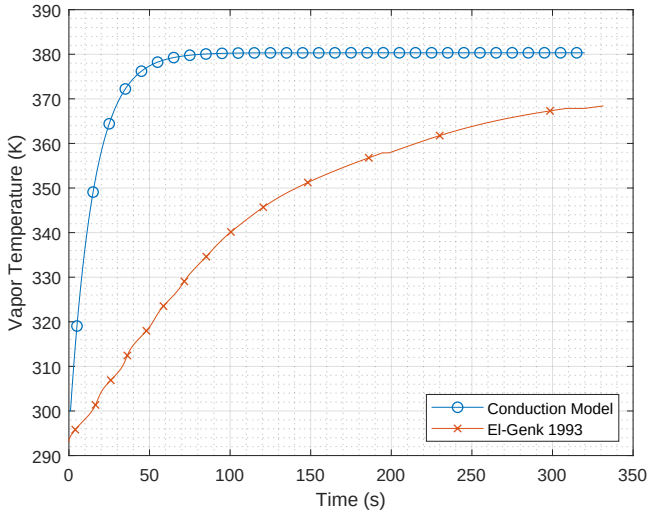

Figure 2.5: Comparison of simulation and copper-water heat-pipe described in [20]

It is clear to see that the transient behavior is not accurately captured. There is obviously excess capacitance not being accounted for that leads to a slower transient. This could be in the vapor, which is not likely, and it could be in the boundary conditions applied as well as material properties. The steady state behavior, however, is captured very accurately being off by around 1% meaning that the accurate determination of the steady state behavior and the 3D conduction approximation can be seen as an accelerated steady state solver. This is evidence for it only being a capacitance issue. In most steady state solutions to the heat equation, the energy storage is not important to the solution. The time and space solutions are separable. With this behavior any correction to the solver to account for the difference in transient behavior will come in the form of a capacitance correction. As was stated previously this is not the only possible cause for the error. This is a flowing system and the true governing equations involve flow possibly adding what could possibly look like a capacitance in reduced equations.

The second case is a benchmark case and is compared to a simulation presented in [17]. This is a sodium heat-pipe with a vapor diameter of 0.014 m and a wall and wick thickness of 0.001 m. The evaporator length is 0.105 m with the condenser being 0.5425 m long. The adiabatic section is 0.0525 m in length. For this benchmark effective constant material properties were used as well as constant boundary conditions. The wall thermal conductivity is 21.7 $Wm^{-1}K^{-1}$ and the wick effective thermal conductivity is 45 $Wm^{-1}K^{-1}$. The effective volumetric specific heat, equal to the density times the mass specific heat, is $1.05x10^{6}Jm^{-3}$. The condenser was exposed to a convective cooling condition with a heat transfer coefficient of 39 $Wm^{-2}K^{-1}$ and an ambient temperature of 300 K. The initial conditions were generated by running the simulation with an evaporator heat input of 623 W until steady state. At that point the heat input was raised to 770 W instantly and ran to steady state. Figure 2.6 shows the comparison of this simulation to the network model developed in [17].

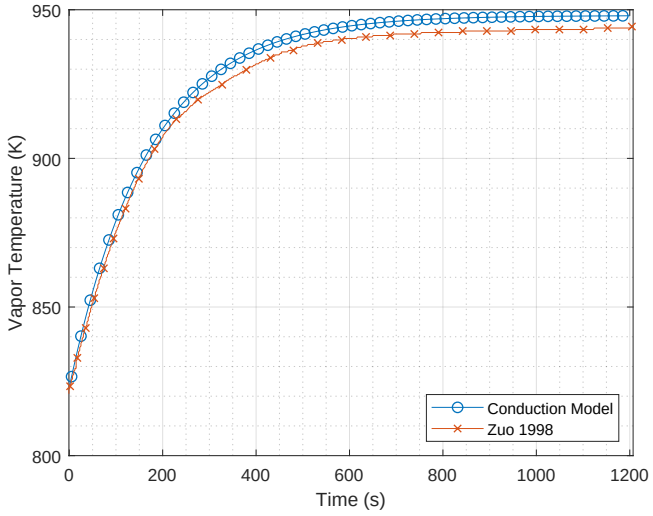

Figure 2.6: Comparison of simulation and sodium heat-pipe described in [17]

The results agree very well and give good confidence for this to capture transient behavior of heat-pipes with metal working fluids. This will allow investigating the FEHP's transient behavior as well as it's steady state properties as compared to previous designs.

2.7 Conclusions

Based on the analysis performed there is motivation for pursuing an integral design. A nearly 17% increase in fuel density with small changes in the ultimate performance of the system is a strong motivator for further study. Characteristic limits for heat-pipe operation of a new FEHP concept were developed. The characteristic limits show that only the capillary limit decreases from this change. This is likely a direct result of the wicks changed geometry. Specifically, the wick increased length. The potassium limit drastically reduced while the sodium limits did not. A 3D conduction model was tested and compared for both transient and steady-state accuracy of heat-pipe operation. For high conductivity working fluids transient and steady-state behavior is captured. This is good for working fluids like sodium or potassium. For low conductivity working fluids this is not the case. There is unaccounted for thermal capacitance in the system. This capacitance needs to be captured to accurately determine the transient behavior of the heat-pipe. The steady-state behavior is captured accurately, however, making this an accurate steady-state solution method for these heat-pipes. Future work can include analysis of the FEHP using the conduction model shown here as well as investigating the effects of neighboring heat-pipes with different power levels. The varying power levels should be captured in the limits as well, as long as the heat addition or heat loss is accurately predicted. There is also work to be done in optimizing the shape and characteristics of the wick structure to improve performance and reduce the impact of having a non-standard geometry. This opens up possible research areas for topological optimization to maximize the power throughput and maximize fuel density within the matrix.

This work open up the possibility of more diverse reactor designs that use more advanced manufacturing techniques and improve performance. The breadth of nonstandard designs that could exist and be analyzed from this research demonstrate the importance.

Bibliography

[1] Brian Wang. Micro-reactors As Cheap As Natural Gas Without Air Pollution – NextBigFuture.com, 2019.

[2] James W Sterbentz, James E Werner, Andrew J Hummel, John C Kennedy, Robert C O'Brien, Axel M Dion, Richard N Wright, and Krishnan P Ananth. Preliminary assessment of two alternative core design concepts for the special purpose reactor. Technical report, Idaho National Lab.(INL), Idaho Falls, ID (United States), 2017.

[3] Ehud Greenspan. Solid-core heat-pipe nuclear battery type reactor. Technical report, University of California, 2008.

[4] C Filippone and KA Jordan. The Holos Reactor: A Distributable Power Generator with Transportable Subcritical Power Modules, 2017.

[5] B.H. Yan, C. Wang, and L.G. Li. The technology of micro heat pipe cooled reactor: A review. *Annals of Nuclear Energy*, 135:106948, jan 2020.

[6] WR Corliss. Power Reactors in Small Packages. Technical report, The United States Atomic Energy Comission, 1968.

[7] Masataka Mochizuki. Latest development and application of heat pipes for electronics and automotive. In *2017 IEEE CPMT Symposium Japan (ICSJ)*, pages 87–90. IEEE, nov 2017.

[8] Charles E. Ahlfeld, Gilleland John Rogers, Roderick A. Hyde, Muriel Y. Ishikawa, David G. McAlees, Nathan P. Myhrvold, Thomas Allan Weaver, Charles Whitmer, and Lowell L. JR. Wood. Heat pipe fission fuel element, may 2008.

[9] Monte Bryce Parker. *Applications of heat pipes to nuclear reactor engineering*. PhD thesis, Iowa State University, 1970.

[10] Patrik Nemec, Alexander Čaja, and Milan Malcho. Mathematical model for heat transfer limitations of heat pipe. *Mathematical and Computer Modelling*, 57(1-2):126–136, jan 2013.

[11] John R Fanchi. *Principles of applied reservoir simulation*. Elsevier, 2005.

[12] CA Busse International Journal of Heat Transfer, Mass, and undefined 1973. Theory of the ultimate heat transfer limit of cylindrical heat pipes. *Elsevier*, 1973.

[13] EK Levy Journal of Engineering for Industry and undefined 1968. Theoretical investigation of heat pipes operating at low vapor pressures. ... *.asmedigitalcollection.asme.org*, 1968.

[14] P. Dunn and D. A. Reay. Heat pipes. *Oxford, Pergamon Press, Ltd., 1976. 305 p.*, 1976.

[15] JT Seo, MS El-Genk Transactions of the 5th Symposium on Space, and undefined 1988. A transient model for liquid metal heat pipes. *osti.gov*, 1988.

[16] Jean-Michel Tournier and Mohamed El-Genk. Current capabilities of "hptam" for modeling high-temperature heat pipes' startup from a frozen state. In *AIP Conference Proceedings*, volume 608, pages 139–147. AIP, 2002.

[17] Z.J. Zuo and A. Faghri. A network thermodynamic analysis of the heat pipe. *International Journal of Heat and Mass Transfer*, 41(11):1473–1484, jun 1998.

[18] C. Ferrandi, F. Iorizzo, M. Mameli, S. Zinna, and M. Marengo. Lumped parameter model of sintered heat pipe: Transient numerical analysis and validation. *Applied Thermal Engineering*, 50(1):1280–1290, jan 2013.

[19] KK Panda, IV Dulera, and A Basak. Numerical simulation of high temperature sodium heat pipe for passive heat removal in nuclear reactors. *Nuclear Engineering and Design*, 323:376–385, 2017.

[20] Mohamed S. El-Genk and Huang Lianmin. An experimental investigation of the transient response of a water heat pipe. *International Journal of Heat and Mass Transfer*, 36(15):3823–3830, oct 1993.

3. A REVIEW OF HEAT-PIPE MODELING AND SIMULATION APPROACHES IN NUCLEAR SYSTEMS DESIGN AND ANALYSIS

3.1 Overview

Nuclear systems are increasingly being designed to operate autonomously with passive safety systems and resilient, robust components. Heat-pipes naturally fit these requirements and are being investigate for use in advanced nuclear systems. These technologies were conceived and designed for this purpose but, recently, have become widely used and are known for use in electronic systems. The modern approach to nuclear safety involves full understanding of the physics at play. It is also important to predict the progression of the accidents from reactor steady-state to the point where either failure occurs or normal operation can be resumed. Understanding the speed of computation, the information obtained, the failures of various models are crucial to determining accurate accident progression. The history of heat-pipes in nuclear systems is reviewed as well as the modeling and simulation performed in that period. Various classes of models are reviewed analyzing their performance, capabilities, and draw backs when performing simulations.

3.2 Introduction

The future of nuclear power is increasingly becoming modular and autonomous. This allows for singular analysis to apply to huge swaths of products in a general sense. Autonomy and modularity also bring nuclear power into the realm of centralized quality control. Current plants have to be designed to the site and as a result have individual safety plans. An autonomous and modular framework would be similar to that of large software suites which allows small teams to push updates and improve the entire product line without custom resources. Jet engines have used this approach to steadily improve products that have been on the market and in use for years as well as improve and validate future designs. Turbine blades, specifically, are notable for this approach

[0]Reprinted with permission from "A review of heat-pipe modeling and simulation approaches in nuclear systems design and analysis" by Cole Mueller and Pavel V. Tsvetkov, 2021. Annals of Nuclear Energy, Volume 160, Copyright 2021 by Annals of Nuclear Energy

with new blade technology being dropped into engines at their next rebuild improving performance with no down time on top of the standard maintenance and inspection schedule. Implementing this approach also allows considerable effort to be placed on computational resources to improve the ability to predict the behaviors of components. From this, better understanding of accidents can be obtained as well as efficient optimization can be performed. This combined with the immense computing resources that are available today give rise to complex multi-physics software that are solving many physical phenomena simultaneously.

The next generation of heat-pipe reactor designs that are beginning to take shape are perfect examples of the modular autonomous power systems of tomorrow. These reactors are being designed to operate without operators for decades with passive safety systems and passive response to changes in grid conditions. This paper will review the models employed to model heat-pipes from the beginning of heat-pipe research until recently. This should serve as a resource for multi-physics simulation and reactor simulations when choosing models that will give quick, accurate, and reliable results. A brief history of heat-pipes will be described as well as their applications in nuclear systems, followed by an overview of modeling efforts since 1970's. Exact solution methods used will not be covered but the governing equations as well as the underlying assumptions will be described.

3.2.1 History of Heat-Pipes

Heat-pipes are an innovative technology that has a widespread appeal. From use in laptops and electronics cooling [1], all the way to satellite thermal control and reactor cooling [2]. Heat-pipes are almost commonplace in the modern world and are used in a variety of industries. How did heat-pipes become such an integral part of technology and when did heat-pipes gain popularity in nuclear systems.

Heat-pipes fall under the classification of two-phase closed thermosyphons. These are a family of devices that transfer heat primarily through the evaporation, and condensation of the working fluid with no mechanical input. All of the energy required to transport the working fluid comes from the evaporation of the working fluid. This all started with the devices manufactured by A.

M. Perkins and his sons. A. M. Perkins specialized in manufacturing single phase and dual phase heat transfer devices for coupling furnaces to boilers [3]. The cleanliness of the systems were the highlight of the inventions. These tubes were able to stay clean longer than traditional approaches and had lifetimes longer than traditional approaches [3]. These tubes also had the ability to operate at extremely high temperatures and pressures that, at the time, were not easily achieved [3]. A. M. Perkins started a career in boiler and heat distribution systems in 1827 [3]. Ludlow Patton Perkins, the son of A. M. Perkins, is credited with the developmental work on the Perkins Tube but based on writings in the late 1800's A. M. Perkins is likely to have done the bulk of the development [3].

The next mention of a heat-pipe like device was in 1942 [4]. At this time, an engineer with General Motors Corporation, Richard S Gaugler patented a device that essentially meets the definition of a heat pipe. The patent describes typical passive closed cycle heat transfer as taking place from low elevation to high elevation [4]. It is described that heat is transferred by heating a volatile fluid causing it to evaporate, allowing the vapor to transport upwards to a cooler area, and then condensing this volatile releasing heat into the condenser region [4]. This is essentially the description of a closed two-phase thermosyphon. Gaugler describes that to deviate from this requires work to be done on the fluid [4]. The goal of the patent, and the originality of the concept, was to create a passive system to transfer heat from a higher elevation to a lower elevation. The approach uses volatile liquid contained in a capillary structure with a space that accumulates the evaporated volatile fluid [4]. The capillary structure was to be made of pure sintered iron particles [4]. A three region device with a capillary structure to provide pressure head is the definition of a heat-pipe. Unfortunately General Motors Corporation did not find immediate use for this at the time and it did not become known based on the work done by Gaugler.

In 1963, at Los Alamos Scientific Laboratory, George M. Grover created a closed two-phased wicked thermosyphon and coined the term "heat-pipe." This is considered the beginning of the modern heat-pipe. Grover created the real scientific focus on heat-pipes and began the effort to define and predict operating characteristics of the devices. Grover's 1963 patent included references to liquid metal working fluids and cryogenic working fluids and in 1964 they published a paper

[5, 6]. With this patent and paper many industries immediately saw the potential of this concept for compact cooling of various kinds. From cooling vacuum tubes to thermal control in space craft and satellites it was very clear that the technology was going to be very useful.

3.2.2 Historical uses in Nuclear Systems

The efforts in nuclear are extensive and to simplify it a general overview of the history is given. The types of models used primarily are described for each era and the efforts to advance those models are also described. It is important to also understand some of the goals for these projects as this has a profound effect on what types of models were developed and the underlying assumptions that led to them.

The advent of the modern heat-pipe and the beginning of heat-pipes in nuclear systems were hand in hand. Today it may not seem that way as most applications of heat-pipes are in electronics and waste heat recovery systems but within the ten years of the initial patent filing by Grover there were numerous papers and conceptual studies of heat-pipe cooled nuclear reactors. In fact, Grover himself patented a nuclear reactor cooled by heat-pipes designed for space applications in 1965, just two years after the initial patent for heat-pipes [7]. At around this same time the European Atomic Energy Community, Euratom, developed a design for a heat-pipe cooled reactor using heat-pipes based off Grover's original concept [8]. This shows an incredible spread that was near global almost immediately after publication. In this early period heat-pipe analysis was limited to resistance models and they are still used in the bulk of design studies as an effective and accurate tool. It is understandable that in the first years after conception design and analysis methods were limited. That combined with most engineering being done with pen and paper hand calculations were going to limit the designers of the day. The resistance models can be seen later in this paper. These were the dominant analysis method until the mid 80's.

By 1968, heat-pipes were being designed into almost every nuclear system intended for space. Heat-pipes were even considered for passive reactivity control in space reactors and in nuclear thermal rockets [9]. It was apparent how versatile heat-pipes were and their potential applications in nuclear. A nuclear reactor that would be designed to passively operate at a predetermined set

point and at the same time dynamically adjust power based on the conditions of the system, is an autonomously operated system. With control systems being considered the transient nature of heat-pipes and their effects on reactivity in core are crucial points of understanding that have to be captured. Computers and software began to become important in modeling the tightly coupled phenomena to get accurate results. These models were almost always application specific and were highly simplified. In fact most heat-pipe models make simplifying assumptions like these such as 2D assumptions. These limit the applicability, generally, for the gain in computational speed. In the 70's the simplifying assumptions were to ensure computer time was not excessive.

In 1970, there were investigations published that looked at the ability to include a fuel based working fluid for enhanced reactivity control [10]. New working fluids and multiple applications allow designs to become more compact and more versatile. The integral nature of this control and cooling system can reduce the cost of components and remove the number of moving components from the core. This will improve safety as solid state components tend to be more reliable. Moving control systems can also become locked leading to runaway reactions.

In the 1970's, enthusiasm about the possibilities of space travel created the need for efficient, and long life power systems. Space reactors were being designed to be reliable, robust, and autonomous. The goal was to develop systems that would not fail and would be able to function without constant operator oversight. These systems needed to be light weight and compact to enhance the portability and needed to be able to provide power for human based missions. With the lighter cooling system and removal of a substantial portion of equipment required, reactors were becoming simpler. For example, a space reactor was designed as a split core to be used for reactivity control [11]. This reactor would be operated with a stationary reflector with half the core attached to it. The other half of the core would be mobile to control reactivity insertion by bringing the two halves closer together. Each half of the core would have heat pipe cooling independently. Thermionic energy conversion systems were eventually investigated for direct power conversion with heat-pipes [12, 13]. These reactors being design for interplanetary exploration and nuclear electric propulsion. These designs show similarities with modern terrestrial nuclear heat-pipe sys-

tems. The hexagonal fuel with central heat-pipe void is a concept being investigated currently [14].

In the conceptual design space individuals were looking for new and unique ways to incorporate heat-pipes. Based on what was mentioned earlier this meant fast models were used to rapidly iterate on design characteristics. Resistance models were those used most often. Investigations into limiting behavior and conditions became important because the models used were not able to capture them. So now, not only were exact operational behavior being determined but the regions in which a heat-pipe reliably operated were being determined as well. The developed limits can be seen in the section about heat-pipe operating principles. These new limits helped give operators and designers confidence in the behavior of heat-pipes when implemented into cooling solutions.

Towards the end of the 1970's with the decline in space exploration and a shift in focus in nuclear to large light water power plants there was a change in heat-pipe research from conceptual design to modeling of existing concepts. This happened in almost every facet of engineering and science, as computational resources became cheaper and better performing, expensive experiments were avoided in favor of computers. The 1980's and 1990's were dominated by the development of computational methods to help focus resources. This can be seen in the many computational papers published in that period some of which include [15, 16, 17, 18, 19]. This period is where the majority of models were developed and make up a significant portion of the review. The models were all closely related and had similar assumptions. It became clear that there were several classes of models that worked well and those developed in their own way. But the motivations were not for detailed modeling but for use in predictive control mechanisms for autonomous systems, specifically space systems. Having substantial communication lag when communicating in space, either the power source needs to be relatively unchanging or the control system needs some sort of autonomous behavior.

In the early 1980's NASA began focusing efforts on a few versatile mission capabilities. The Space Shuttle began completing missions in 1981 with the goal of providing a much less expensive route to access space, similar approaches were taken with other capabilities. Custom missions were

avoided in favor of general mission capabilities. Capabilities were being developed for all mission aspects, including power. The SP-100 reactor was intended to be one of these capabilities. It being a heat-pipe cooled reactor to provide power for space missions. The SP-100 project was started in 1983 under the supervision of DARPA in conjunction with the Department of Energy office of Nuclear Energy to develop a reactor that could be used on a variety of missions to meet the military's needs as well as other potential future users [20]. The program never advanced beyond ground testing and was eventually terminated in 1994.

Plant design and operation began shifting from a performance perspective to a safety perspective. Better predicting the results of plant casualties and operational decisions was a goal of research and development. This motivated designs that were isolated from the environment to mitigate the consequences of an accident; [21] discussed a heat-pipe cooled reactor that was meant to be buried deep underground. The heat-pipes would be designed to carry the heat from the buried reactor long distances to the surface where it could be used. The heat-pipes could do this with no mechanical work input and with little thermal losses. Maintenance issues have long been known with buried systems and this system is likely included. Heat-pipes at this time were known to be extremely reliable and made sense for transporting heat long distances without the ability to maintain them. Fast reactor systems were also designed using heat-pipes as the primary coupling between the sodium coolant and the steam generator [22]. With the lessons learned at EBR I and the reliability and safety demonstrated at EBR II, incorporating components that aided in the reliability of the system made sense for the design of a terrestrial power plant.

Throughout the 1990's heat-pipes were either incorporated into emergency core cooling systems or into space reactors. There was little research investigating the performance and capabilities of small nuclear power plants for earth. Space systems can be adapted for terrestrial use, but typically space systems employed specialized technology developed in a research environment as a single use case or demonstration technology. These space concepts had low system efficiencies and power such as [23] with 12% efficiency and 40 kW_e which is not a realistic design point for commercial power systems. Converting this to a terrestrial style power plant would require ma-

jor design changes likely changing the entire nature of the reactor. This is because space design requirements are vastly different than terrestrial design requirements. There are a few reactors in this design range as well such as [24, 25] both of which are designed for kW levels. This only means designs cannot be easily converted, but the concepts used in the designs can be. That being said there were some designed in this period for megawatt level operation, such as [26]. This used heat-pipes for the radiator to ultimately reject heat away from the brayton cycle.

In the 2000's, heat-pipe applications in reactors grew. With the war in Iraq, private space exploration maturing quickly, and confidence in nuclear technology building, reactors were becoming more popular for power production, desalination, and process heat. In this period the AP-1000 reached a deployment phase and in some places began construction. The AP-1000 has advanced passive cooling measures to ensure safety in the event of an accident. There were small reactor concepts that employed heat-pipes for this very purpose. The SMART reactor out of Korea is one example of a reactor containment being cooled with heat-pipes [27]. There were also investigations into using heat-pipes to further isolate the nuclear cooling fluid from the desalination plant by coupling the desalination process to the heat source with heat-pipes [28]. The fear was that radiation could contaminate the desalinated water and heat-pipes could prevent this. The space system SAFE-400a was also proposed and designed at Los Alamos for future space missions [29]. There was also the beginning of modern solid core heat-pipe reactors. The University of California designed a solid state heat-pipe cooled reactor [30]. This design is likely one of the main contributors to heat-pipe's current popularity and interest in modern reactors use of heat-pipes. The concerted effort between space reactor research and the promise of micro-grid capabilities created a strong push to develop these smaller reactor types.

In the period of 2010 to 2020 heat-pipe reactors have taken off. With several private companies designing and rapidly progressing through the design process there is a lot of promise for heat-pipe reactors. With reactors like KRUSTY being designed for space missions and components for this reactor being tested as well, there is rapid progress occurring [31]. There are also terrestrial reactors being designed and nearing a regulatory phase. Such as the eVinci Reactor from Westinghouse

[32], or the MegaPower reactor also designed at LANL [33, 14]. These are all progressing quickly and show promise for the future of heat-pipes in nuclear systems. There have been several recent reviews discussing the technology of used in conjuction with modern heat-pipe reactors that help understand the design goals associated with these systems [34, 35].

3.2.3 Description of Heat-Pipes and Thermosyphons

Heat-pipes are thermosyphon devices. A thermosyphon is a device that transports heat based on flow phenomena that is generated naturally from the system properties. There are no mechanical pumps and no internal means of generating flow. They can be separated into single-phase and multi-phase fluid devices. Multi-phase thermosyphons can have more than two phases such as nanofluid based heat-pipes; those with nano-particles dispersed into the flow to improve certain characteristics of the device [36]. Only single-phase and two-phase devices will be discussed further. Single-phase thermosyphons operate with a single fluid phase with no distinct separation between the component fluids within the device.

3.2.3.1 Thermosyphon Operating Principles

The thermosyphon most individuals picture when the topic is brought up is a single phase device that strictly relies on the density differences and gravity to provide the required pressure head to induce flow and transport the heat. This is probably the most common type but is far from the only type. Under a broader definition thermosyphon devices can be thought of as any device that is entirely self contained and transports heat passively without moving parts using a working fluid or mixture of working fluids with intent of eliminating conduction losses. Based on this definition operating principles or goals can be defined.

The first goal is that heat must be transported. Either conduction through this device or fluid movement within this device must move heat energy from a source to some sort of sink. In a thermosyphon this is always done with a moving fluid. Natural convection is used in some cases, evaporation and condensation enhances this natural convection process as gravity is the primary fluid mover, in other cases it could be the rapid expansion of vapor bubbles.

The second goal is that they are passive. Passive operation requires no operator or control input. It must dynamically reach stable operating conditions. A turbine-compressor combination can do this, but it is a very complicated system, and moving parts violate the definition.

This leads to the final goal, no moving parts. Without moving parts the only way to establish flow is from the physical characteristics of the system. This is primarily where the types of thermpsyphons differ. This can be heat-pipes, pulsating heat-pipes, vapor chambers, reboilers, and what is colloquially known as a thermosyphon. It is standard to break these into subcategories of two-phase closed thermosyphon and single-phase closed thermosyphons.

3.2.3.2 Heat-Pipe Operating Principles

Heat-pipes are a distinct subset of thermosyphons that use a wicking structure to passively generate flow caused by differences in capillary pressures. They have several regions that will be discussed later. Heat-pipes, as was previously mentioned, use capillary effects to generate the primary system head to create flow and energy transport. This gives heat-pipes unique operational characteristics. If they are designed properly, they can operate inverted or against gravity or whatever acceleration is present and acting on the device.Vapor chambers and heat-pipes are very similar and act on the same principles. There is a distinction for several reasons. The main reason is that they are designed to accomplish different goals. Typically heat-pipes are designed to transport large amounts of heat over a significant distance. This is in contrast to vapor chambers, which are designed to dissipate heat, or spread it out efficiently. Vapor chambers have frequently been incorporated into heat-spreaders because of the near isothermal behavior of the vapor within them [37]. The isothermal properties essentially allow an amplification of the of the effective heat-transfer area available for the heat source. This results in lower temperatures with similar performance when compared to traditional heat-sinks.

With capillary pressure creating the majority or all of the pressure head in some cases certain operating behaviors can be intuitively determined. First is, a maximum amount of pressure can be developed by any capillary based device. There is only a maximum pressure differential that can be generated between the two phases present. In the case of a heat-pipe this is the vapor and the

liquid phase. This leads to the derivation of the capillary limit. This limit describes the maximum heat transfer rate possible based on the maximum capillary pressure attainable as can be seen in Equation 3.1.

$$\Delta P_{capmax} \geq \Sigma \Delta P_i \tag{3.1}$$

P in this equation refers to the pressure, with the Δ indicating the change. The subscript i denotes the specific component of pressure change, being frictional, gravitational or others [38]. It is also known that two phase flow results in higher pressure drop. In a heat-pipe true two phase flow is hoped to be avoided using the wick. But, there is the possibility that fluid droplets can be pulled from the wick caused by high speed vapor flow creating increased pressure losses, limiting heat-pipe performance. This droplet entrainment leads to the derivation of the entrainment limit which can be seen in Equation 3.2.

$$Q_e = h_{fg} A_v \sqrt{\frac{We \cdot \rho \cdot \sigma}{L}} \tag{3.2}$$

Where Q_e is the entrainment limit, h_{fg} is the latent heat of vaporization, A_v is the vapor flow area, We is the Weber number, ρ and σ are the density and surface tension respectively, and L is the characteristic length of the porous interface, typically the effective pore diameter [39]. If the flow is then analyzed there are certain properties that can lead to operational limitations. If the flow velocity is high enough compressible effects may become important. This can even lead to the choking of flow within the heat-pipe. This choked flow condition is commonly referred to as the sonic limit which can be seen in Equation 3.3.

$$Q_{sonic} = \sqrt{\frac{\gamma \rho P}{2(\gamma + 1)}} \cdot h_{fg} A_v \tag{3.3}$$

P represents the pressure and γ is the heat capacity ratio [39]. With all liquid heat transport systems, boiling phenomena must be considered. With a heat-flux that is too large boiling can occur blocking the flow return to the rest of the evaporator section. This can be catastrophic and

leads to the creation of the boiling limit that can be seen in Equation 3.4.

$$Q_{boil} = \frac{4\pi l_{eff} k_{eff} T_v \sigma_l}{h_{fg} \rho_v ln\frac{r_i}{r_v}} \left(\frac{1}{r_n} - \frac{1}{r_{eff}} \right) \tag{3.4}$$

l_{eff} is the effective length of the heat-pipe and r is the radius with the subscripts i and v representing the inner tube radius and the vapor radius respectively. And the subscripts n and eff represent the nucleation site radius and the effective pore radius for the wick[39]. k_{eff} is the effective thermal conductivity of the wick, T_v is the vapor temperature or the saturation temperature, σ_l is the surface tension of the liquid, h_{fg} is the latent heat of evaporation, and ρ_v is the vapor density. These limitations are used to to do baseline analysis for design and define an operational envelope in which a heat-pipe can be safely operated. These are conservative limits that give designers confidence in producing a product that will not fail under the design conditions. It also gives the designers knowledge on certain upper bounds of connecting components to the heat-pipes. Other models are used to obtain exact information about the heat-pipes operating conditions.

3.2.3.3 Distinguishing features of Heat-Pipes

Heat-pipes are easily distinguished from other types of thermosyphons by their wicking structure. This creates two dedicated flow paths, one for the liquid and one for the vapor. This also gives capillary pressure helping to drive the flow rather than just density differences. This gives them the ability to operate in many different orientations without a loss of performance. There are design consideration that have to be accounted for but it is possible. This gives them the ability to act as“wires" in a connection from the source to the sink. Many times they are ignored in thermal analysis or the effective conductivity is made very high. They are also long, narrow and, within in reason, can be bent and guided tortuously to the source. This allows much more compact geometries to be created and allows heat sources to be placed closer together.

There are several other devices that either share a similar name or similar features that could cause confusion. As stated earlier vapor-chambers share a common wick structure but the primary reason they are named differently is because their primary goal is to spread heat and not move it as

can be seen in the diagram in Figure 3.1.

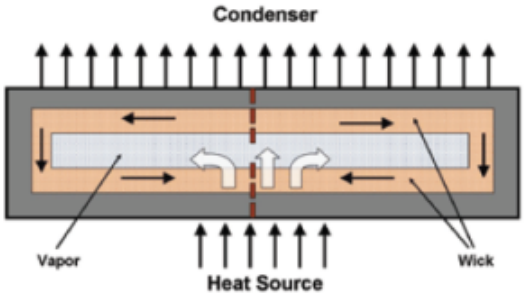

Figure 3.1: Drawing of a basic Vapor Chamber designed for spreading heat [40]

In Figure 3.1 we can see the three components of a vapor chamber or heat-pipe, the envelope, the wick, and the vapor region. The envelope contains the fluid to prevent losses, the wick transports liquid back to the heat source from the condenser region, and the vapor transports heat from the evaporator region back to the condenser region.

There is also devices known as a loop heat-pipe. These have a wick structure and operate according to similar principles, but the liquid is returned along a dedicated line. This slightly simplifies manufacturing of a wick structure, and somewhat eliminates the entrainment limit.

There are also devices known as oscillating heat-pipes that have no wick structure and operate using the boiling phenomena. When boiling occurs the expansion of the vapor pushes the fluid through the pipes. The momentum of the fluid then carries the vapor off the heat source. When the vapor reaches the condenser it condenses and pulls fluid behind it. This cycle allows the fluid to be pumped using the growth and retraction of vapor bubbles. There are many heat-pipe types there are several recent reviews on their applications and some of the unique challenges and motivations that brought them about [42]. Heat-pipe heat exchangers are not necessarily a different type of heat-pipe but, they are a unique application for them and have similar heat-pipe requirements to reactors [43].

These were covered because some perform substantially better than tradition wicked heat-

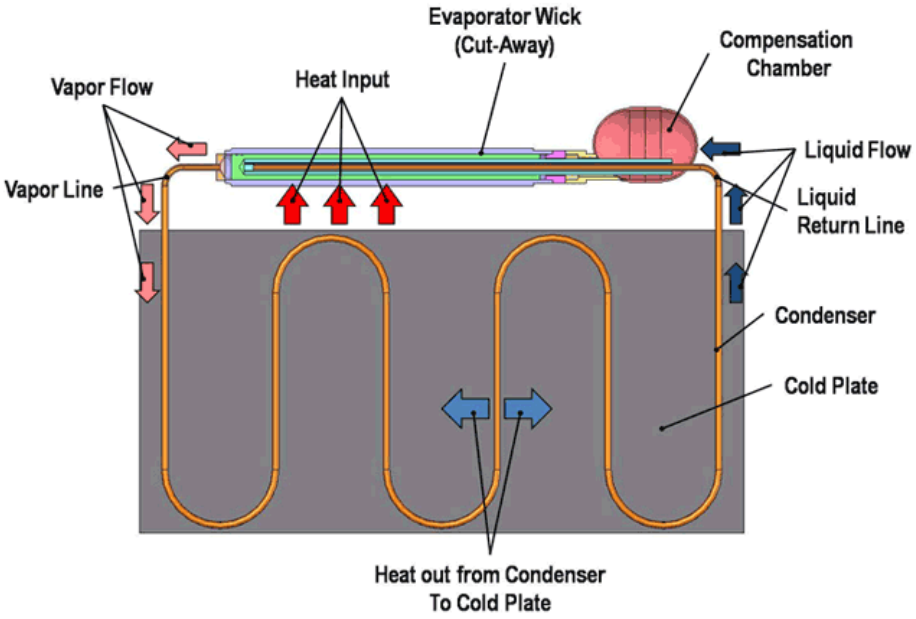

Figure 3.2: Drawing of Loop Heat Pipe to understand operation [41]

pipes. This performance comes with increased system complexity, increased size, and loss of desirable properties such as compactness. For a single heat source this increased complexity could justify the cost, but when there are many the system could become too complex to properly manage. This is the main reason they have not been adopted into nuclear systems at this point. Nuclear reactors would often require 100's-1000's of individual cooling connections, it just would not be worth the cost. This is why modern nuclear plants, if passive for any period of operation, rely on large scale thermosyphon behavior to drive the flow. This can simply provide the needed results. This is until distributed power generation became popular. Now micro and small reactors can reasonably consider traditional heat-pipes for primary cooling. With factory made standard reactors, large numbers of complex systems can be made without incurring substantial costs. This is especially true if the sub-components of the system are manufactured independently and at a large scale. This requires knowledge of the available models to accurately determine operating conditions. To do this drawing on the historical research will be incredibly useful.

3.3 Physics of Heat-Pipe Systems

Understanding the physics of the system will give a foundation for defining governing equations that properly capture the behavior within the heat-pipe. There is both compressible gas flow and incompressible liquid flow within the system. Phase change is also present and is what gives heat-pipes their isothermal nature. This is an important part of heat-pipe behavior and accurately capturing this behavior is necessary. Gas flow is the primary energy carrier from the evaporator to condenser. Thermal diffusion is present as well and is one of the more influential behaviors in the system when it comes to transient and steady state behavior. Figure 3.3 shows the standard approach represented by a 2-D axisymmetric geometry. It will be useful to reference this figure when reading.

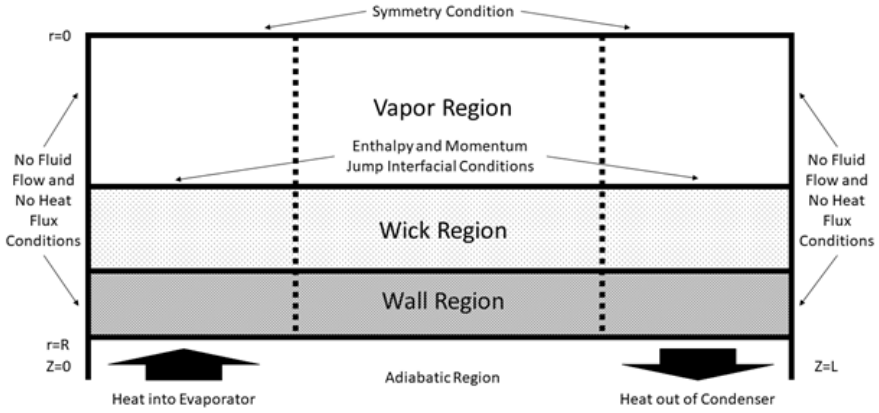

Figure 3.3: General Heat-Pipe layout for a convenient reference

When analyzing the models and methods developed previously an understanding of the system physics is important. It is also important to determine the contribution from those physics to the system behavior. When are these important, and why are they or are they not important in general. This type of analysis will allow future engineers and scientists to better build models for their specific application or focus their efforts to improve the detail and accuracy of these models. It

also lends to the understanding of why previous researchers made specific decisions when building there methods and models.

3.3.1 Physical Regions Within a Heat-Pipe

Figure 3.3 will be a useful reference when describing heat-pipes. It shows the axis of the heat-pipe along the z axis which is horizontal in the image. The radial axis is shown vertically. It is displayed in this manner to more efficiently use the space. The standard approach has zero heat-flux conditions at the ends with some sort of symmetry condition along the central axis and then variable conditions along the wall region depending on the heat-pipe design.

There are three principle regions within a heat-pipe. The solid envelope or wall region, the wick region, and the vapor region. The solid envelope region is required to contain the working fluid within the heat-pipe. The wick region is the primary fluid return. It brings fluid from the condenser to the evaporator. The vapor region transports the thermal energy from the evaporator to the condenser.

Governing equations for each region are presented for various and common heat-pipe models as well as a general overarching set of equations that governs the behavior and from which most other models can be derived. This will serve as a starting point for future engineers to investigate the common equations, and assumptions used for modeling heat-pipes and why those assumptions occurred. For most prior engineers a common reasoning was speed of calculation but there are some special cases.

3.3.2 Solid Envelope Region

The solid region of a heat-pipe is a required component within the heat-pipe. It defines the boundaries of the system and is where the heat both enters and exits the system. In traditional heat-pipes this is a tube with end caps. This is always a solid material and, in every case found, is metallic such as copper, aluminum, or stainless steel.

3.3.2.1 Importance to System Behavior

The solid envelope is very important to system behavior. Being a solid region there is two very important properties of interest. The first is the thermal conductivity. Envelopes with higher thermal conductivity will have lower temperature drops when compared to those with lower conductivity. This is very straight forward and intuitive and is not specific to heat-pipes. This is a significant portion of the thermal resistance associated with a heat-pipe making it very important to the steady state behavior of the heat pipe. The second property is the heat capacity of the envelope. The amount of energy the envelope can hold has a noticeable impact on the transient behavior of the system. The more heat storage the slower the transient will progress. Again this is not specific to heat-pipes.

3.3.2.2 Governing Equations Used

The solid region is very simple to model. The heat equation has been solved repeatedly and has been shown to be accurate, given your inputs are also accurate. For steady state solutions the heat equation takes the form of Equation 3.5 and the transient form takes the form of Equation 3.6

$$0 = k\Delta T \tag{3.5}$$

$$\frac{\delta T}{\delta t} = \frac{k}{\rho C_p}\Delta T \tag{3.6}$$

This is standard for the wall region. In most cases this is simplified into 2D axisymmetric equations but that is a decent assumption for standard heat-pipes and for verification and validation purposes. Modifications to this equation for simpler or faster calculations will be discussed.

For steady state heat-pipe modeling a common approach is to form a resistance network. This occurs between the wick and the wall for the evaporator, adiabatic region, and condenser and then the vapor region. This starts by assuming radial conduction in the evaporator and the condenser. From this the resistance for those regions can be defined by Equation 3.7.

$$R = \frac{\ln(\frac{r_o}{r_i})}{k2\pi L_j} \tag{3.7}$$

Where R is the resistance of the section, r is the radius with i and o being the inner and outer radius respectively, k is the thermal conductivity, and L is the length with j representing the specific section of evaporator or condenser and wick or wall. For the axial conduction through the adiabatic region a similar resistance is used that can be seen in Equation 3.8.

$$R = \frac{L_j}{k\pi(r_o^2 - r_i^2)} \tag{3.8}$$

In this case j represents the specific section of the adiabatic section whether that is the wick or wall. There are many correlations for the vapor resistance as it is more complex than conduction and the exact style of heat-pipe will affect it. It also is not a bad assumption to assume there is no resistance in the vapor region [44] but for the purposes here it will take an arbitrary value. Figure 3.4 shows an example of the circuit. This is not an exhaustive diagram as there can be resistances added for the interfaces in the system.

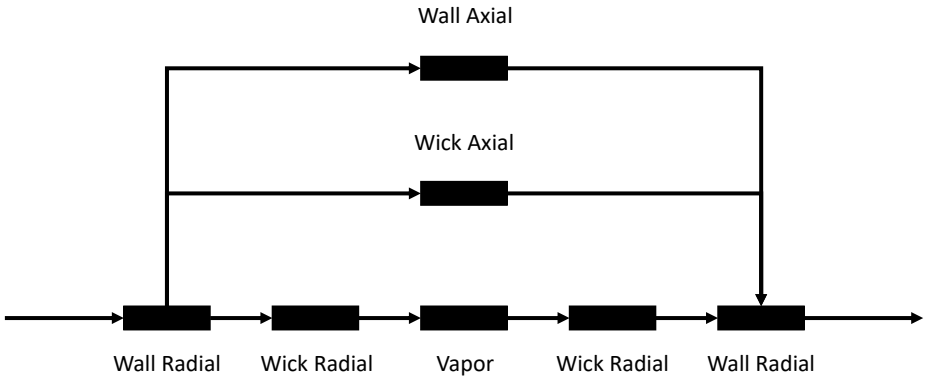

Figure 3.4: Electrical Resistance Network as represented in [44]

The arrows represent “wires" in this analogy and the blocks represent the resistors. The wires are regions of coupled temperatures meaning the temperatures are equal at those points in the region. For example the wall axial and the wick axial have the same inlet and outlet temperature. These two have the same inlet temperature of the wall radial region of the evaporator and the same outlet temperature of the wall radial region of the condenser. These can also be organized in various ways to better represent the system. Using a resistance analysis for each section we know that the temperature drop is represented by Equation 3.9.

$$\Delta T = Q \cdot R \tag{3.9}$$

Where Q is the heat flowing through the resistor section. This can naturally be organized into a system of equations and solved simply to get a decent estimation of the temperature of each segment. A natural assumption is that the entire heat-pipe can be accurately represented as a pseudo solid material with a sort of conductive resistance between all the components.

This same analysis can be extended into a transient form. First, the previously derived resistances cannot be used as they were derived specifically for steady state. Second, a capacitance or energy storage term is necessary. This will be based off analysis performed by [44]. The final result will be presented and readers will be encouraged to view the original paper to see more details of the derivation. The solution requires two assumptions. The first is that the temperature is continuous at the vertex. The second is that at any vertex the heat input flows must equal the heat output flows. These are just statements of the conservation laws captured by the heat equation. In essence the derivation of this method becomes a method of lines solution with a pseudo 2-D finite difference discretization of the spatial equations. This can be seen in Equation 3.10.

$$\frac{dT_i}{dt} = \frac{2\alpha_i}{\lambda_i^2}(T_{i,1} + T_{i,2} - 2T_i) \tag{3.10}$$

Where T is the temperature of the segment with subscript i representing the specific segment. λ is the length of the of the segment and α is the thermal diffusivity of the segment. The actual

method of lines equations for these were derived in [44] so applying the actual conditions and getting the six equations will not be performed here. Knowing that these are simply a method of lines solution of the heat equation another analysis method can be performed. This is a conduction only analysis. This is solving the transient heat-equation with appropriate boundary conditions and effective thermal conductivity's. The major assumption here is that convective behavior is not a major contributor to the movement of energy in the heat-pipe. For liquid metal heat-pipes this is a perfectly valid assumption. For water or other working fluids with low conductivity this may not be. This is seen in [38] where the transient behavior occurs much quicker than expected in the conduction model and is partially attributed to the low conductivity of the fluid.

3.3.3 Wick Region

The wick region of the heat-pipe is a necessary component to ensure the evaporator has liquid. Without liquid in the evaporator a dry out condition occurs and the heat-pipe goes from a very high thermal conductivity to essentially an insulator. This could cause failure in the heat-pipe, or failure to the components being cooled. This region dominates pressure drop behavior and is a significant component of the thermal mass. Special care is needed to accurately determine the characteristic limits created by the features of the wick like the capillary limit and the entrainment limit.

3.3.3.1 Importance to System Behavior

This region is very important to system behavior. It is a very large thermal mass relative to the vapor and is on par with the thermal mass of the envelope. This property alone will cause an increase in the time to reach a steady operating condition. It is a large thermal inertia component in the system. Compounding on that, the fluid is moving, albeit slowly, it is still moving heat as it flows and if the effective thermal conductivity of the wick is low enough it will change the behavior of the system.

3.3.3.2 Governing Equations Used

It was discussed in previous sections that conduction approximations have been used to describe both transient and steady state heat-pipe behavior. This will not be discussed again but it

is worth noting that it is used. At the start of heat-pipe research there was really only one type of wick. This was a homogeneous porous wick for the complete length of the wick section. This was approached initially with Darcy flow equations. Darcy flow works well in porous structures at very low Reynolds numbers. This is a regime in which inertial effects, and turbulence do not occur. In most heat-pipes, creating turbulent flow is near impossible because the prevailing limits prevent flow rates of that magnitude. The momentum equation can be seen in Equation 3.11.

$$q = -\frac{K}{\mu}(\nabla p + F) \tag{3.11}$$

Where q is the volumetric flow rate, K is the permeability tensor, μ is the fluid viscosity, and p is the pressure of the system. F are body force terms or momentum sources and is where gravity would be included. This is still used to investigate heat-pipe wick behavior. If the flow rate is known as a function of height the pressure gradient can be integrated over the length of the heat-pipe and pressure drop can be determined. This allows for the calculation of capillary limits or the associated pressure drop of the wick. Combined with mass conservation equations and energy conservation a transient type analysis can be done that accounts for heat transfer.

With the advancement of wick styles Darcy laws became inadequate to describe the flow behavior within them. With wick styles still having capillary behavior the need to capture the behavior of porous flow is necessary but the new wick styles typically have properties to allow for non-porous channel flow. These wick styles include arterial wicks, grooved wicks, and annular wicks. All provide open channel flow to the liquid to decrease pressure drops and increase heat-pipe performance. Figure 3.5 shows some of the different types of wicks that have been studied.

This brought forth models to describe flow behavior in a heat-pipe that can account for inertial effects more directly. The pressure drop through some of these wicks were so small that the full navier stokes could be solved for laminar flow without much loss in accuracy. Others retained the porous media models and adjust the porosity, permeability, and other constants such that it would reduce to navier stokes in that region. The most general of these was the Darcy-Brinkman-Forchheimer extended model. This includes all the terms used. From this model the Darcy mo-

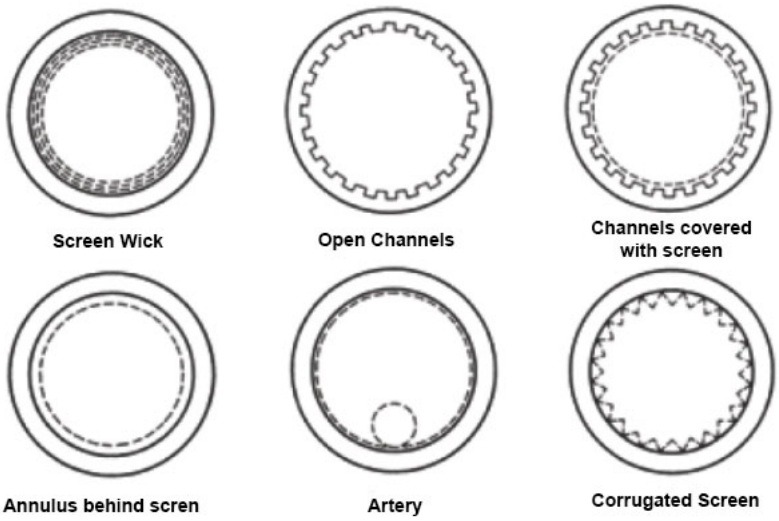

Figure 3.5: Some Wick Structures used in Modern heat-pipes [40]

mentum equations can be derived by neglecting Brinkman and Forchheimer terms as well as the transient terms. Equation 3.12 is the Darcy-Brinkman-Forchheimer extended momentum equation.

$$\frac{1}{\epsilon}\frac{\delta(\rho\vec{q})}{\delta t} + \frac{1}{\epsilon^2}\nabla\cdot(\rho\vec{q}\otimes\vec{q}) = \rho\vec{F} - \nabla P - \frac{\mu}{K}\vec{q} - \frac{C\rho}{K}|\vec{q}|\vec{q} + \frac{\mu}{\epsilon}\Delta\vec{q} \tag{3.12}$$

In these equations ρ is the density, ϵ is the porosity, $\vec{q}$ is the volumetric flux or darcy velocity, K is the permeability of the porous structure, C is the inertia coefficient, and μ is the viscosity of the fluid. P and $\vec{F}$ is the pressure and body force terms respectively. The porous mass continuity equation is also needed which is applicable to Darcy flow as well. This is shown in Equation 3.13.

$$\epsilon\frac{\delta\rho}{\delta t} + \nabla\cdot(\rho\vec{q}) = 0 \tag{3.13}$$

In the wick, energy conservation is probably the most important aspect of this evaluation. This is supported by the fact that the system can be modeled well with only conduction in some cases. So the true temperature profile should be captured by the energy equation. A general form of the energy equation is shown in Equation 3.14.

$$\frac{\delta}{\delta t}\left[\epsilon(\rho h)_L + (1-\epsilon)(\rho h)_m\right] + \nabla \cdot \left[(\rho h)_L \vec{q}\right] = \frac{\delta P}{\delta t} + \vec{q} \cdot \nabla p - \nabla \cdot (-k \nabla T) \tag{3.14}$$

This is without viscous dissipation. Viscous effects may be important so ignoring them may cause error. To see a 2D analysis with full viscous dissipation accounted for refer to [45] and the related work. Here the subscripts L and m are to represent the liquid and the metal matrix respectively. These three equations can be simplified and manipulated to recreate almost all the available simulation tools for modeling wick behavior.

One of the more widely used models developed by [46] is the THROHPUT code. This is a 1-D axial model that accounts for freezing and thawing heat-pipes. It is a well characterized code and is used for modern heat-pipe simulations because it is computationally fast and simple to understand. The wick region is coupled to both the vapor and the solid by source terms. Each region is 1-D axial like the wick region with momentum, mass, and energy source terms for each respective region being solved. The solid region has no momentum or mass equations to be solved. This model also accounts for freezing and thawing of the wick. It assumes an area averaged formulation making it difficult to account for geometries with varying areas. The radial shape used for area averaging is well approximated by a quadratic function. If the flow is not one dimensional then the area averaging will cause deviation from actual results. The exact formulation can be found in [47] and readers are encouraged to read the report in detail.

3.3.4 Vapor Region

The vapor region is the primary transporter of energy from the evaporator to the condenser. In a properly designed heat-pipe the majority of the energy is carried by the vapor and small amounts are carried through the wick and the envelope. The vapor region is in most cases isothermal. There are scenarios when that is not the case, such as when the fluid is operating in a free-molecular flow condition, but in steady-state and most operating scenarios isothermal assumptions allow physics to be accurately captured.

3.3.4.1 Importance to System Behavior

This is the primary transporter of energy but that does not mean it is important to system behavior. During startup and shutdown transients where the vapor does not behave as a continuum, the vapor dynamics play an important role in the behavior of the heat-pipe but near the operational point the vapor becomes unimportant to system behavior. It has almost no thermal inertia compared to the solid and wick regions so it is not driving the behavior of the system transient. The vapor velocity can also be very high. This means that, with appropriate assumptions, the energy can be treated as traveling from the evaporator to the condenser instantly and the vapor can be ignored. Treating the vapor as a lumped mass with near zero heat capacity is very common as most steady state applications only need this.

The vapor region has very small thermal inertia, and it is that reason that it does not drive over heavily influence the behavior of the heat-pipe. As long as the vapor region remain relatively isothermal it will be unimportant to the system from a modeling perspective. The vapor region becomes important when the heat-pipe gets "cold." Cold refers to the point where the vapor pressure is very low and the sonic velocity drops as a result. In this situation the flow becomes choked and the flow approaches the sonic limit. This can easily occur during transients, and in the context of reactor safety, during accident transients. For example, if cooling is introduced to quickly to high temperature heat-pipes during an accident, the flow could be choked and heat could be trapped in the fuel. But this is an accident scenario, and so resolving the vapor behavior to high precision is only important then.

3.3.4.2 Governing Equations Used

Governing equations in the vapor region are relatively simple. It is usually a compressible fluid flow model with species accounting to ensure capturing of non-condensible gases in variable conductance heat-pipes. This can then be reduced to 1D or 2D equations. The real difference is the energy equations. In some models the vapor is assumed saturated and so the energy equation takes the form of the Clausius-Clapeyron equation. The continuity equation is seen in Equation 3.15

$$\frac{\delta \rho}{\delta t} + \nabla \cdot (\rho \vec{u}) = 0 \tag{3.15}$$

Where ρ is the density, t is time, and $\vec{u}$ is the velocity vector. The momentum conservation equation is seen in Equation 3.16

$$\frac{\delta \rho \vec{u}}{\delta t} + \nabla \cdot (\rho \vec{u} \otimes \vec{u}) = -\nabla p + \mu \Delta \vec{u} + \frac{1}{3} \mu \nabla (\nabla \cdot \vec{u}) + F \tag{3.16}$$

Where p is the pressure, μ is the viscosity, and F are the momentum source terms. The energy conservation equation in it's general form can be seen in Equation 3.17

$$\frac{\delta}{\delta t}(\rho h) + \nabla \cdot (\rho h \vec{u}) = \frac{\delta P}{\delta t} + \vec{u} \cdot \nabla p - \nabla \cdot (-k \nabla T) \tag{3.17}$$

Again viscous dissipation is left out. Errors could occur from ignoring viscous effects in the vapor. If the vapor is assumed saturated then the energy equation does not need to be solved and the temperature, and therefore enthalpy, are dependent on the pressure of the region. To account for this the Clausius-Clapeyron equation is used to obtain the temperature in the vapor region from the pressure solution. This simplifies the solution procedure allowing the temperature field to be easily determined.

3.3.5 Wick-Vapor Interface

The wick vapor interface is an important aspect because it acts as a divider between the flow regimes. It allows the heat-pipe to be considered as multiple single phase regions rather than two phase regions. Two phase behavior is very difficult to model and, in fact, the wick-vapor interface adds a considerable amount of instability to the problem because of it's sensitivity to temperature and pressure.

3.3.5.1 Importance to System Behavior

This specific interface is very important to system behavior as it generates the momentum to drive flow, it allows energy to be carried isothermally, and it is the fundamental principle that

makes a heat-pipe work. That being said there are ways to avoid or improve on the poor stability of this component of the models. This part of the model effectively models the evaporation and condensation of the heat-pipe. Evaporation and condensation occur on very short time scales meaning near equilibrium models can be used to effectively capture the behavior. One of these conditions is fairly simple and is universal and this is conservation of mass flux at the interface. This means liquid flow into the interface equals the vapor flow out of the interface. This also works in the reverse direction and is just a conservation property. The second conditions has to do with how the flow is driven, mostly how does the temperature affect the evaporation flux. For this condition there is three general approaches to the solution to determine the mass flux from evaporation. The first and most detailed is the kinetic theory of gases relationship as was used in [48] and is represented by Equation 3.18.

$$\bar{\dot{m}} = \left(\frac{M}{4\pi R T^{int}}\right)^{1/2} (P_v^{equ} - P_v) \tag{3.18}$$

Where $\bar{\dot{m}}$ is the mass flux from evaporation, M is the molecular weight of the fluid, T^{int} is the interface temperature, P_v^{equ} is the equilibrium vapor pressure of the liquid at the interface temperature, and P_v is the vapor pressure of the vapor. So this equation really just represents a vapor pressure differential from the interface. There are other equations that often use an accommodation coefficient to account for evaporating gases that have extra repulsive or attractive forces in their liquid state. This gives very good results and is arguably the most accurate form to capture the phenomena. But in this state it contributes to numerical instabilities and difficulties with solution. If this equation is instead viewed as a vapor pressure differential then it is easy to jump to the most commonly used forms of the equation which is what is used in the full flow model presented later in this paper.

With it being a vapor pressure differential we can assume that the pressures correlate directly to temperatures and then this can be replaced with a temperature differential. The constants are different but the constants tend to be easier to understand in this form and that will become apparent. A temperature differential that correlates to mass flow tends to be in terms of power. So this

becomes a power balance across the interface that takes temperature gradients and mass fluxes. So this condition is represented in Equation 3.19.

$$h_{fg}\ \bar{\dot{m}}\ dA = -k\vec{\nabla}T\ \vec{n}\ dA \tag{3.19}$$

Where h_{fg} is the latent heat of evaporation, dA is the differential in area, and $\vec{n}$ is the normal to the surface. This states that the evaporated mass is equal to the heat across the differential area element. Now there is still a degree of freedom in the vapor that needs to be handled and this is the temperature of the vapor. To handle this the common approach is to say the vapor is saturated and then the pressure defines the temperature. Assigning this temperature to the interface will allow for closure and this approach works well. There is one last closure relation for models that does not solve the vapor and that effectively sets the temperature of the vapor in such a way that the net energy flow into the vapor is zero. This also works well and is the basis behind most conduction models especially for steady state. This was discussed prior but it was worth reiterating.

3.4 Heat-Pipe Models

A collection of papers from the foundation of heat-pipe modeling to the present are shown here. The strengths and weaknesses will be highlighted to give an idea of how they perform and what may be a good selection when looking to perform full multi-physics calculations with them. The boundary conditions will not be covered as they tend to be a simple continuity of flux and temperature but the interface between the liquid and the vapor will be discussed briefly as this is a major component in determining exact behavior of the heat-pipe. This interface condition can be as simple as a thermal continuity accounting for evaporation and condensation or as complex as a Volume of Fluid type approach to monitor the capillary radius to dynamically account for the changing capillary pressure. This second approach allows the model to directly limit the minimum and maximum capillary pressure generated and therefore allows for the determination of the capillary limit.

Author	Envelope Region	Wick Region	Core Region	LV Interface
[44]	Pseudo 2-D Conduction	Pseudo 2-D Conduction	Zero Resistance	Evaporator Coupled to Condenser
[49]	Transient 2-D Axisymmetric Conduction	Transient 2-D Axisymmetric Conduction	1D Quasi-Steady, Compressible	Kinetic Theory of Gases Mass Transfer Rate
[50]	1-D Axial Conduction	1-D Axial Conduction	Steady 2-D Axisymmetric and 2-D Cartesian	Simple heat flux balance with a latent energy term
[51]	Steady 2-D Axisymmetric Conduction	Steady 2-D Axisymmetric Conduction	Steady 2-D Axisymmetric Compressible	Simple heat flux balance with a latent energy term
[52]	Transient 2-D Axisymmetric Conduction	Transient 2-D Axisymmetric Conduction	Transient 2-D Axisymmetric Compressible	Energy Balance that satisfies mass flow rate with calculated saturation pressure

Author	Envelope Region	Wick Region	Core Region	LV Interface
[53]	Transient 2-D Axisymmetric Conduction	Transient 2-D Axisymmetric Conduction	Ignored	Energy Balance over whole interface must be 0
[54]	Transient 2-D Axisymmetric Conduction	Transient 2-D Axisymmetric Conduction	1-D, Area Averaged, Steady, Compressible, Vapor Flow	Kinetic Theory of Gases Mass Transfer Rate
[16]	Transient Lumped Conduction	Transient Lumped Conduction	Negligible Capacitance	Non-Existent
[55]	Transient Lumped Conduction	Transient Lumped Conduction	Negligible Capacitance	Non-Existent
[56]	Transient Lumped Conduction	Transient lumped with porous pressure losses	Transient Lumped with effective resistance, capacitance, and inductance derived for evaporator and condenser	A capillary pressure balance is performed at the evaporator

Author	Envelope Region	Wick Region	Core Region	LV Interface
[57]	Transient 2-D Axisymmetric Conduction	Transient 2-D Axisymmetric Conduction	Lumped Vapor Mass with Effective Heat Capacity	Simple Energy Balance
[58]	Transient 1-D Radial Conduction	Transient 1-D Radial Conduction	1-D Transient Compressible Flow	Heat Flux in the Wick is equal to the evaporation mass flux multiplied by the latent heat
[18]	Transient 2-D Conduction	Transient 2-D Incompressible Flow	Transient 2-D Compressible Flow	Full Energy Balance between convection, conduction, and evaporation
[19]	Transient 3-D Conduction	Transient 3-D Conduction	Transient Compressible Quasi 1-D Flow	Simple Energy Balance with latent energy term
[59]	Transient 2-D Conduction	Transient 2-D Incompressible Flow	Transient 1-D Compressible Flow	Simple Energy Balance with latent energy term
[60]	Steady 3-D Conduction	Steady 3-D Darcy Flow (Pressure Gradients determine Velocity)	Steady 1-D Flow	Energy balance over the vapor wick boundary

Author	Envelope Region	Wick Region	Core Region	LV Interface
[61]	Transient 2-D Axisymmetric Conduction	Transient 2-D Axisymmetric Darcy-Brinkman-Forchheimer Flow	Transient 2-D Compressible Flow with 1-D Rarefied gas corrections	Kinetic Theory of Gases Mass Transfer Rate with a radius of curvature to couple pressure
[62]	Not Analyzed	Steady 2-D Incompressible Flow with Porous Terms	Steady 2-D Incompressible Flow	Simple Energy Balance with latent energy term
[63]	Transient 2-D Solid Conduction	Transient 2-D Incompressible Porous Flow	Transient 2-D Compressible Flow with rarefied gas corrections	Simple Energy Balance with latent energy term
[64]	Steady 3-D Conduction	Steady 3-D Darcy Flow	Steady 3-D Compressible Vapor Flow	Simple Energy Balance with latent energy term
[17]	Transient 2-D Conduction	Transient 2-D Incompressible Flow	Quasi-steady 1-D Compressible Flow	Simple Energy Balance with capillary relationship for pressure coupling
[46]	Transient 1-D Conduction with radial coupling terms	Transient 1-D Porous Flow with radial coupling terms	Transient 1-D Compressible Flow with radial coupling terms	Kinetic Theory of Gases Mass Transfer Rate

3.5 Performance and Capabilities

The tables presented do not represent all the work done but show a plurality of approaches to modeling and simulating heat-pipes for design and analyses purposes. These models should help with formulating models in the future for fast, and accurate simulation of heat-pipes in large systems such as nuclear power plants. To do this, the performance and capabilities of each model class is reviewed as well as the information attainable from the simulation. This is an important aspect as only certain models can give information about characteristic limits such as sonic limiting effects or capillary limiting effects. It is important to note that complex two-phase flow phenomena like entrainment or boiling have not been captured in any heat-pipe modeling efforts. This phenomena may be possible to capture through Volume of Fluid modeling but the mesh resolution may become prohibitive. Lagrangian methods may also allow this but it is common that these fall back on empirical correlations to obtain droplet size and entrainment rate from the interfacial sheer stress or the Weber number. Boiling phenomena is studied extensively for light water reactors. The same processes and standards could be applied to reactor heat-pipes to ensure nucleate boiling heat fluxes are not exceeded. Any nucleation is going to harm heat-pipe performance and rather than avoiding film boiling, it is desirable to avoid nucleation.

To better describe the performance and capabilities of these models they will be divided in to several classes of models. These classes range from simple for use in design and optimization studies to complicated full flow analyses for determination of true operational limits and exact behavior in transient analyses. With faster computing resources becoming available complicated analyses can be used more readily in optimization studies but computational time could still be prohibitive. The classes of models analyzed are lumped capacitance, no flow or conduction only, wick conduction, ignored vapor, and full flow analyses.

3.5.1 Lumped Capacitance Models

Lumped capacitance models are some of the simplest models defined and usually have their basis in conduction approaches. These models define control volumes in the domain of interest with

associated variables. When it comes to heat-pipes though, a single control volume can represent the entire domain. this is useful analytically but more domains can increase accuracy and reveal more information about the behavior of the system. Then transfer functions are created that couple control volumes in a physically realistic way. This can be a network analyses such as in [44], or a true lumped model with fluidic accounting such as in [56]. For design purposes these models can be very effective in determining operational behavior quickly and help to make informed design decisions. Even for transient behavior these models can yield descent results.

These models solve very quickly and can be easily generalized to different geometries. Sonic limits can be obtained using compressible flow behavior within the lumps and between the lumps. All limits are approximate and conservative and serve as good upper bounds to operational performance. The same is with capillary limits when coupling the vapor and liquid lumps a capillary jump relationship can be defined using a radius of curvature. Surface curvature is always present in two phase flow and is a result of pressure differences and surface free energy in the respective fluids. The surface tension of the liquid creates this curvature and an approximation for analysis is to assume that this curvature is spherical in nature. That spherical curvature can be fully defined through an effective radius.

Lumped capacitance models are good choices for design studies and potentially optimization procedures because of their quick, simple, and robust solution schemes. The accuracy is not as great as more complicated models but it is enough for rough design. They can give information, in an approximate manner, for even sonic and capillary limits. But for exact operational and transient information these do not compare to the more complicated models.

3.5.2 Conduction Only Models

These models are the next step up in complexity from lumped capacitance models. Conduction only models are a resistance network type model. Effective resistances and capacitance's can be defined for the wick, wall, and vapor coupled at the interfaces to describe the system in both transient and steady state. In the extreme this is simply a lumped model but if the geometry is meshed a high resolution solution can be obtained for the whole domain as an approximate temperature

solution. Essentially solving the heat equation with effective properties where it matters.

The heat equation is simple to solve numerically and many methods have been created to do so. These methods perform very well and can give accurate temperature distributions for the whole domain. The problems arise when the wick flow is high. With high liquid flow, convection can become important in the solution process. This will change the shape of the temperature solution in the wick. This is essentially a change in the effective thermal conductivity of the wick in a non-isotropic way as well as a change in the heat-capacity of the wick. If the liquid flow is low, this will give accurate results.

From these simulations approximate information can be determined about the pressure drop in the system and the flow profiles in the system. Using the temperature gradient at the wick vapor interface as an evaporation or condensation source the vapor profile can be approximately determined at every time step or at steady state. The capillary limit can be determined in a similar fashion. With various relationships the radius of curvature at each location can be determined as well as the flow rate in the wick and corresponding pressure drop.

Conduction models are extremely useful if applied correctly and proper care is taken in the analysis including analysis of the Biot number of the wick. They are fast and robust with many available tools for solving them. If proper care is not taken, they can mislead designers in their results.

3.5.3 Wick Conduction Models

Wick conduction models take conduction models one step further by assuming that there is still vapor flow. With this, sonic limitations can be directly determined from the simulations. These models still run into accuracy issues at high liquid flow rate but they gain the advantage of being able to directly determine sonic limitations in the heat-pipe with information from that being fed back into the simulation online. Fortunately, the sonic limit is only encountered at low temperatures or during startup making the model accurate in this regime. Analyzing Biot number will still be necessary and the ability to determine capillary limits can be done after simulation in a post processing situation.

These models can still be very quick but adding flow into the analysis will drastically reduce the computational speed in most cases. This is especially true with low density gas flow where low heat loads can lead to sonic velocities in the geometry. What is useful is that it is generally laminar flow eliminating the need for turbulence modeling. In some cases it is also not a bad assumption to assume inviscid or 1-D flow as the pressure drop in the vapor is very small compared to the wick pressure drop. Another common assumption is steady state as the vapor response time is orders of magnitude shorter than the wick and wall. This will allow the simulation to retain some of the speed benefits to the simpler conduction models.

Like conduction models these models are fast and robust and again proper analysis of Biot will lead to good results. The added vapor region directly incorporates the sonic limit into the calculations and allows for online information about how it is encountered. These models are also going to take slightly longer to calculate and with a true transient formulation the vapor region will drastically limit computational speed.

3.5.4 Ignored Vapor Models

Ignored vapor models are models that simply do not consider most of the physics of the vapor during calculations. These models assume the vapor is either a lump and couple it to all the wick faces or it is assumed that the wick face temperature is equal to the average of all the wick faces ignoring it entirely. This is because the vapor is computationally expensive compared to simulating anything else in the system. The wick is low velocity, incompressible flow where the vapor is high velocity, compressible flow. By ignoring the vapor, transient simulation can occur much more rapidly.

These models are fast and very robust because the behavior of incompressible flow is heavily studied at this point and has been simulated. Including the laminar behavior improves the stability of the solution methods. There are drawbacks, however, the sonic limit is once again only able to be recovered in post-processing and does not provide feedback to the simulation. Models like this will give accurate temperature profiles in any operational situation that does not contain sonic limited operation. If shocks appear this will further harm accuracy. With appropriate boundary

conditions online determination of the capillary limit can be obtained. A properly designed heat-pipe will not be sonic-limited during normal operation. This model would be appropriate to use in those situations. Standard operational behavior should not be sonic limited and as a result this will be a good model for that purpose.

Models like this, as long as flow is captured in the wick, will have higher computational costs than similar conduction models but give the advantage of capturing the convective behavior in heat-pipes that leads to inaccuracies in conduction models. At the same time the wick pressure drop can be determined and possibly the capillary limit of the heat-pipe. These models are also robust but the computational speed can become a factor, especially with large systems of heat-pipes.

3.5.5 Full Flow Models

Full flow models are the most complex a heat-pipe simulation can get with continuum mechanics. The wicks flow is modeled as well as the compressible vapor flow. It will give the most accurate solutions as far as temperature profile and the sonic limit will be determined online while providing feedback to the simulation. You cannot obtain info about the capillary limit without appropriate boundary conditions but there are several models that have been analyzed that do provide this inherently.

These models will provide the most accurate results, with information on the sonic limit and capillary limit. Without adding Volume of Fluid capabilities, then entrainment behavior cannot be determined and neither can the boiling limits. This is the most computationally expensive model because the vapor is severely limited by CFL. CFL being the Courant–Friedrichs–Lewy condition which is a useful measure for stability in advective simulations. In an explicit formulation a CFL condition greater than 1 will lead to instability in the simulation. With implicit formulations you can achieve higher CFL conditions due to the reduce sensitivity but the flow velocity in the vapor can reach velocities several orders of magnitude larger than in the wick. With clever simulation procedure the vapor region can be simulated on a different time step size than the wick and wall regions. It is possible to assume steady vapor flow to reduce computation time, but in some geometries and meshes, steady solutions take longer to converge than transient time steppers.

These models would be very useful in accident analysis as the accuracy is good and there is an inherent feedback on sonic and capillary limits. These limits will likely be those encountered in an accident progression and will give the most information. Accident analysis is usually not performed until a design is complete therefore, rapid analysis of various geometries is not required and a long detailed analysis will be the most informative. This does not mean these are the only types of models that can be used for accident analysis but the slow computational speed of these models limit their use to analysis of existing designs.

A comparison of lumped capacitance, conduction based, and full flow methodologies is shown in Figure 3.6. The heat-pipe geometry used was taken from the experimental setup of [65, 66]. The heat transfer coefficient between the cooling water and the heat-pipe was assumed to be near infinite. Ignored vapor was not shown because it would have been redundant to the full flow model for the heat pipe analyzed. The physical description of this simulation is described in Table 3.1

The sink temperature was in the form of an ODE so an accurate average Coolant flow temperature could be determined. The form can be seen in Equation 3.20

$$\frac{d\bar{T}}{dt} = \frac{Q}{2mC_p} + \frac{\dot{m}}{m}(T_{in} - \bar{T}) \tag{3.20}$$

Where $\bar{T}$ is the average coolant temperature, m is the coolant mass in the cooling volume of the flow loop, $\dot{m}$ is the flow rate through the coolant loop, Q is the rejected power calculate from the integral of the heat flux over the area of the condenser region, C_p is the heat capacity for the water, and T_{in} is the inlet cooling temperature. All temperatures were initialized at the same temperature specified in the following table.

The simulation is similar to the experiment presented in [65, 66] except the heat transfer coefficient was not the same due to the ODE nature of the boundary condition. The validity of the models used have been compared to experiments in prior papers and the accuracy has been demonstrated as long as the boundary conditions are accurate. The goal of this test was to demonstrate the similarities of the models on the same problem as well as discuss the weaknesses of the various classes of models.

Table 3.1: Description of Simulations

Evaporator Length	393 mm
Adiabatic Length	37 mm
Condenser Length	170 mm
Outer Radius	9.55 mm
Envelope Thickness	0.9 mm
Wick Thickness	0.3 mm
Working Fluid	Water
Ultimate Sink Type	Water Cooled
Ultimate Sink Temperature	Equation 3.20
Heat Transfer Coefficient to Ultimate Sink	1,000,000 $\frac{W}{m^2-K}$
Power Input	575 W
Cooling Loop Working Fluid	Water
Cooling Loop Length	170 mm
Cooling Loop Volume	0.0188 kg
Cooling Loop Flow Rate	0.0024 $\frac{kg}{s}$
Cooling Loop Inlet Temperature	295 K
Insulation Effective Mass	0.716 kg
Insulation Effective Specific Heat	838 $\frac{kJ}{kg-K}$
Initial Temperatures	295 K

In this analysis the lumped capacitance model was based on [16] and the calculation completed almost instantly for the full transient. Temperature was assumed to be the vapor temperature and as such the resistance between the cooling water and the vapor was calculated based on the thermal resistance of cylindrical annulus. The two regions were wick and wall region. The capacitance of the system was calculated from the wall, the wick material, and the insulation used in the experiment. The conduction model was the next fastest computed model as it was only solving the heat equation. The slowest was the full flow model as it was solving several non-linear equations simultaneously. The full flow model was a transient conduction model in the wall, with a transient flow model in the wick, and a steady state 3D flow model in the vapor region. The full flow model involved solving the equations with OpenFOAM. For the wall Equation 3.6 was solved, for the wick regions Equation 3.12, Equation 3.13, and Equation 3.14 were solved, and for the vapor Equation 3.15, Equation 3.16, and Equation 3.17 were solved simultaneously without a transient

term. The wall wick interface were coupled with an equal temperature and heat-flux condition. The interface condition between the wick and the vapor assumed the heat-flux out of the wick and into the vapor translated to the evaporation rate similar to Equation 3.19. This completed the model used and it led to results similar to the other models despite having substantially more detail. This can be seen in Figure 3.6 very clearly.

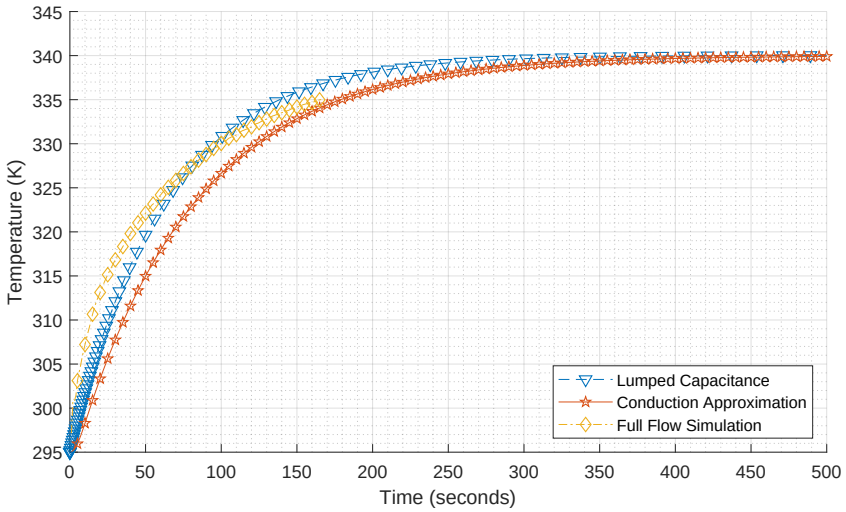

Figure 3.6: Comparison of the behavior of various heat pipe models on the vapor temperature

This figure demonstrates several concepts. First, all the models show very similar transient behavior. This is important because it shows that very simple fast solving models can be very robust and accurate as long as accurate properties are used. But there are subtle differences that outside of design conditions could be important. The first is that the lumped model had a steeper transient initially than the conduction model. This is likely caused by the assumption that the whole geometry is at the same temperature so information is passed a little faster. The second difference is that the shape of the full flow simulation is slightly different. The temperature starts out changing faster before eventually slowing down to a slower rate than the other two models. The only explanation for this is that the fluid motion in the wick causes a preferential heat flow into the vapor. Once this is established the heat can then transfer from the vapor into various parts of the wick. This leads to a smaller than expected thermal capacitance initially that grows as the vapor heats up and gains the ability to heat the wick along its full length. The Full Flow simulation ran slowly and as a result only 165 seconds are presented.

3.5.6 Potential Approaches to Heat-Pipe modeling in the future

With Multi-Physics modeling becoming popular, the desire to get results quickly at low costs remains a priority. These simulations can take days to run even with reduced order models and large assumptions in the behavior of the system. Some multi-physics models involve changing the model used when it becomes inaccurate. In this scheme you would always use the model that is the least computationally expensive without sacrificing accuracy.

With these several classes of models covered potential approaches and uses become apparent to ensure efficient design and simulation techniques. This means that full flow models are only used when there is large uncertainty in the operational performance of a design. This can be in the early stages of transients or when expected operation is very near to predicted characteristic limits. When operating away from the characteristic limits, ignored vapor or conduction based models can be used depending on the flow conditions in the wick. There is nothing preventing these models from being activated when the uncertainty in the current regime is high. Flow can be approximated in conduction models so if conduction models are turned off and full flow is turned on those predicted profiles can easily be used.

These types of approaches can be used to ensure that operational performance is near the heat-pipes peak capability. This will also ensure that heat-pipes designed outside of the traditional cylindrical or planar configurations can be analyzed efficiently and quickly. Typical heat-pipe systems don't contain hundred or even thousands of heat-pipes operating in different configurations like the next generation nuclear plants are expected to. In a multi-physics environment where densities and concentrations are important to the coupled physics, like neutronics, understanding the temperature and density distribution is critical not only to safety, like in accident scenarios, but also in ensuring the plant is operating at or near its peak performance.

3.6 Conclusions

A review of various heat-pipe models and the over arching classes of heat-pipe models that exist were conducted. The advantages and disadvantages were discussed as well as some of the

motivating engineering that was occurring in the periods they were developed. A numerical test was performed comparing the models and how they perform in terms of accuracy. The similar results indicated that the additional model detail and captured physics changed the solution in a significant way. This is apparent when looking at the underlying models of the numerical test. In the last section an approach is recommended to perform accurate heat-pipe models in multi-physics simulations or even high-fidelity standalone simulations at minimal computational cost. This recommendation accounts for a more efficient approach to gain the required information but also reduce the computational time used. It would be ideal to use a minimal amount of work to obtain the best results.

When formulating complex coupled and uncoupled models it is important to understand the underlying physics of the components and what behaviors are dominant. As engineers it is always a goal to get the best performance with the least effort. In simulation space this comes to the accuracy of the information that is attained and the computational effort expended to get that information. With the review work performed researchers now gain a resource to determine the needed modeling effort to simulate specific operating conditions for heat-pipes. It allows the needed information to be gained while knowing the trade offs in accuracy that is being made when making simplifying assumptions to the modeling effort. This review work allowed an advanced model to be made directly for this research effort.

Bibliography

[1] Heng Tang, Yong Tang, Zhenping Wan, Jie Li, Wei Yuan, Longsheng Lu, Yong Li, and Kairui Tang. Review of applications and developments of ultra-thin micro heat pipes for electronic cooling, aug 2018. ISSN 03062619.

[2] Hassam Nasarullah Chaudhry, Ben Richard Hughes, and Saud Abdul Ghani. A review of heat pipe systems for heat recovery and renewable energy applications, may 2012. ISSN 13640321.

[3] D. A. Reay. The Perkins Tube-a noteworthy contribution to heat exchanger technology. *Journal of Heat Recovery Systems*, 2(2):173–187, 1982. ISSN 01987593. doi: 10.1016/0198-7593(82)90045-5.

[4] Gaugler Richard S. Heat Transfer Device, 1944. URL `https://lens.org/039-405-146-456-723`.

[5] Grover George M. Evaporation-condensation Heat Transfer Device, 1966. URL `https://lens.org/137-356-119-991-880`.

[6] G. M. Grover, T. P. Cotter, and G. F. Erickson. Structures of Very High Thermal Conductance. *Journal of Applied Physics*, 35(6):1990–1991, jun 1964. ISSN 0021-8979. doi: 10.1063/1.1713792. URL `http://aip.scitation.org/doi/10.1063/1.1713792`.

[7] Grover George M, Busse Claus A, and Josef Bohdansky. Nuclear Reactor With Thermionic Converter, 1967. URL `https://lens.org/070-424-404-776-402`.

[8] Peter Fiebelmann. Nuclear Reactor, 1968. URL `https://lens.org/114-677-671-705-043`.

[9] VE Hampel and RP Koopman. REACTIVITY SELF-CONTROL ON POWER AND TEMPERATURE IN REACTORS COOLED BY HEATPIPES. *Transaction of the American Nuclear Society*, 1968. URL `https://www.osti.gov/biblio/4813461`.

[10] Monte Bryce Parker. *Applications of heat pipes to nuclear reactor engineering*. PhD thesis, Iowa State University, 1970. URL https://lib.dr.iastate.edu/cgi/viewcontent.cgi?article=5258{&}context=rtd.

[11] G Niederauer, E Lantz, and R Breitweiser. Split-core heat-pipe reactors for out-of-pile thermionic power systems. *N/A*, 1971.

[12] Daniel R Koenig, William A Ranken, and Ernest W Salmij. Heat-Pipe Reactors for Space Power Applications. *J. ENERGY*, 1(4), 1977. doi: 10.2514/3.62334. URL http://arc.aiaa.org.

[13] Eugene V Pawlik and Wayne M Phillipsf. A Nuclear Electric Propulsion Vehicle for Planetary Exploration. *J. SPACECRAFT*, 14(9), 1977. doi: 10.2514/3.57233. URL http://arc.aiaa.org.

[14] James W Sterbentz, James E Werner, Andrew J Hummel, John C Kennedy, Robert C O'Brien, Axel M Dion, Richard N Wright, and Krishnan P Ananth. Preliminary assessment of two alternative core design concepts for the special purpose reactor. Technical report, Idaho National Lab.(INL), Idaho Falls, ID (United States), 2017.

[15] Mohamed S. El-Genk and Huang Lianmin. An experimental investigation of the transient response of a water heat pipe. *International Journal of Heat and Mass Transfer*, 36(15):3823–3830, oct 1993. ISSN 0017-9310. doi: 10.1016/0017-9310(93)90062-B. URL https://www.sciencedirect.com/science/article/pii/001793109390062B.

[16] Amir Faghri and Charles Harley. Transient lumped heat pipe analyses. *Heat Recovery Systems and CHP*, 14(4):351–363, 1994.

[17] Jong T Seo and Mohamed S El-Genk. A transient model for liquid metal heat pipes. In *Transactions of the 5th Symposium on Space Nuclear Power Systems*, pages 114–119, 1988.

[18] Yiding Cao and Amir Faghri. Transient two-dimensional compressible analysis for high-temperature heat pipes with pulsed heat input. *Numerical Heat Transfer*, 18(4):483–502, 1991.

[19] Y Cao and A Faghri. Transient multidimensional analysis of nonconventional heat pipes with uniform and nonuniform heat distributions. *Journal of Heat Transfer*, 1991.

[20] VC Truscello. SP-100, the US Space Nuclear Reactor Power Program. Technical information report. Technical report, JPL, 1983. URL https://www.osti.gov/biblio/10184691.

[21] Hampel Viktor E. Underground Nuclear Power Station Using Self-regulating Heat-pipe Controlled Reactors, 1989. URL https://lens.org/065-065-553-054-275.

[22] Huebotter Paul R and Mclennan George A. Fast Reactor Power Plant Design Having Heat Pipe Heat Exchanger, 1985. URL https://lens.org/088-538-890-111-13X.

[23] Lester L Begg, Thomas j. Wuchte, and William D Otting. Star-C thermionic space nuclear power system. *AIP Conference Proceedings*, 246(1):114–119, 1992. doi: 10.1063/1.41774. URL https://aip.scitation.org/doi/abs/10.1063/1.41774.

[24] W.A. Ranken and J.A. Turner. Design studies of the moderated thermonic heat pipe reactor (mohtr) concept. *N/a*, 1 1991.

[25] W.A. Ranken and M.G. Houts. Heat pipe cooled reactors for multi-kilowatt space power supplies. *N/a*, 1 1995.

[26] Mohamed S El-Genk, Nicholas J Morley, and Albert Juhasz. Pellet bed reactor concept for nuclear electric propulsion. *AIP Conference Proceedings*, 271(2):631–639, 1993. doi: 10.1063/1.43209. URL https://aip.scitation.org/doi/abs/10.1063/1.43209.

[27] Si-Hwan Kim, Keung Koo Kim, Ji Won Yeo, Moon Hee Chang, and Sung Quun Zee. Design Verification Program of SMART. Technical report, Korea Atomic Energy Research Institute, 2003. URL https://www.ipen.br/biblioteca/cd/genes4/2003/papers/1047-final.pdf.

[28] Hussam Jouhara, Vladimir Anastasov, and Ibrahim Khamis. Potential of heat pipe technology in nuclear seawater desalination. *Desalination*, 249(3):1055–1061, 2009. ISSN 0011-9164. doi: https://doi.org/10.1016/j.desal.2009.05.019. URL http://www.sciencedirect.com/science/article/pii/S0011916409009540.

[29] DI Poston. Nuclear Design of the SAFE-400a Space Fission Reactor. *ANS Conference Proceedings*, 2002. URL https://inis.iaea.org/search/search.aspx?orig{_}q=RN:40044672.

[30] Ehud Greenspan. Solid-core heat-pipe nuclear battery type reactor. Technical report, University of California, 2008.

[31] David I Poston, Marc Gibson, Patrick McClure, Thomas Godfroy, and Rene Sanchez. Results of the krusty nuclear system test. *NETS-2019, ANS*, 67:1–7, 2019.

[32] A Levinsky, JJ van Wyk, Y Arafat, and MC Smith. Westinghouse eVinciTM Reactor for Off-Grid Markets, 2018. URL http://answinter.org/wp-content/2018/data/pdfs/404-26706.pdf.

[33] PR Mcclure. Special Purpose Reactors. *OSTI*, 2019. URL https://www.osti.gov/servlets/purl/1529523.

[34] B.H. Yan, C. Wang, and L.G. Li. The technology of micro heat pipe cooled reactor: A review. *Annals of Nuclear Energy*, 135:106948, jan 2020. ISSN 0306-4549. doi: 10.1016/J.ANUCENE.2019.106948. URL https://www.sciencedirect.com/science/article/pii/S0306454919304359{#}f0070.

[35] DQ Wang, BH Yan, and JY Chen. The opportunities and challenges of micro heat piped cooled reactor system with high efficiency energy conversion units. *Annals of Nuclear Energy*, 149:107808, 2020.

[36] Leonard M Poplaski, Steven P Benn, and Amir Faghri. Thermal performance of heat pipes using nanofluids. *International Journal of Heat and Mass Transfer*, 107:358–371, 2017. ISSN 0017-9310. doi: https://doi.org/10.1016/j.ijheatmasstransfer.2016.10.111. URL http://www.sciencedirect.com/science/article/pii/S0017931016315204.

[37] Jung Chang Wang, Rong Tsu Wang, Tien Li Chang, and Daw Shang Hwang. Development of 30Watt high-power LEDs vapor chamber-based plate. *International Journal of Heat and Mass Transfer*, 53(19-20):3990–4001, sep 2010. ISSN 00179310. doi: 10.1016/j.ijheatmasstransfer.2010.05.018.

[38] Cole Mueller and Pavel Tsvetkov. Novel design integration for advanced nuclear heat-pipe systems. *Annals of Nuclear Energy*, 141:107324, jun 2020. ISSN 0306-4549. doi: 10.1016/J.ANUCENE.2020.107324. URL https://www.sciencedirect.com/science/article/pii/S0306454920300220?dgcid=author.

[39] Patrik Nemec, Alexander Čaja, and Milan Malcho. Mathematical model for heat transfer limitations of heat pipe. *Mathematical and Computer Modelling*, 57(1-2):126–136, jan 2013. ISSN 0895-7177. doi: 10.1016/J.MCM.2011.06.047. URL https://www.sciencedirect.com/science/article/pii/S0895717711003888.

[40] How Does the Wick and Orientation of a Heat Pipe Affect its Performance? | Advanced Thermal Solutions, 2015. URL https://www.qats.com/cms/2015/03/11/how-does-the-wick-and-orientation-of-a-heat-pipe-affect-its-performance

[41] Advanced Cooling Technologies. Pchps for precise temperature control, 2020. URL https://www.1-act.com/resources/

heat-pipe-fundamentals/different-types-of-heat-pipes/pchps-for-precise-temperature-control/.

[42] Amir Faghri. Review and advances in heat pipe science and technology. *Journal of heat transfer*, 134(12), 2012.

[43] Hamidreza Shabgard, Michael J Allen, Nourouddin Sharifi, Steven P Benn, Amir Faghri, and Theodore L Bergman. Heat pipe heat exchangers and heat sinks: Opportunities, challenges, applications, analysis, and state of the art. *International Journal of Heat and Mass Transfer*, 89:138–158, 2015.

[44] Z.J. Zuo and A. Faghri. A network thermodynamic analysis of the heat pipe. *International Journal of Heat and Mass Transfer*, 41(11):1473–1484, jun 1998. ISSN 0017-9310. doi: 10.1016/S0017-9310(97)00220-2. URL https://www.sciencedirect.com/science/article/pii/S0017931097002202.

[45] Jean-Michel Tournier and Mohamed El-Genk. Current capabilities of "hptam" for modeling high-temperature heat pipes' startup from a frozen state. In *AIP Conference Proceedings*, volume 608, pages 139–147. AIP, 2002.

[46] Michael L. Hall and Joseph M. Doster. Transient thermohydraulic heat pipe modeling. In *Space Nuclear Power Systems*, pages 407–410, January 1987.

[47] Michael L Hall. Transient Thermohydraulic Heat Pipe Modeling: Incorporating throhput into the caesar Environment ARTICLES YOU MAY BE INTERESTED IN. *AIP Conference Proceedings*, 654:106, feb 2003. doi: 10.1063/1.1541284. URL https://doi.org/10.1063/1.1541284.

[48] Jean-Michel Tournier and Mohamed El-Genk. "hptam" heat-pipe transient analysis model: an analysis of water heat pipes. *AIP Conference Proceedings*, 246:1023–1037, 01 1992.

[49] Chenglong Wang, Jing Chen, Suizheng Qiu, Wenxi Tian, Dalin Zhang, and GH Su. Performance analysis of heat pipe radiator unit for space nuclear power reactor. *Annals of Nuclear Energy*, 103:74–84, 2017.

[50] N Zhu and K Vafai. Analytical modeling of the startup characteristics of asymmetrical flat-plate and diskshaped heat pipes. *International Journal of Heat and Mass Transfer*, 41(17): 2619–2637, 1998.

[51] Ming-Ming Chen and Amir Faghri. An analysis of the vapor flow and the heat conduction through the liquid-wick and pipe wall in a heat pipe with single or multiple heat sources. *International journal of heat and mass transfer*, 33(9):1945–1955, 1990.

[52] C Harley and A Faghri. Transient two-dimensional gas-loaded heat pipe analysis. *Journal of Heat Transfer*, 1994.

[53] PR Mistry, FM Thakkar, S De, and S DasGupta. Experimental validation of a two-dimensional model of the transient and steady-state characteristics of a wicked heat pipe. *Experimental heat transfer*, 23(4):333–348, 2010.

[54] Chenglong Wang, Dalin Zhang, Suizheng Qiu, Wenxi Tian, Yingwei Wu, and Guanghui Su. Study on the characteristics of the sodium heat pipe in passive residual heat removal system of molten salt reactor. *Nuclear Engineering and Design*, 265:691–700, 2013.

[55] B Rashidian, M Amidpour, and MR Jafari Nasr. Modeling the transient response of the thermosyphon heat pipes. In *Proceedings of the World Congress on Engineering*, volume 2, pages 2–4, 2008.

[56] C. Ferrandi, F. Iorizzo, M. Mameli, S. Zinna, and M. Marengo. Lumped parameter model of sintered heat pipe: Transient numerical analysis and validation. *Applied Thermal Engineering*, 50(1):1280–1290, jan 2013. ISSN 1359-4311. doi: 10.1016/J.APPLTHERMALENG.2012.07.022. URL `https://www.sciencedirect.com/science/article/pii/S1359431112005042`.

[57] Won Soon Chang and Gene T Colwell. Mathematical modeling of the transient operating characteristics of a low-temperature heat pipe. *Numerical Heat Transfer*, 8(2):169–186, 1985.

[58] Jerry Bowman and RICHARD SWEETEN. Numerical heat-pipe modeling. In *24th Thermophysics Conference*, page 1705, 1989.

[59] Frederick A Costello, Allen F Montague, and Michael A Merrigan. Detailed transient model of a liquid-metal heat pipe. Technical report, Costello (FA), Inc., Herndon, VA (USA); Los Alamos National Lab., NM (USA ..., 1986.

[60] Ji Li and GP Peterson. 3d heat transfer analysis in a loop heat pipe evaporator with a fully saturated wick. *International Journal of Heat and Mass Transfer*, 54(1-3):564–574, 2011.

[61] Jean-Michel Tournier and Mohamed S El-Genk. Hptam, a two-dimensional heat pipe transient analysis model, including the startup from a frozen state. Master's thesis, The University of New Mexico, 1995.

[62] KAMAL AR'ISMAIL, MAURICIO ARAUJO ZANARDI, and CHANG YU LIU. Two dimensional analysis of flow and heat transfer in a porous heat pipe. *6th International Heat Pipe Conference Proceedings*, 1986.

[63] JH Jang, A Faghri, WS Chang, and ET Mahefkey. Mathematical modeling and analysis of heat pipe start-up from the frozen state. *Journal of Heat Transfer*, 1990.

[64] Yeong Shin Jeong, Kyung Mo Kim, In Guk Kim, and In Cheol Bang. Hybrid heat pipe based passive in-core cooling system for advanced nuclear power plant. *Applied Thermal Engineering*, 90:609–618, 2015.

[65] Lianmin Huang and Mohamed S El-Genk. Experimental investigation of transient operation of a water heat pipe. In *AIP Conference Proceedings*, volume 271, pages 365–374. American Institute of Physics, 1993.

[66] Mohamed S. El-Genk and Huang Lianmin. An experimental investigation of the transient response of a water heat pipe. *International Journal of Heat and Mass Transfer*, 36 (15):3823 – 3830, 1993. ISSN 0017-9310. doi: https://doi.org/10.1016/0017-9310(93)90062-B. URL http://www.sciencedirect.com/science/article/pii/001793109390062B.

4. A NETWORK APPROACH TO FULL CORE TEMPERATURE ANALYSIS IN ADVANCED NUCLEAR HEAT-PIPE SYSTEMS

4.1 Overview

Advanced heat-pipe systems are becoming more popular for micro-grid applications globally. With this increase in interest, methods for rapid analysis of the system are necessary for quick design iterations. The method proposed is bench marked against an OpenFOAM conduction approximation for two reactor like geometries. One geometry is a more traditional approach and the other geometry is a novel approach. The method is designed to rapidly attain heat-pipe power throughput to compare with characteristic limits of the heat-pipe design. For the traditional geometry the predicted peak temperatures were within 7% of the OpenFOAM solutions and the novel geometry is within 1% of the OpenFOAM solution giving high confidence that this can be used to rapidly evaluate and analyze new core geometries.

4.2 Introduction

As heat-pipes become a common design element of modern nuclear reactors the need for modern modeling a simulation techniques becomes more important. There is also a need to rapidly evaluate designs to ensure near optimal behavior is achieved. To adequately evaluate the performance of the design, the analysis method needs to be accurate, robust, and easily handle various design configurations. This paper develops a network approach to determine approximate full core steady state temperatures and heat-pipe rejection loads.

4.2.1 Heat-Pipe Operation

A heat-pipe is a two-phase wicked heat-transport device. It operates in a manner similar to most thermosyphons except it uses a capillary structure, or wick, to generate the primary pressure head. Because phase change is the primary method of heat transport the heat is moved in an isothermal

[0]Reprinted with permission from "A network approach to full core temperature analysis in advanced nuclear heat-pipe systems" by Cole Mueller and Pavel V. Tsvetkov, 2021. Annals of Nuclear Energy, Volume 160, Copyright 2021 by Annals of Nuclear Energy

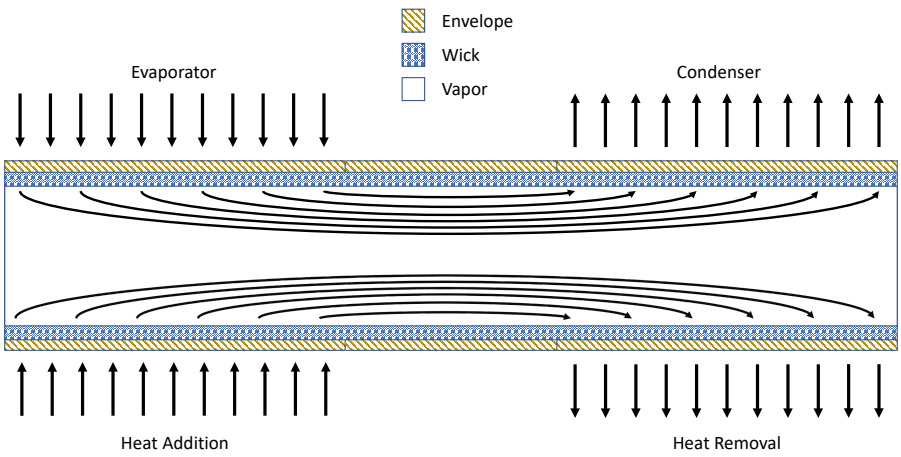

Figure 4.1: A basic illustration of a heat-pipe

condition. This property gives them very high effective thermal conductivity's.

There are three pieces to a traditional heat-pipe that are necessary to generate the required performance. The vapor region, the wicking structure, and the envelope structure. The vapor region is a continuous space that allows vapor to occupy and flow through it. It allows heat to be transported from the evaporator section to the condenser section easily. The wick can be considered a flow return path for the working fluid. Once the fluid condenses it must return to the evaporator so the cycle can continue. It also generates the head pressure required to induce flow based on capillary behavior in the wick. The envelope maintains the desired separation from the environment. The designed fill gas over pressure is something that must be maintained to ensure heat transport occurs as the designers intended. There can be no fill gas, a vacuum, as in a standard representation, or there can be a slight over pressure as is seen in variable conductance heat-pipes. A simple heat pipe representation can be seen in Figure 4.1.

Given the high effective conductivity a natural assumption for modeling purposes is a perfect conductor. This is very useful but does not hold always. Because a heat-pipe is primarily driven by flow there are flow limiting behaviors that must be accounted for when using simplified models for a heat-pipe. The common limits are capillary limit, sonic limit, boiling limit, and entrainment limit. Each limits the operation in a different way and needs to be considered when making conductive

assumptions.

Much research has been performed investigating various working fluids and structure combinations to ensure the product does not become compromised from adverse behavior between them. This research has been continuously carried out to determine reliability of the products and to create rejection sampling procedures to catch defective products before shipment. This research will be continued as nuclear reactors begin to be constructed with heat-pipe components.

4.2.2 Prior Work

There are many methods and software's out there for analyzing single heat-pipes but there are limited examples of analysis of large systems. This method employs a network type structure where node values at key points are evaluated and then for an extra step are unfolded into a 3D evaluation in an attempt to regain some spatial accuracy. There are many examples of a network type analysis being performed on heat-pipes such as [1] where a single heat-pipe is reduced to a network of blocks and transient analysis is performed. This approach can be described as a method of lines type analysis where the spatial discretization is performed and the transient term is left as is. Then the resulting system of first order equations are solved with the tool of choice. A lumped capacitance approach is very similar and sometimes indistinguishable and an example of that can be seen in [2] where a detailed fluidic model is added to ensure convective transport is at least partially captured. But these approaches are only for analyzing single heat-pipes. There are many more heat-pipe models but the network approach to singular heat-pipes is useful and well established.

With micro modular reactors becoming more popular and heat-pipe cooling being a popular choice for them the number of methods addressing the interaction between heat-pipes is growing. From direct multi-physics coupling of the singular heat-pipe models to large systems level analysis they are being explored and used to get results quickly. Especially with the access to HPC resources these extremely large models become more common. [3, 4] developed tools for full core reactor analysis including temperature solutions. A more primitive approach involves setting heat-pipe vapor temperatures to a constant predetermined value such as in [5]. This will give valuable

information but is not recommended because the core power profile will cause different heat-pipe loading's and as a result different temperatures.

4.2.3 Motivations

The motivation for this method are specifically for these scoping studies and parametric analysis. Rapid design iterations are necessary and exact accuracy is generally not needed when getting to a good base or point design. If true multivariate optimization is desired then speed of evaluation is very important to get to converged solutions. Accuracy isn't ignored but approximate solutions are preferred if they can gain substantial speed ups. A caveat to this is if the behavior relative to the true solution is predictable. In more precise terms does the provide a bound on the true solution or is it random to the true solution. A fast approximate solution will be more desirable if it always over estimates the true solutions compared with if it was an over estimate in certain cases but an under estimate in others.

This method is an approximate solution that requires fractions of the computational time of the high fidelity simulations delivered by tools like OpenFOAM. There are other reasons methods like this may be useful and it could act as an initial guess to higher fidelity simulations thus reducing the number of iterations to converge and, also, potentially getting over instability barriers for certain iterative schemes. This isn't very important with the heat-equation, from which the method is derived, but coupled to fluid solvers or radiation transport solvers could help convergence substantially. This method was developed for optimization so this is just something worth noting.

4.2.4 Optimization

Full core optimization has been investigated for various reasons from design to core shuffling considerations [6, 7, 8, 9]. In nuclear reactors this optimization problem becomes incredibly expensive as the typical solver methods involve monte-carlo approaches. For core shuffling the combinatorial problem itself is very large involving many possible or feasible solutions that are sub-optimal. Searching this solution space becomes very difficult and so algorithms to efficiently

find a near optimal solution have been developed to save computational time.

Genetic algorithms and simulated annealing algorithms are popular to build from because they do not rely on perfect information to function and they only promise near optimal results. But others have tested more complex algorithms with good results [6, 8]. In order to get accurate results to evaluate constraints and objects complex function evaluations must be performed. Neutronics and thermal-hydraulics are the main physics considered in most design studies and can be expensive. Because of the high computational cost parallel schemes are typically implemented so that multiple evaluation can be performed simultaneously. With a faster method the number of available optimization algorithms increase and create more opportunity for finding better designs.

4.3 Theory

The model is a network analysis approach and as a result the geometry needs to be described in that way. A traditional network is described with nodes and edges. The nodes tend to describe a state and the edges tend to describe a transformation between one node and another. Thus an edge describes a state to state transition or a relationship between the states. To apply this to this problem nodes need to be established. This is simple and are intuitively selected at the fuel center line and the vapor. These are natural locations where information is desired and could bound performance. The edges are defined as thermal resistances. Most mesh based simulations result in a network type description. In this case a resistance approximation is used and this naturally results in a network structure.

For most heat-pipe systems, resistance analysis is appropriate and accurate within the safe operating region for a heat-pipe. In nuclear systems there is some additional complexity associated with the relationships between neighboring heat-pipes and fuel-elements that could cause problems with accuracy. This method could be described as a pseudo-2D method with a 3D unfolding. The pseudo-2D is because the geometry is represented in 2D but the relational terms are 1D approximations to the heat equation.

4.3.1 Model Derivation

To begin the derivation of this model several pre-requisites need to be established. The first is that the heat-pipe must be operating and be analyzed within the established safe operating region of the heat-pipe. The second is that within the safe operating region the vapor temperature is nearly isothermal. The last assumption was already discussed briefly, but it is assumed that a resistance network or conduction scheme accurately captures steady state heat-pipe behavior [10, 11, 12]. These assumptions are pretty widely accepted in heat-pipe analysis and have even shown acceptable accuracy in transient analysis.

Once the network is setup a system of linear equations is solved giving temperatures at all the nodes. A secondary matrix can be setup that acts as a translation from temperature to power. This will become clearer after the derivation is demonstrated, but from this power the rejected power can be obtained for each heat-pipe. With this the characteristic limits and how close the heat-pipe is operating to them can be obtained. This allows a more direct analysis of heat-pipe safety and could allow a slightly higher total core power.

In nuclear design it is useful to analyze based on unit cell properties. Traditionally the unit cell consists of fuel surrounded by coolant but in the case of heat-pipe cooling the heat-pipes and the fuel are generally independent unit-cells and must be treated as such. So for this analysis we will start by defining two neighboring cells, with these the method will be defined. Beyond two cells the method can be scaled up to any number of neighboring cells. The two cells will be known as the "Owner" and the "Neighbor". Intuitively we will center ourselves around the "Owner" cell and begin describing the method. Figure 4.2 will be useful to reference when deriving the method.

There are three conditions enforced that create the systems of equations. The first is that the heat leaving through the surfaces is equal to the heat produced in the cell. A mathematical description is seen in Equation 4.1.

$$Q_O = \sum_{i=1}^{6} Q_{O \to i} \tag{4.1}$$

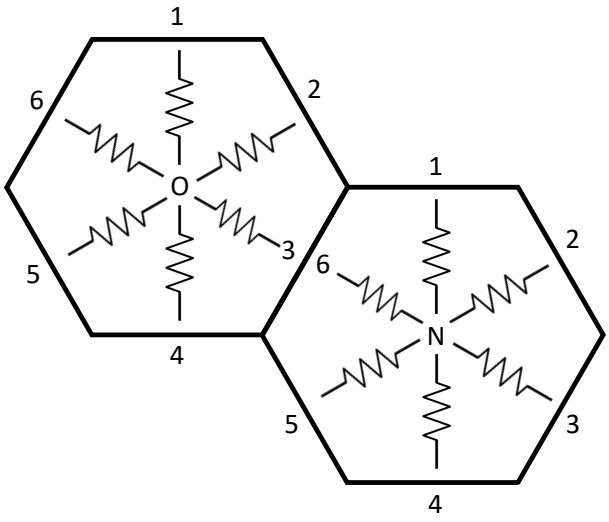

Figure 4.2: Simple two cell drawing to describe system of equations

Where Q is the heat and i indicates the specific surface heat is flowing to. This is a simple conservation of energy rule that needs to exist. The second condition required is that heat flowing across a surface must be conserved. Taking the specific relationship from Figure 4.2, the "Owner" and "Neighbor" relationship can be seen and then mathematically described in Equation 4.2 .

$$Q_{O\to 3} = Q_{N\to 6} \tag{4.2}$$

This is just a conservation relationship that conserves heat flow across the surface. It is now necessary to define what the heat-flow to each surface is. To do this Fourier's law is useful and can be seen in Equation 4.3.

$$q" = -k\vec{\nabla}T \tag{4.3}$$

Where q" is the local heat flux, k is the thermal conductivity, and T is the temperature. Assuming the local heat-flux is constant over some area, this can be integrated over that local area to get the heat flow across that area and a one dimensional equation can be obtained that can be seen in Equation 4.4.

$$q" A = Q_{O \to i} = -kA \frac{dT}{dx} \tag{4.4}$$

$Q_{O \to i}$ being the total power transferred from Owner to i, and the one reference dimension is x. Noting that A is a function of the reference dimension, x, and that the power is constant with respect to the reference dimension. The equation can be reorganized to get a fairly common formulation for a resistance network in Equation 4.5.

$$Q_{O \to i} \int_{x1}^{x2} \frac{1}{-kA(x)} dx = Q \cdot R_a = \Delta T \tag{4.5}$$

Where R_a is the effective resistance and there is an implied subscript from Owner to face i. From this equation it is simple to see that accurate temperature relationships can be attained if an accurate resistance can be found between the cell center and the cell face. This brings in the third condition that requires temperature continuity at the interface. Describing this formally for consistency can be seen in Equation 4.6.

$$T_{O \to i} = T_{N \to j} \tag{4.6}$$

Where T is the temperature and i and j are numbers corresponding to the shared surface. With this it is relatively trivial to apply boundary conditions such as periodic, sinks, sources, and convective boundaries to gain the needed system description.

When viewing this derivation there are terms that could be a function of temperature, specifically the thermal conductivity, and this reduces the accuracy for unfolding the 2D information into a 3D profile.

4.3.2 Proof of Peak Fuel Equivalence

With the assumption that the resistance is accurate to the temperatures involved within the region the temperature difference represents an average. With it being an average to gain 3D information about the temperature profile an unfolding process needs to occur and proving that the

3D information retains the appropriate average information is important.

In order to do this Equation 4.3 is a good start, it can be assumed that the heat flux is a function of x and z and the gradient in the x direction is the only significant contributor to the gradient. This gives Equation 4.7.

$$q"(x,z) = -k\frac{dT(x,z)}{dx} \tag{4.7}$$

This is a fairly consistent approach to sub channel analysis in nuclear reactors as it is a conservative estimate on peak fuel temperature. With this form, the area can be again multiplied. Area is assumed to be independent of axial location and the result of this can be seen in Equation 4.8.

$$q"(x,z)P(x)dz = Q(z) = -kP(x)dz\frac{dT(x,z)}{dx} \tag{4.8}$$

Where $P(x)dz$ is surface area at position x, and $Q(z)$ is the power at location z. From here the same process can be followed as previously to obtain the resistance form displayed in Equation 4.9

$$Q(z)\int_{x1}^{x2}\frac{1}{-kP(x)dz}dx = \int_{x1}^{x2}\frac{dT(x,z)}{dx}dx \tag{4.9}$$

From here it will be useful to collapse several terms and carry the integration through on others. This gives Equation 4.10 that defines several new terms.

$$Q(z)\frac{1}{dz}R_b = \Delta T(z) \tag{4.10}$$

Where R_b is the resistance for this term and is distinctly different from the prior resistance term that was defined. This difference will be analyzed later and will be important. It will be helpful to define a linear power term as it is more convenient to work with and is commonly used in analysis of nuclear fuel. This is defined in Equation 4.11.

$$Q(z) = q'(z)dz \tag{4.11}$$

The assumption is that linear power is known from neutronic analysis or other means within a nuclear system. This definition makes it clear to see that if linear power is known then the temperature difference is also known directly because dz cancels out. From here an integration over z needs to occur yielding Equation 4.12 which provides a relationship with the total power.

$$Q \cdot R_b = \int_Z \Delta T(z) dz \tag{4.12}$$

This is not a useful relationship as is, but by multiplying by a special form of unity in Equation 4.13, the average temperature difference can be obtained.

$$Q \cdot R_b = \frac{\int_Z \Delta T(z) dz}{\int_Z dz} \int_Z dz = \bar{\Delta T} \Delta L \tag{4.13}$$

To prove the temperature temperature difference obtained in Equation 4.4 is the average temperature difference, a ratio of Equation 4.4 and Equation 4.13 can be taken which results in Equation 4.14.

$$\frac{R_a \Delta L}{R_b} = \frac{\Delta T}{\bar{\Delta T}} \tag{4.14}$$

Looking at this it is simple to see that the LHS is unity because the surface area at location x is equal to the perimeter at that same location extruded by length ΔL which proves that the temperature change attained in the method is the true average. Substituting Equation 4.11 into Equation 4.10 begins the unfolding process and is seen in Equation 4.15.

$$q'(z) \cdot R_b = \Delta T(z) \tag{4.15}$$

By assuming or forcing the functional form of both $q'(z)$ and $\Delta T(z)$ to be those seen in Equation 4.16 the unfolding is very simple.

$$q'(z) = \frac{Q}{\Delta L} \cdot f(z)$$
$$\Delta T(z) = \bar{\Delta T} \cdot g(z) \tag{4.16}$$

From this equation our goal is to determine what g(z) is. By substituting these into Equation 4.15, g(z) can be solved for and it is determined that the shape of the temperature difference is the same shape as the linear power. This is a relatively obvious understanding but it is useful to have a proof. With the assumption that the vapor axial temperature is constant more information is obtained. This information is represented in Equation 4.17

$$T(z) = \Delta T(z) + T_v \tag{4.17}$$

This represents the entire unfolding and as long as the resistance is accurate to the point of interest an accurate temperature can be obtained from this method. This is nearly the same as many sub channel approximations but with heat-pipes gain an added aspect of accuracy. With the unfolding complete the peak temperature can be obtained by finding the maximum of the temperature function inside the pin. There are many methods to determine this so going into the specifics is not important.

4.3.3 Resistance Derivations

For this resistances need to be determined for the system of linear equations. For the two geometries analyzed in this paper there are four geometries to be considered in our resistances. They are a cylinder with internal heat generation, a cylindrical annulus with no internal heat generation, a hexagonal annulus with no internal heat generation, and an infinte slab with no internal heat generation. These are relatively straight forward and have been derived elsewhere but they will be derived here for completeness.

To start the resistance for a cylindrical geometry with internal heat generation will be derived representing the fuel element in both cases. They have slightly different forms but that will be shown later. To start the derivation the steady state heat equation is taken with the cylindrical

laplacian used. The azimuthal and axial terms are assumed negligible. This can be seen in Equation 4.18

$$\frac{1}{r}\frac{d}{dr}(kr\frac{dT}{dr}) + q''' = 0 \tag{4.18}$$

Solving this equation gives a pretty well known general solution represented in Equation 4.19.

$$T(r) = -\frac{q'''r^2}{4k} + C_1 ln(r) + C_2 \tag{4.19}$$

Applying boundary conditions is all that is needed to find a specific solution to this equation. What is needed is not just a specific equation but a resistance relationship in the form of Equation 4.5. To get the ΔT component only the C_1 constant needs to be determined. To get this the inner condition that the heat flux is zero is applied and solved. An equation for ΔT can be determined and is seen in Equation 4.20.

$$\Delta T = \frac{q'''}{2k}\left(R_i^2 ln\left(\frac{R_o}{R_i}\right) + \frac{R_i^2 - R_o^2}{2}\right) \tag{4.20}$$

The RHS now needs to be forced into a form that resembles QR. To do this Q is extracted from the volumetric heat generation. Assuming the volumetric heat generation term is an average it is relatively simple and we end up with the relationship in Equation 4.21.

$$\Delta T = Q\frac{1}{2k\pi(R_o^2 - R_i^2)L}\left(R_i^2 ln\left(\frac{R_o}{R_i}\right) + \frac{R_i^2 - R_o^2}{2}\right) \tag{4.21}$$

Where the volume of the heat generating medium is added to the denominator to the lead term with a power term on top. L is the length of the fuel element. It is now clear that there is a temperature difference term, a power term and then leftover terms that represent the resistance terms. To simplify it into what will be actually used the inner radius is assumed to be zero and resistance is simplified dramatically. This can be seen in Equation 4.22.

$$\Delta T = Q\frac{1}{4k\pi L} \tag{4.22}$$

This resistance is used in one geometry. For the other geometry another step is needed. Because it is a repeating hexagonal lattice this represents six parallel resistors. Adding resistances in parallel is trivial and Equation 4.23 represents the six equal resistors and what the specific value is.

$$\frac{1}{R} = \frac{6}{R_s} \tag{4.23}$$

Where R_s is the specific resistance for the parallel representation and the 6 is because a hexagonal representation is broken into six parts. So for the fuel portion this is the resistances that will be used. Similar logic will be applied to breaking up the resistors in the annular representations of other components.

Now to derive resistances for annular components which can include cladding, annular gaps, and capillary structure but is needed for both geometries. The general solution for an annular geometry with no internal heat generation is seen in Equation 4.24.

$$T(r) = C_1 ln(r) + C_2 \tag{4.24}$$

By conserving power or heat flux into the inner radius the constant C_1 can be determined. From this point, a similar process can be carried out to obtain an equation in the form of Equation 4.5. The math is repetitive and will not be shown. The final equation can be seen in Equation 4.25.

$$\Delta T = Q\frac{1}{2k\pi L} ln\left(\frac{R_o}{R_i}\right) \tag{4.25}$$

The resistance value is now clearly represented for an annulus with no heat generation. Using Equation 4.23 the needed forms can be obtained for each geometry.

The next geometry that needs to be handled is a hexagon with a circular cylinder removed from its center. To make it easier only a wedge will be analyzed that represents a sixth of the

geometry with periodic boundaries. This derivation requires assuming 1D heat transfer normal to the cylindrical inner hole. This is done by assuming the area change is linear from the inner cylinder to the outer hexagon. Because heat is conserved the total power through the segment remains constant. Figure 4.3 shows the geometry and the parameters for determining the resistance.

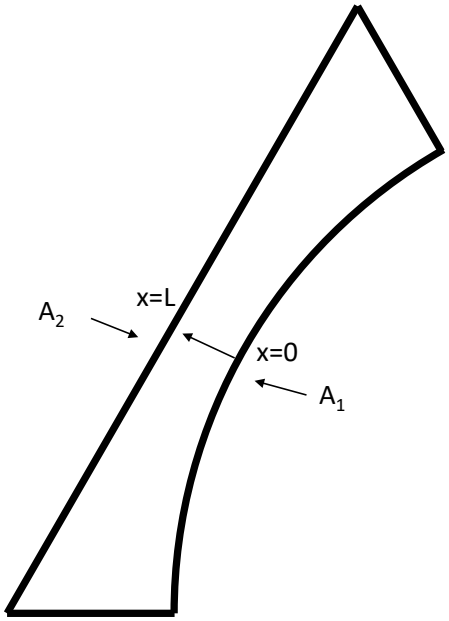

Figure 4.3: Wedge used for determining resistance of Hexagonal annulus portion of geometry

Choosing the area position relationship is up to the individual, linear was chosen hear because it is simple and easy to handle. For most of the derivation it will be left as an arbitrary function. Equation 4.26 shows the first step of the derivation.

$$Q = -kA(x)\frac{dT}{dx} \tag{4.26}$$

Reorganizing this an initial value problem can be obtained. Because the bounds are known, being 0 and L this can be set up in it's most general form seen in Equation 4.27.

$$T(L) - T(0) = \Delta T = -Q\frac{1}{k}\int_0^L \frac{1}{A(x)}dx \tag{4.27}$$

Where L is the thickness of the piece between the cylinder and the hexagon. It becomes clear what the resistance term becomes and so for a general case this is the solution. If the area is assumed to be linear from 0 to L then the integral can be solved. The linear relationship is seen in Equation 4.28 and the result of the integral is seen in Equation 4.29.

$$A(x) = \frac{(A_2 - A_1)}{L}x + A_1 \tag{4.28}$$

$$\int_0^L \frac{1}{\frac{(A_2-A_1)}{L}x + A_1}dx = L\frac{ln(\frac{A_2}{A_1})}{A_2 - A_1} \tag{4.29}$$

The integral clearly shows that the log mean area is present which is a nice confirmation that the calculation makes sense. The final form that will be used for these calculations is presented in Equation 4.30.

$$\Delta T = -Q\frac{L}{k \cdot LMA} \tag{4.30}$$

Where LMA is the log mean area of the piece using the inside and outside areas of the piece. It is worth noting that if the piece is very conductive relative to the rest of the geometry then the 1D assumption could introduce error. There could be substantial conduction tangential to the inner cylinder and not just perpendicular to it.

After this there is only one geometry left and it is a simple wall or plane with no heat generation internally. This is a geometry that is well understood and analytical solutions are readily available for similar to the cylinder. The temperature profile is a simple linear relationship so jumping straight to a Fourier assumption is appropriate. A reasonable starting point is seen in Equation 4.31.

$$Q = -kA\frac{\Delta T}{\Delta x} \tag{4.31}$$

Where A is the area and it is constant over the thickness, Δx. With minimal effort this can be rearranged into a very well known resistance form to get the final resistant required for this analysis. This is shown in Equation 4.32.

$$\Delta T = Q\frac{\Delta x}{kA} \tag{4.32}$$

There is a need to be aware of the signs on each and every term as steps were skipped that would clarify them but the resistances should always be positive and that is all that is necessary to define them properly.

4.4 Geometries Analyzed

Two geometries were analyzed here. The first is described in [5, 13] and the specific geometric parameters will be specified in a later table, and the second is similar to that described in [14] with the specifics again described in a a later table.

These geometries were specified based on the fuel and heat-pipes so that it was not necessary to analyze the whole core. This method can analyze large geometries very quickly but for bench marking purposes, getting results from a higher fidelity solution like OpenFOAM takes substantially longer. Both geometries used approximately 3,000,000 mesh elements to ensure an adequate resolution was obtained for comparison.

4.4.1 MegaPower Geometry

The MegaPower geometry is a fairly standard configuration for heat-pipe reactors and is comprised of a hexagonal lattice with fuel elements and heat-pipes. The ratio of fuel elements to heat-pipe is typically around 2 fuel elements to each heat-pipe and is contained in some sort of structural material. Designs like this have been described in [5, 15, 16] and there are other examples as well but the key characteristic is that there are exactly two repeated unit cells in the system. To begin describing the simulation criteria two unit cells will be drawn and described and then these cells will be mapped to a hexagonal grid defining the geometry. A general fuel unit cell can be seen in Figure 4.4 which shows the three major variables describing the geometry.

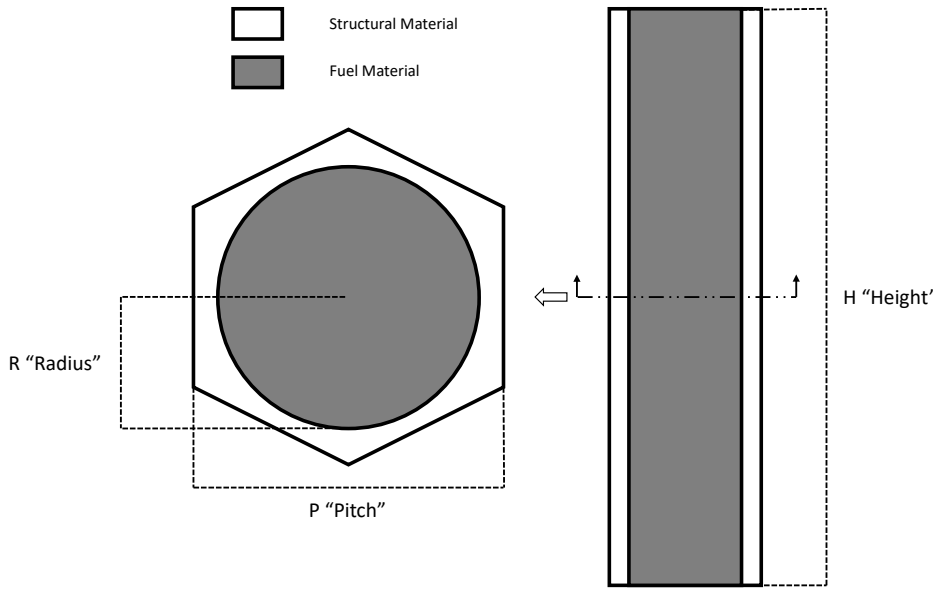

Figure 4.4: Unit Cell representing the fuel portion of the geometry

As can be seen in Figure 4.4 the three variables that describe the cell is the Pitch, P, of the hexagonal geometry, the radius, R, of the fuel element, and the height, H, of the fuel element. The only dimension unique to this cell is the fuel radius, with height and pitch being a dimension that is shared between the two in some way. Now the heat-pipe geometry will be described and there are several other variables here unique to this cell and they can be seen in Figure 4.5.

Figure 4.5 shows there are eight total variables that fully define the geometry of this unit cell. These are the evaporator length, L_e, which corresponds to the fuel height, the adiabatic length, L_a, the condenser length, L_c, the radius of the heat-pipe, HR, the pitch of the unit cell, P, then the thicknesses of each component, that being the wall thickness, the annular gap thickness, and the capillary structure thickness represented by W_t, A_t, and C_t respectively. With these dimensions meshed geometries can be obtained as well as all the parameters necessary for this method.

For the layout of the geometry a hexagonal grid will be described with a pitch equal to that of the unit cell Pitch. The layout of the MegaPower geometry is made up of 19 hexagonal locations with 7 heat-pipes and 12 fuel elements. The exact layout is displayed in Figure 4.6

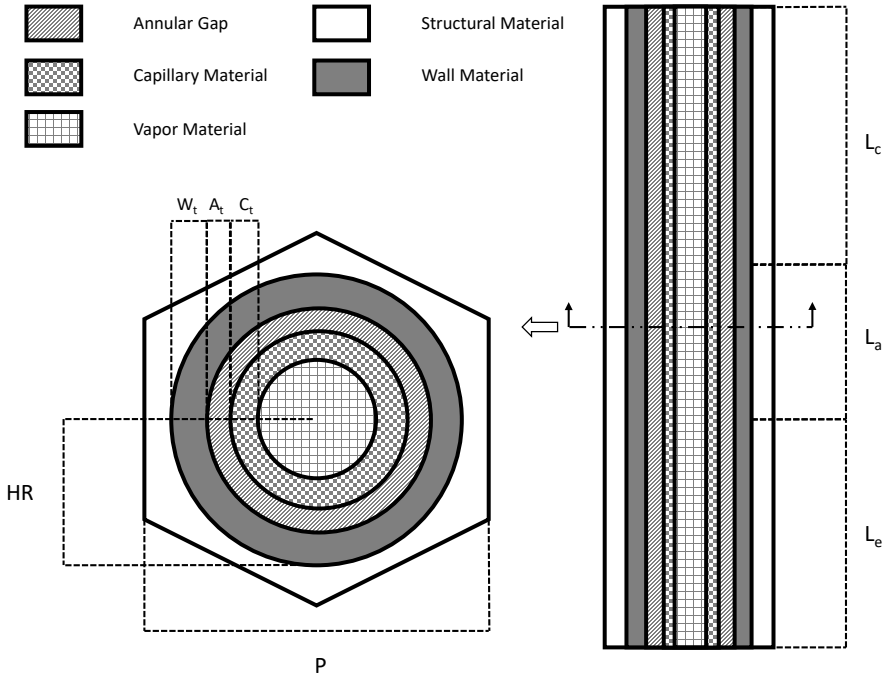

Figure 4.5: Unit Cell representing the heat-pipe portion of geometry

The numbers describe each heat-pipe and fuel element respectively and will be used in future sections to describe the specific power produced within each element. The boundary conditions to the steady state simulation performed in OpenFOAM and for this method will now be described as well as the specific properties. These are shared between the two geometries but will be described for both for clarity.

The properties used are identical in both geometries but as was said both will be described. It is assumed that properties are constant with temperature for a direct comparison between the detailed simulation and this method. For this simulation, thermal conductivity is all that is needed from each material and the effective thermal conductivity that is calculated in the capillary structure. There are four materials that need to be defined, those being stainless steel, UO_2, liquid sodium, and then the capillary structure which is assumed to be a mix of stainless steel and sodium with a porosity of 70%. Table 4.1 presents these conductivity's as used in the MegaPower geometry's calculations. The exact geometric parameters used in the simulation are presented in Table 4.2

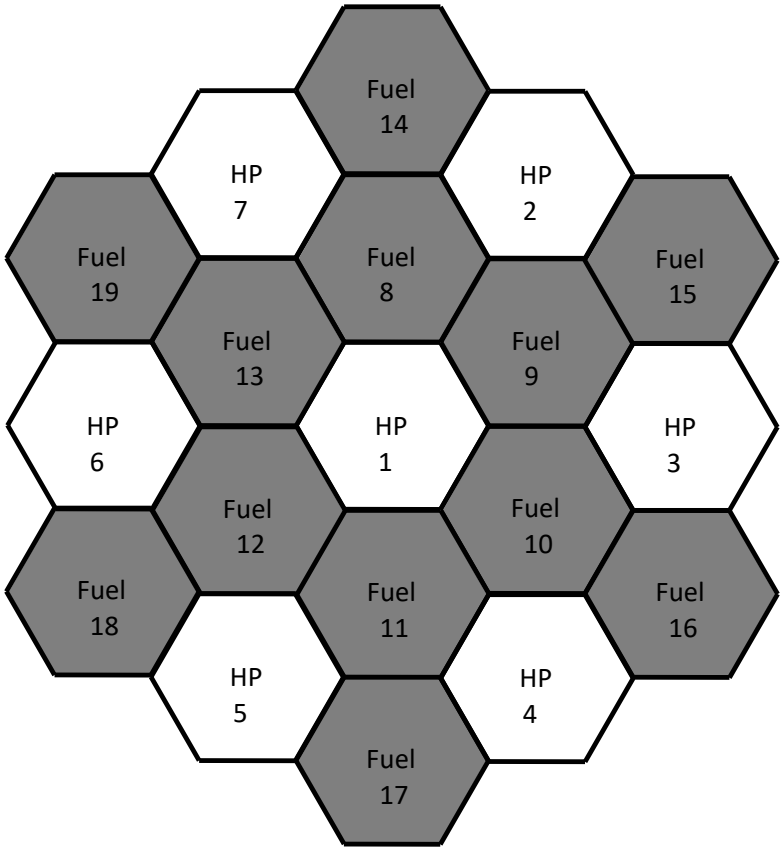

Figure 4.6: Unit cell layout of the analyzed MegaPower geometry

The outward facing surfaces of the geometry all have adiabatic conditions except for the condenser which has a convective cooling condition applied. The heat-pipes have inner faces that correspond to the liquid vapor interface of the heat-pipe. Each heat-pipe has it's own interface being calculated independently from the others. The interface temperature is set such that the net heat flow into or out of the surface is zero. This sounds complicated but in a steady state simulation this consists of two parts. Guessing the temperature that makes this condition true and then updating that temperature based on the resulting error which happens to be the net heat-flow. Knowing how OpenFOAM performs heat transfer calculations is required to create an updated temperature. If this is known the error can be defined as a function of the interface temperature and then updated with any number of 1D root finding algorithms. For this specific case a Newton-Raphson approach was used because it required few iterations to converge and the surface integration could become

Table 4.1: Material Properties used in the Simulations

Material	Thermal Conductivity
Stainless Steel	16.00 $\frac{W}{m-K}$
UO_2	3.60 $\frac{W}{m-K}$
Liquid Sodium	61.25 $\frac{W}{m-K}$
Sodium and Stainless Steel	43.66 $\frac{W}{m-K}$

Table 4.2: Geometric Definitions used in the Simulations

Evaporator Length	1.50 m
Adiabatic Length	0.30 m
Condenser Length	2.10 m
Fuel Length	1.50 m
Fuel Radius	0.706 cm
System Pitch	1.6 cm
heat-pipe Radius	0.8875 cm
heat-pipe Wall Thickness	0.10 cm
heat-pipe Annulus Thickness	0.07 cm
heat-pipe Capillary Thickness	0.10 cm
heat-pipe Capillary Porosity	0.70

costly for the net heat flow. In the proposed method the vapor is assumed to be a node and this allows it to automatically handle the steady condition. To ensure clarity if the boundary does not have an explicitly defined condition it is an adiabatic boundary. Table 4.3 describes the parameters used in the boundary conditions for this simulation.

Table 4.3: Boundary Conditions used in the simulations

Condenser Surface	Convective Boundary Condition
Heat Transfer Coefficient	326 $\frac{W}{m^2-K}$
Ambient Temperature	725 K
All Other External Surfaces	zero gradient
Fuel Pin Heat Generation	Pin dependent function that varies axially

This allows for the simulation to take place. The fuel pin heat generation rates will be described in more detail in future sections as they are problem dependent. A conduction approximation is now fully defined and can be performed with OpenFOAM and the method described.

4.4.2 MegaPower Mesh Description

The meshes used in OpenFOAM for both analysis were generated using all hexahedral meshes. Given the high aspect ratio of the geometry the mesh structure was developed such that accurate gradient information can be obtained in each constituent direction. A 2D mesh was first developed and then extruded into the remainder of the geometry.This results in large mesh sizes along the axis of the geometry with small mesh sizes orthogonal to the axis of the geometry. This is not problematic as the steepest gradients are orthogonal to the axial direction.

For the MegaPower mesh approximately 3.7 million mesh elements were used in the final mesh presented in Figure 4.7. Because of the high aspect ratio and skewness in parts of the mesh, a single refinement study was performed between a coarse mesh and this final mesh to determine the level of convergence of our solution. The vapor temperature was the quantity of interest that was analyzed to determine the mesh was sufficiently converged. From the coarse mesh to this final mesh the number of mesh elements roughly doubled (1.8 Million) uniformly in all directions and resulted in a less than 1% (0.95%) increase between the coarse solution and the solution presented on this mesh. This convergence study was only performed on the simplest power profiles used. This gives reasonable confidence that the solution provided is accurate, however, additional convergence studies could be performed to get order of convergence, as well as determine the effect of skewness and aspect ratio on the solutions in depth.

4.4.3 Fuel-Element Heat-Pipe Geometry

For the Fuel-Element Heat-Pipe Geometry a similar process is used to describe the geometry. Unlike the MegaPower Geometry this geometry contains a single unit cell that is repeated throughout the core. This simplifies the process of explanation but there are more variables in the single unit cell that need to be defined. A little background shows this configuration is from [14] and

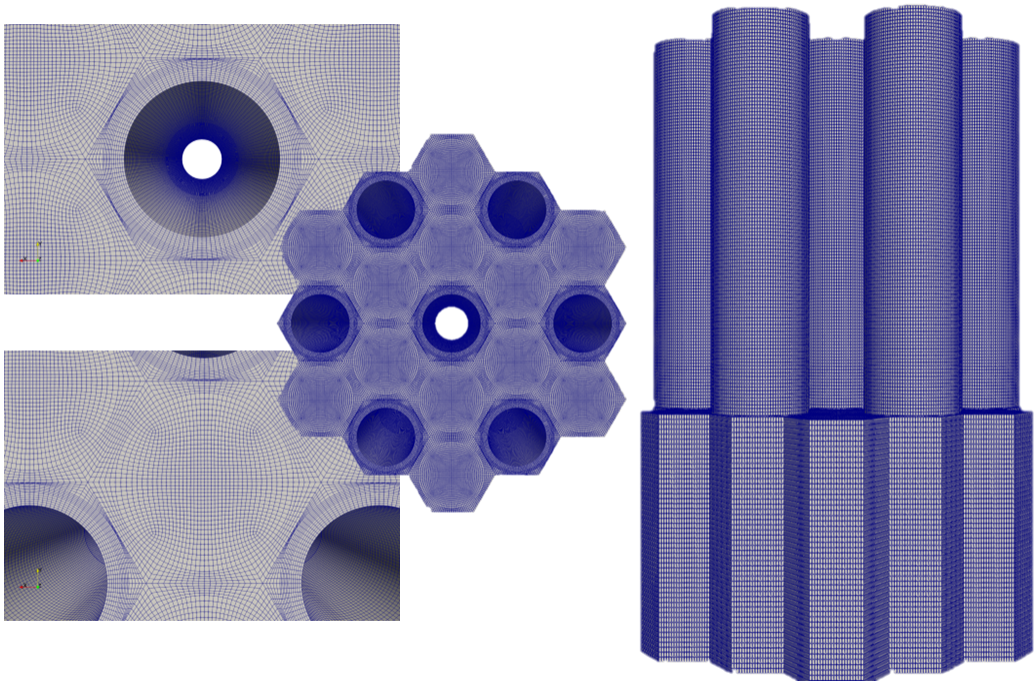

Figure 4.7: Mesh used for the MegaPower Geometry OpenFOAM Analysis

will be a good reference in understanding the geometry. A figure of the unit cell is represented in Figure 4.8 for easier understanding of the geometry and to aid in the description of the dimensions of the geometry.

The C indicates the capillary structure thickness, the A is the annulus thickness, the W is the wall thickness, and the subscripts of i and o indicate the inner and outer respectively. F_r is the Fuel radius, and P is the pitch of the geometry. There is one more item that needs to be specified and this is the radius of the condenser section. To get this, continuity of the vapor area is enforced. The vapor area in the evaporator region is the same as the area in the condenser region. The lengths are defined the same as previously.

The layout of the geometry needs to be described. This may seem redundant since all the fuel elements are the same but they are needed to describe the power profiles of each fuel element and then to describe the temperatures of each major component. For this geometry 13 Unit cells were used with there being 13 vapor regions and 13 fuel regions to solve temperatures for. This layout

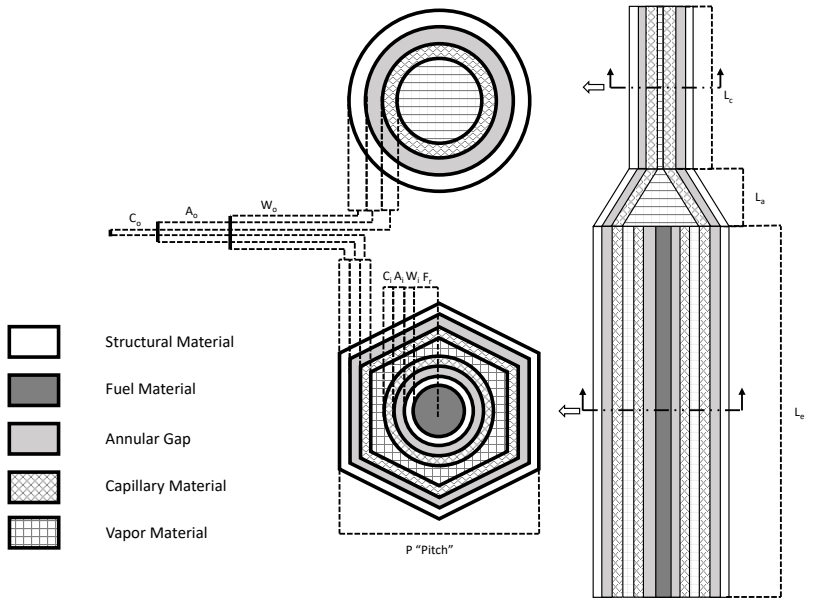

Figure 4.8: Fuel-Element Heat-Pipe unit cell geometry to aid in description

can be seen in Figure 4.9 where the numbers represent the vapor regions and to get the fuel element numbering you simply add 13 to each number to get the respective fuel elements.

This layout contains two layers as the calculation computes the fuel temperatures and the vapor temperatures of the heat-pipe. Each unit cell contains both a vapor region and fuel region. To distinguish, each region gets their own number. The vapor regions correspond to the numbers presented in the figure. The fuel region, as was described earlier, is the layout number with 13 added to it. This makes it easy to determine the relationships.

The material properties are the same as in the prior simulation but they will be reiterated for clarity. There are four conductive materials used in this simulation and for ease of calculation the properties were considered constant. These four materials are stainless steel, sodium, sodium stainless mix, and UO_2. The assumed properties can be seen in Table 4.4.

The geometric definitions for each of the labeled components in the unit cell diagram need to be described to define the full simulation. These were generated to handle a heat-pipe through-put of around 7 kW which is similar to what the MegaPower is designed for. This was done by ensuring

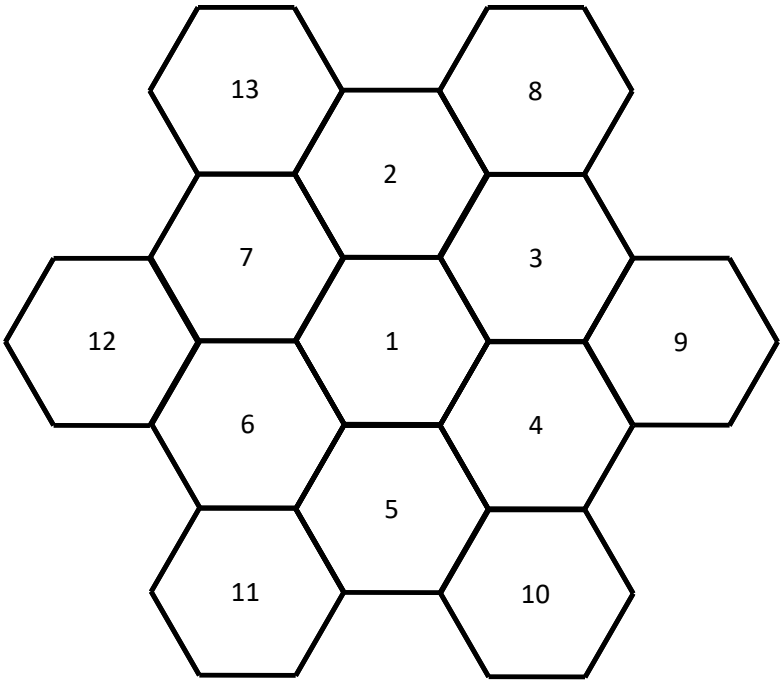

Figure 4.9: Unit cell layout of the analyzed Fuel-Element Heat-Pipe Geometry

the prevailing limits were greater than 7 kW at the operating temperature of around 1000 K which is again similar to the MegaPower requirements. The details of obtaining prevailing limits for a geometry like this can be seen in [14]. Table 4.5 shows the geometric parameters used.

Like the prior simulation all outward facing surfaces have adiabatic conditions except the condenser surface. The condenser surface has an identical convective condition on it. It is worth noting that these simulations are not intended to compare the designs and are only meant to show the ability to capture the relevant information. This is clarified because these two designs have different geometries in the condenser region and that would result in different heat transfer coefficients. The liquid vapor interface is calculated in the same way here as in the MegaPower simulations. This being each interface is independent from the next and the temperature is set so the net heat flow into or out of the vapor region is zero. The boundary conditions are shown in Table 4.6.

Table 4.4: Material Properties used in the Simulations

Material	Thermal Conductivity
Stainless Steel	16.00 $\frac{W}{m-K}$
UO_2	3.60 $\frac{W}{m-K}$
Liquid Sodium	61.25 $\frac{W}{m-K}$
Sodium and Stainless Steel	43.66 $\frac{W}{m-K}$

Table 4.5: Geometric Definitions used in the Simulations

Evaporator Length	1.50 m
Adiabatic Length	0.30 m
Condenser Length	2.10 m
Fuel Length	1.50 m
Fuel Radius	0.706 cm
System Pitch	2.115 cm
Outer Capillary Thickness	0.050 cm
Inner Capillary Thickness	0.050 cm
Outer Annular Thickness	0.035 cm
Inner Annular Thickness	0.026 cm
Outer Wall Thickness	0.050 cm
Inner Wall Thickness	0.050 cm
Condenser Vapor Radius	0.500 cm

This ensures a fully defined conduction problem that can be solved with any generic solver and the method presented here. Again, OpenFOAM was used as the bench-marking tool in this case to compare to the method presented here.

4.4.4 Fuel-Element Heat-Pipe Mesh Description

The mesh used for the OpenFOAM analysis of the Fuel-Element Heat-Pipe can be seen in Figure 4.10. This mesh has similarly high aspect ratios to allow the gradients to be resolved appropriately. This mesh contained approximately 3.2 million hexahedral elements. This mesh was a little more complicated to produced but an extruded quad mesh was successfully used to create the hexahedral mesh with uniform axial discretization used. Again a single mesh convergence study was performed using the simplest power profiles demonstrated with the finer mesh being

Table 4.6: Boundary Conditions used in the simulations

Condenser Surface	Convective Boundary Condition
Heat Transfer Coefficient	326 $\frac{W}{m^2-K}$
Ambient Temperature	725 K
All Other External Surfaces	zero gradient
Fuel Pin Heat Generation	Pin dependent function that varies axially

used for the studies. The coarse mesh contained roughly half (1.6 Million) the number of elements as the fine mesh and resulted in a vapor temperature difference between the two geometries of just over 1% (1.13%). This gives confidence in our results, but again, it will be better to perform additional refinement studies to determine directional dependence, order of convergence, and the effects of skew and aspect ratio on the solution. It is worth noting here that this is a heat equation solution and most solvers are fairly robust as the heat equation has desirable properties and has well known analytical solutions that can be used for verification purposes. But this should not be relied on in determining the veracity of any single solution. The mesh refinement was to ensure our discretization error is sufficiently small and our comparisons to the methods solution are useful.

4.5 Power Distributions Analyzed

There are four power profiles analyzed for each geometry. In these sections the profiles will be described and the results and analysis will be performed showing the strengths and weaknesses of this method. The derivation of this method involves 1-Dimensional assumptions and as a result there may be inaccuracies due to those but the purpose of the bench-marking is to show where those arise and to glean potential solutions to those inaccuracies.

The numbering scheme presented in Figure 4.6 and Figure 4.9 will be used to describe the peak fuel temperatures, the vapor temperatures, and the powers and power profiles within the pins. The motivation for this is for optimization, this means peak fuel temperatures are an important property of the design and will represent bounding behavior for this method.

In all of these simulations the OpenFOAM result will be visualized using Paraview as a visualization tool. Because the novel geometry and the simulated solution are so close in all cases only

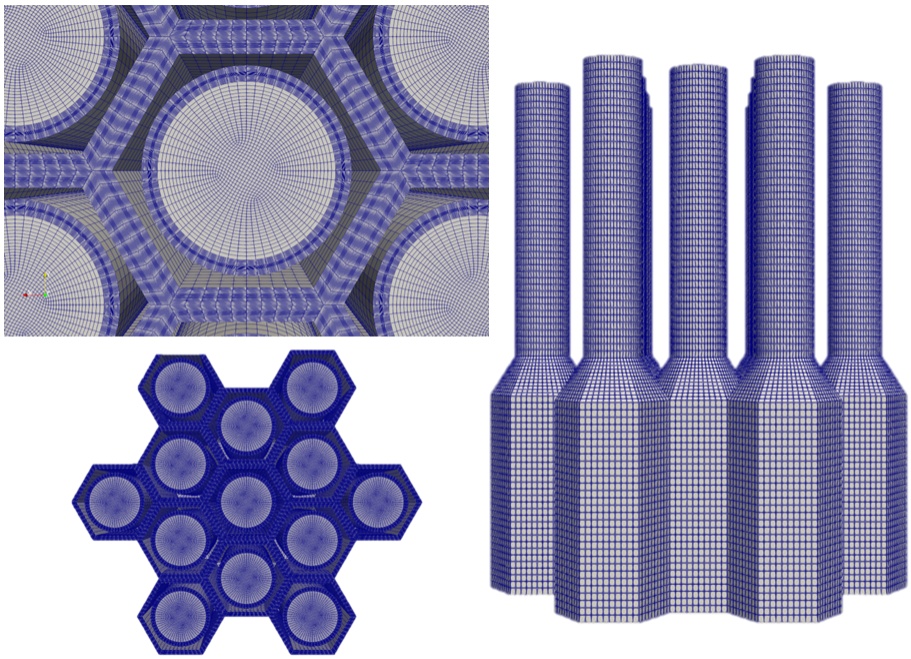

Figure 4.10: Mesh used for the Fuel-Element Heat-Pipe Geometry OpenFOAM Analysis

the OpenFOAM geometry will be presented with results. For the MegaPower like geometry both will be presented because it provides insight into why the error is more dramatic.

4.5.1 Constant Pin Power

For the first analysis all the pins have the same total power and power profile. This is a relatively simple problem and is simple to analyze. The total pin power is 2367 W and the average power density is equal to the local power density. The first analysis that will be presented is the MegaPower layout with a constant axial profile and no variation between each pin with respect to total power.

Table 4.7: Pin Power and axial power density function for the MegaPower geometry

Pin Number	Axial Power Density Function	Total Pin Power
8 - 19	$q'''(z) = 10,077,382.06\frac{W}{m^3}$	2367 W

Now to reiterate, the analysis will be comparing the peak fuel temperature as calculated by OpenFOAM and then by this method, and then the vapor temperatures will be compared as well. This should give confidence in this method for use in fast analysis for design studies. Table 4.8 is where the comparison is shown

Table 4.8: Results of the OpenFOAM analysis and this method

Cell Number	OpenFOAM (K)	Method (K)	% Difference
1 (Vapor)	842	846	+0.5
2-7 (Vapor)	834	833	-0.1
8-13 (Fuel)	884	918	+3.8
14-19 (Fuel)	915	942	+3.0

For a better visual on the specific behaviors occurring and why there is more error in this geometry compared to the other a 2D plot of temperature is presented as generated from OpenFOAM solutions within Paraview in Figure 4.11a and from the new methods solutions within MATLAB in Figure 4.11b. The color scales are identical and cover the same range so that it is simple to compare the figures. What is very clear is the bulk of the error comes from the relatively high conductivity of the stainless steel. This adds two dimensional heat transport where one dimensional was assumed. This leads to an over estimate of the temperature and is actually a desirable characteristic for design studies because reality will outperform the simulation. This gives confidence in this being an upper bound for the performance characteristics of a design and would indicate that this method would work well in optimization iterations. This is repeated in the other cases as well and shows patterns in where the error originates. As the tables indicate this actually holds for both geometries and gives good confidence in it for this use. But once again 2D plots of the new methods results won't be displayed because the results are near identical and it doesn't provide any additional information unlike for the MegaPower geometry.

It is easy to see in this analysis that the major differences are in the fuel regions. There are a lot of reasons this could occur but the likely culprit, as was mentioned previously, is that the

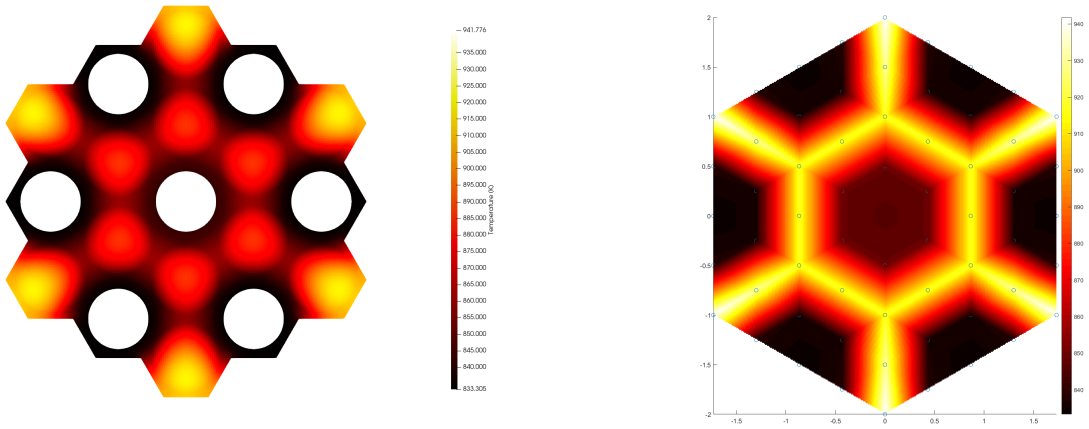

(a) OpenFOAM Results

(b) New Methods Results

Figure 4.11: Results from each analysis for a constant axial power distribution

1D assumption of the hex annulus is slightly off. The tangential heat-flux contributes to improved heat-flow in the lattice. It is good that for this case it is not a substantial contributor to the error and it leads to a conservative estimate to the temperature. This is exactly the behavior that is desired in early design iterations.

Now the second geometry is analyzed and, again, all 13 pins have the same power and a constant axial profile. The total pin power is 2367 W with the average power density being constant. The pin power is shown in Table 4.9.

Table 4.9: Pin Power and axial power density function for novel design integration

Pin Number	Axial Power Density Function	Total Pin Power
14 - 26	$q'''(z) = 10,077,382.06\frac{W}{m^3}$	2367 W

In the same way as the MegaPower analysis, the vapor temperatures, and peak fuel temperatures will be presented for both calculations. The percent error or difference will also be presented to get an idea of where the errors are presenting and what could be potentially causing it. This table can be seen in Table 4.10.

Table 4.10: Results of the OpenFOAM analysis and this method

Cell Number	OpenFOAM (K)	Method (K)	% Difference
1-13 (Vapor)	815	815	0.0
14-26 (Fuel)	851	852	+0.1

The 2D results for the novel geometry can be seen in Figure 4.12. The new method produces nearly identical results to OpenFOAM and so the high resolution results from OpenFOAM are presented as they are nicer to view. There is not much to be gleaned from this but it helps to present the data provided in the table.

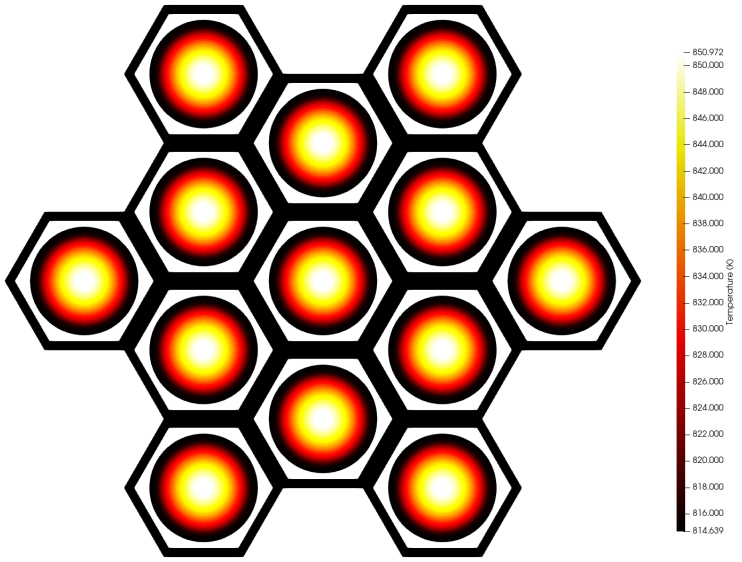

Figure 4.12: OpenFOAM Results for a Constant axial distribution

It is worth noting that there was around a one kelvin difference for both but with rounding they ended up at the same temperature. It is clear to see that this is much more accurate and analytically it is because this is a geometry that much more closely resembles the primitive shapes that can be analyzed with 1D methods. The assumptions are effectively matched much more accurately by this geometry than the MegaPower geometry.

4.5.2 Cosine Axial Profile

This profile demonstrates the unfolding procedure and the accuracy of it. Each pin will have the same total power but will have a cosine axial profile. The MegaPower geometry will be analyzed first. The table of power profiles for each of the twelve pins is presented in Table 4.11.

Table 4.11: Pin Power and axial power density function for the MegaPower geometry

Pin Number	Axial Power Density Function	Total Pin Power
8 - 19	$q'''(z) = 15,829,514.72\, cos(\frac{\pi}{L}z)\frac{W}{m^3}$	2367 W

After unfolding the temperatures are then reported. Table 4.12 shows the results after the unfolding procedure to get the peak fuel temperature.

Table 4.12: Results of the OpenFOAM analysis and this method

Cell Number	OpenFOAM (K)	Method (K)	% Difference
1 (Vapor)	836	846	+1.2
2-7 (Vapor)	835	833	-0.2
8-13 (Fuel)	910	959	+5.4
14-19 (Fuel)	962	1004	+4.4

The 2D temperature plots are presented for the cosine axial distribution in Figure 4.13a and in Figure 4.13b. Like the previous power distribution the 2D behavior of the stainless steel adds error. This error seems to be small and creates a situation where the values over estimate the high fidelity solution slightly. This gives good confidence for the intended purpose.

The error here is larger than the prior example and this is expected. The prior solution had effectively no axial conduction because of the uniform axial profile. By adding a shape to the axial profile conduction axially is introduced. This makes other assumptions inaccurate, specifically

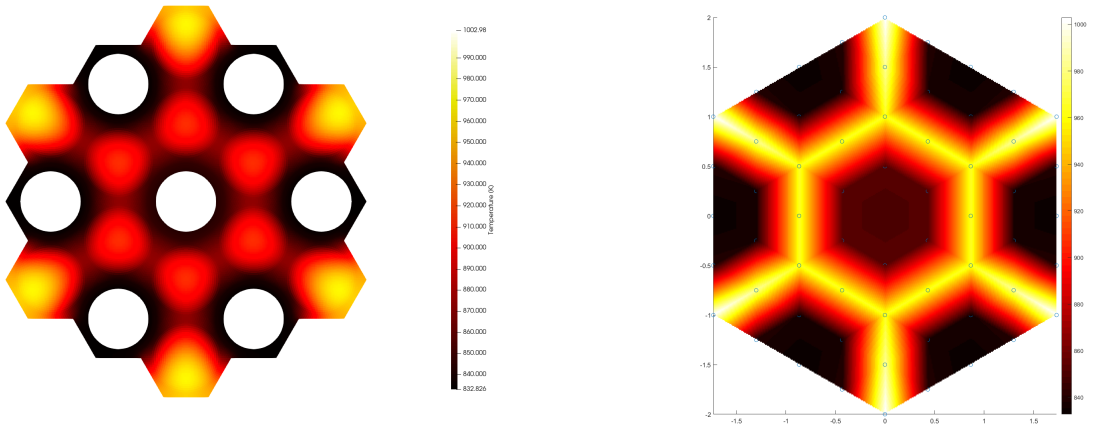

(a) OpenFOAM Results

(b) New Methods Results

Figure 4.13: Results from each analysis for a cosine axial power distribution

neglecting axial conduction. Despite this inaccuracy the solution presents values that are near the expected values and it is still conservative in nature.

Now the novel design integration will be analyzed with all pins producing the same power and the same axial profile for heat generation. The functional form used for the profile can be seen in Table 4.13.

Table 4.13: Pin Power and axial power density function for novel design integration

Pin Number	Axial Power Density Function	Total Pin Power
14 - 26	$q'''(z) = 15,829,514.72\ cos(\frac{\pi}{L}z)\frac{W}{m^3}$	2367 W

Now the unfolding procedure is done to obtain the peak temperatures in the fuel. The results of the unfolding can be seen in Table 4.14.

The 2D plot for the novel geometry with a cosine axial distribution can be seen in Figure 4.14. Again, the plot demonstrates the assumptions made are more appropriate with this geometry and the results are much more accurate. This allows the reader to compare the results in the table with the high fidelity results directly.

Table 4.14: Results of the OpenFOAM analysis and this method

Cell Number	OpenFOAM (K)	Method (K)	% Difference
1-13 (Vapor)	815	815	0.0
14-26 (Fuel)	872	873	+0.1

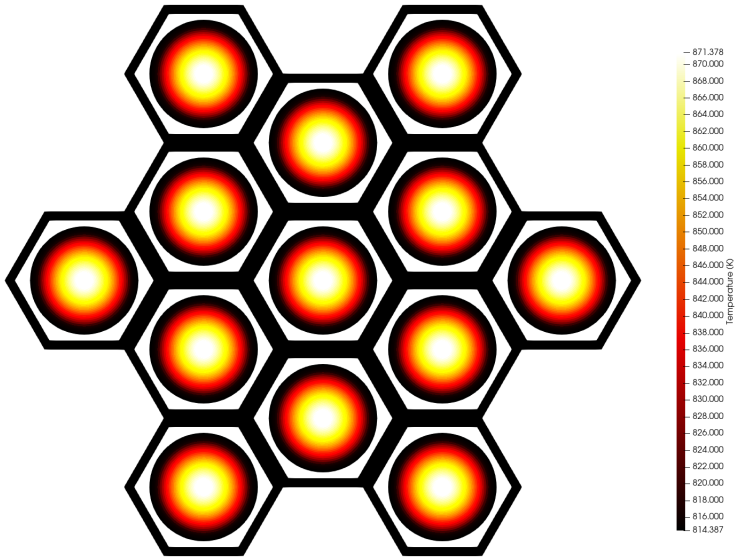

Figure 4.14: OpenFOAM Results for a Cosine axial distribution

4.5.3 Constant Pin Power with Planar Tilt

The next profile involves investigating power imbalances between fuel elements and how well the vapor temperatures are predicted from that. To do this a planar tilt is implemented to the power profile in a specific way. Total power for the whole geometry is the same as the previous runs. Then the fuel elements are grouped into five groups. These five groups have the same pin power and adjacent groups have a 20% higher or lower power level than the current group. The specific values used can be seen in Table 4.15.

When looking at the number combinations it becomes very obvious what the grouping criteria was. This simulation was performed to demonstrate the method can predict the natural balancing between the pins and the heat-pipes when the nearby power loads are not equal. In a reactor there

Table 4.15: Pin Power and axial power density function for the MegaPower geometry

Pin Number	Axial Power Density Function	Total Pin Power
15, 16	$q'''(z) = 14,116,685.87\frac{W}{m^3}$	3315 W
9, 10	$q'''(z) = 11,763,904.54\frac{W}{m^3}$	2763 W
8, 11, 14, 17	$q'''(z) = 9,803,253.43\frac{W}{m^3}$	2302 W
12, 13	$q'''(z) = 8,169,376.44\frac{W}{m^3}$	1919 W
18, 19	$q'''(z) = 6,807,815.26\frac{W}{m^3}$	1599 W

is rarely a case where each pin is producing the same power as the next and those differences can lead to over engineering to ensure adequate cooling in all scenarios. The results of this is presented in Table 4.16.

Table 4.16: Results of the OpenFOAM analysis and this method

Cell Number	OpenFOAM (K)	Method (K)	% Difference
1 (Vapor)	841	845	+0.4
2, 4 (Vapor)	843	843	0.0
3 (Vapor)	853	853	0.0
5, 7 (Vapor)	824	823	-0.1
6 (Vapor)	816	814	-0.2
8, 11 (Fuel)	883	916	+3.7
9, 10 (Fuel)	902	941	+4.3
12, 13 (Fuel)	867	894	+3.1
14, 17 (Fuel)	913	939	+2.8
15, 16 (Fuel)	962	995	+3.4
18, 19 (Fuel)	875	896	+2.4

The 2D results for OpenFOAM and for the new method are shown in Figure 4.15a and in Figure 4.15b respectively. 2D behavior in some regions make the 1D assumptions less valid. In either case the errors are low enough to be acceptable for design studies.

As can be seen, the differences are under 5% in magnitude. All the peak fuel temperatures are conservative in nature which is a desired property as well. Like the other situations this geometry shows more error and it is likely due to the 1D assumption in the high thermal conductivity region.

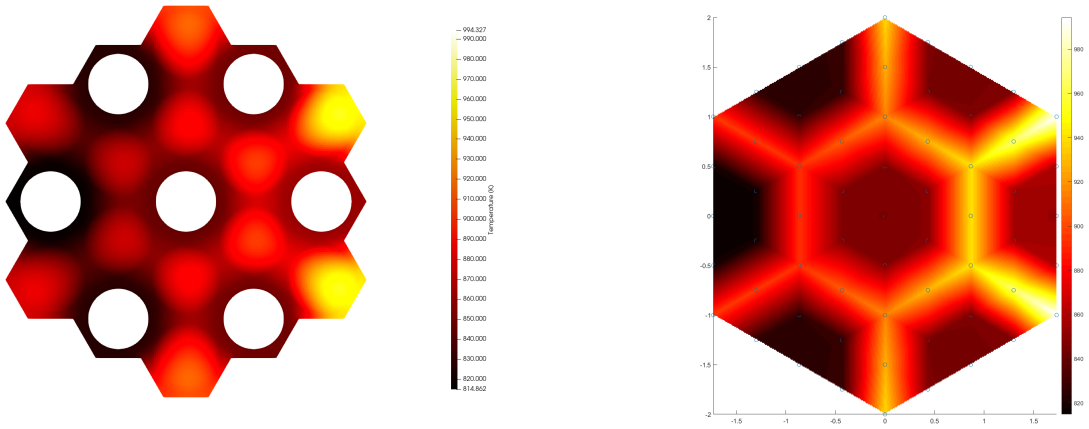

(a) OpenFOAM Results

(b) New Methods Results

Figure 4.15: Results from each analysis for a constant axial power distribution with a planar tilt

This error will grow when a cosine profile is used and may become problematic but currently it is acceptable accuracy for design studies.

Moving onto the novel geometry, a similar method was used to give a planar tilt in the power. The fuel elements were again broken into five different groups. Adjacent groups have a 20% difference in power and the total geometry power generation is the same as in the prior runs. The power specifications for each pin can be seen in Table 4.17.

Table 4.17: Pin Power and axial power density function for novel design integration

Pin Number	Axial Power Density Function	Total Pin Power
22	$q'''(z) = 14,218,551.73\frac{W}{m^3}$	3340 W
16, 17, 21, 23	$q'''(z) = 11,848,791.69\frac{W}{m^3}$	2783 W
14, 15, 18	$q'''(z) = 9,873,995.20\frac{W}{m^3}$	2319 W
19, 20, 24, 26	$q'''(z) = 8,228,286.78\frac{W}{m^3}$	1933 W
25	$q'''(z) = 6,856,919.82\frac{W}{m^3}$	1611 W

The results here are expected to be more accurate than with the MegaPower geometry based on the previous runs performed. There is also the expectation that the heat-pipes are much more similar in temperature than in the MegaPower geometry as they have little resistance between them.

This is a load balancing feature of this integration scheme [14]. The results of the analysis can be seen in Table 4.18.

Table 4.18: Results of the OpenFOAM analysis and this method

Cell Number	OpenFOAM (K)	Method (K)	% Difference
1, 2, 5 (Vapor)	815	815	0.0
3, 4 (Vapor)	815	818	+0.4
6, 7, 11, 13 (Vapor)	815	813	-0.2
8, 10 (Vapor)	815	817	+0.2
9 (Vapor)	815	820	+0.6
12 (Vapor)	815	811	-0.5
14, 15, 18 (Fuel)	851	851	0.0
16, 17 (Fuel)	858	860	+0.2
19, 20, 24, 26 (Fuel)	845	843	-0.2
21, 23 (Fuel)	858	860	+0.2
22 (Fuel)	866	872	+0.7
25 (Fuel)	840	836	-0.5

The OpenFOAM results are presented in Figure 4.16 for the visuals as both simulations provide near identical results and, again, not much is gleaned from the plots as the geometry behaves much more 1-Dimensional than the MegaPower geometry.

It is clear to see that this method is very accurate for certain problems. So far the accuracy is good enough where design studies could be quickly and easily performed without much concern that there will be significant error in results. A benefit to using this method for design studies is that when a design is found that meets the criteria specified a more detailed analysis can be done, as is done with normal design procedures.

4.5.4 Cosine Profile with Planar Tilt

The last power profile is the logical next step in this analysis by incorporating all the complexity that has been investigated up to this point. This is the planar tilt with an axial profile in the shape of a cosine function. What is expected is that the MegaPower geometry will have the larger of the error and it will increase from the prior problem slightly. The second geometry is expected to

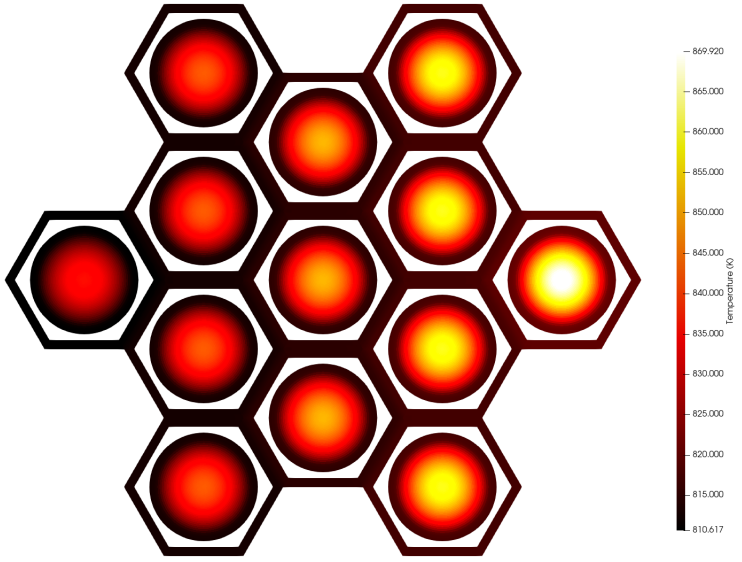

Figure 4.16: OpenFOAM Results for a Constant axial distribution with a planar tilt

be fairly accurate keeping with the prior problems. The planar tilt remains the same as in prior problems and the cosine shape function is the same. The only difference is the leading constants for the shape function.

Table 4.19: Pin Power and axial power density function for the MegaPower geometry

Pin Number	Axial Power Density Function	Total Pin Power
15, 16	$q'''(z) = 22,174,438.31 \cdot cos(\frac{\pi}{L}z)\frac{W}{m^3}$	3315 W
9, 10	$q'''(z) = 18,478,698.03 \cdot cos(\frac{\pi}{L}z)\frac{W}{m^3}$	2763 W
8, 11, 14, 17	$q'''(z) = 15,398,914.47 \cdot cos(\frac{\pi}{L}z)\frac{W}{m^3}$	2302 W
12, 13	$q'''(z) = 12,832,426.50 \cdot cos(\frac{\pi}{L}z)\frac{W}{m^3}$	1919 W
18, 19	$q'''(z) = 10,693,691.20 \cdot cos(\frac{\pi}{L}z)\frac{W}{m^3}$	1599 W

The total pin power is the same as the planar tilt problem but instead of a constant axial power density profile there is a cosine power density profile centered around the mid-plane of the fuel pin. This is somewhat representative of a true reactor profile but a normal profile will have a shallower curvature due to the the profile not going to zero at the edge of the pins. This is because of leakage

from the geometry and is normally handled with modified vacuum boundary conditions called an extrapolation length. An important rule is the power density at the edge's of a reactor does not got to zero. Again we expect this to be the worst accuracy because it deviates from the 1D assumptions the most. The results can be seen in Table 4.20.

Table 4.20: Results of the OpenFOAM analysis and this method

Cell Number	OpenFOAM (K)	Method (K)	% Difference
1 (Vapor)	841	845	+0.5
2, 4 (Vapor)	843	843	0.0
3 (Vapor)	854	853	-0.1
5, 7 (Vapor)	825	823	-0.2
6 (Vapor)	816	814	-0.2
8, 11 (Fuel)	909	956	+5.2
9, 10 (Fuel)	934	995	+6.5
12, 13 (Fuel)	888	922	+3.8
14, 17 (Fuel)	958	1004	+4.8
15, 16 (Fuel)	1026	1082	+5.5
18, 19 (Fuel)	906	938	+3.5

The 2D results for OpenFOAM and for the new method are presented in Figure 4.17a and Figure 4.17b respectively. This simulation combines all the attributes from the previous simulation and is expected to have the greatest error as it deviates the farthest from the assumptions made.

It is clear to see here that the errors are small and the method is very good at approximating the solution. It is an over estimate of the OpenFOAM solutions which is good for design iterations. This property gives confidence that the final design will be within specifications and not exceed any constraints placed on the system during the design phase. The second geometry is expected to give better results. The descriptions of the power profile are necessary to understand the simulation and are presented in Table 4.21.

The powers in each pin remain the same as prior analysis but the shape has changed which really tests the unfolding procedure and its ability to accurately capture the peak fuel temperatures.

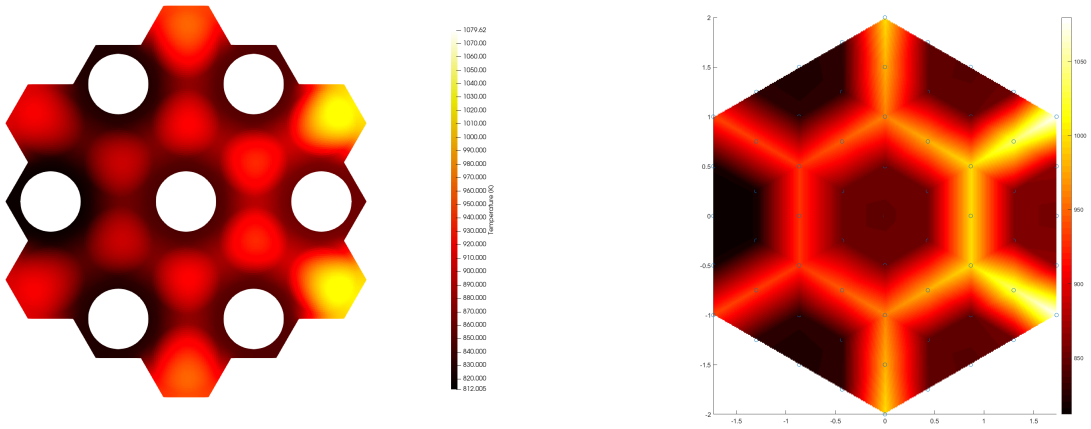

(a) OpenFOAM Results

(b) New Methods Results

Figure 4.17: Results from each analysis for a cosine axial power distribution with a planar tilt

Table 4.21: Pin Power and axial power density function for novel design integration

Pin Number	Axial Power Density Function	Total Pin Power
22	$q'''(z) = 22,334,448.83 \cdot cos(\frac{\pi}{L}z)\frac{W}{m^3}$	3340 W
16, 17, 21, 23	$q'''(z) = 18,612,038.46 \cdot cos(\frac{\pi}{L}z)\frac{W}{m^3}$	2783 W
14, 15, 18	$q'''(z) = 15,510,035.40 \cdot cos(\frac{\pi}{L}z)\frac{W}{m^3}$	2319 W
19, 20, 24, 26	$q'''(z) = 12,924,962.65 \cdot cos(\frac{\pi}{L}z)\frac{W}{m^3}$	1933 W
25	$q'''(z) = 10,770,824.47 \cdot cos(\frac{\pi}{L}z)\frac{W}{m^3}$	1611 W

In the other geometry it was seen to be within 10% of the OpenFOAM simulation and for this geometry it is expected to be more accurate. These results can be seen in Table 4.22

The OpenFOAM results are presented in Figure 4.18. With all the simulations parameters being the farthest from the assumptions made this method being within 1% of the high-fidelity solutions just attests to the capabilities of this method for certain geometries.

This geometry works very well with this method and results in less than 1% error for all regions of interest. This gives confidence in using this for optimization studies. For certain geometries this method is extremely accurate and results in a very useful tool for design analysis. This could also be used to form initial guesses for high fidelity models as was previously mentioned. This would allow more accurate material properties to obtained rapidly and with confidence. The higher

Table 4.22: Results of the OpenFOAM analysis and this method

Cell Number	OpenFOAM (K)	Method (K)	% Difference
1, 2, 5 (Vapor)	814	815	+0.1
3, 4 (Vapor)	816	818	+0.2
6, 7 (Vapor)	812	813	+0.1
8, 10 (Vapor)	816	817	+0.1
9 (Vapor)	819	820	+0.1
11, 13 (Vapor)	812	812	0.0
12 (Vapor)	811	811	0.0
14, 15, 18 (Fuel)	870	871	+0.1
16, 17 (Fuel)	883	885	+0.2
19, 20 (Fuel)	859	860	+0.1
21, 23 (Fuel)	883	885	+0.2
22 (Fuel)	899	901	+0.2
24, 26 (Fuel)	859	860	+0.1
25 (Fuel)	849	850	+0.1

fidelity model could then be iterated on until converged.

Looking at the LANL geometry for all runs there are absolute errors at most of 61 K and this could be a cause for concern when looking for design analysis methods such as this. But there are often additional assumptions made in design analysis that are intentionally introducing error as well to gain speed. Heat transfer coefficients are a great example of this trade-off. The thermal conditions in a heat exchangers are never constant and because of the 3D nature of turbulence can very widely over time. Heat transfer coefficients are an attempt to capture average behavior to make design decisions quickly. On the same side, heat transfer coefficients can very widely and produce very large errors in design if used outside their domain. Inside their tested region, errors can be as high as 15%. As engineers, it is important to understand when and where error is going to occur and what the worst case implications for that error are. With the specific discretization and resistance formulations used for these analyses several statements can be said with certainty. There is error intentionally introduced in the hopes of gaining computational speed, those errors are expected to cause an over estimate in fuel temperatures specifically. This overestimate in fuel temperatures is caused additional avenues for heat transfer being ignored in the pseudo 1-D

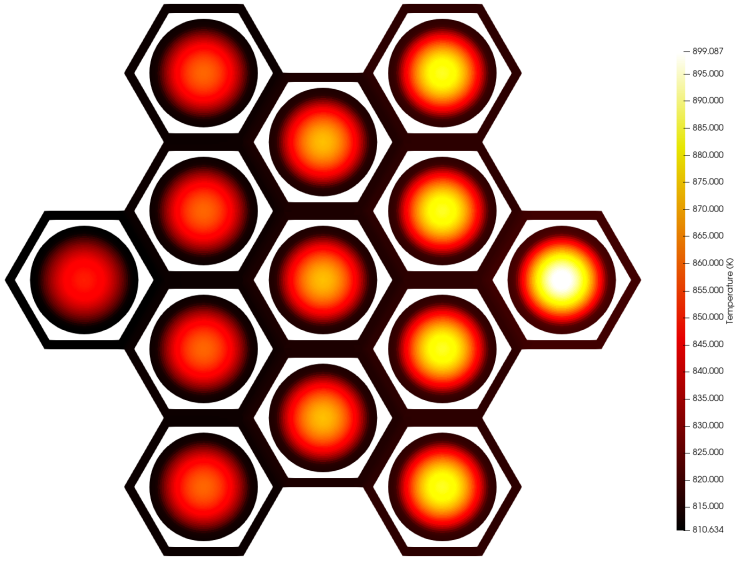

Figure 4.18: OpenFOAM Results for a Cosine axial distribution with a planar tilt

resistance relationships. This creates the guarantee that conservative decision making is performed.

Currently, computational cost is lower than it ever has been and it will likely continue to decrease. With these decreases it is important to shift perspective as designs develop. Starting with basic iterative approaches to investigate large swaths of the design space, to detailed physical modeling as the design space shrinks and eventually experimental validation for the design itself. Knowing how a system behaves is important to operations and from a financial and health risk perspective.

4.6 Conclusions

The exceptional accuracy of this method and it's inherent simplicity give large amounts of potential uses. The bench-marking performed gives confidence in the results of design iterations and makes this useful to engineers and analysts. With every example analyzed giving an over estimate of peak fuel temperatures this could also be used for simple check on the performance of a reactor design to ensure the design meets certain safety thresholds or constraints. Since heat-pipes are an important feature in several micro modular designs, methods like this become important for improving the designs quickly and for analyzing them quickly and accurately. This method

demonstrates good characteristics when solving various different geometries and provides accurate results in a variety of situations. The reasons for accuracy loss are very clear and could potentially be accounted for in simple ways. With some geometries, a near exact answer can be obtained such as in the novel geometry analyzed here, and in others good approximations can be obtained that allow quick evaluations to be done. With this method being faster than higher fidelity models more designs can be analyzed and designs can be improved at a lower cost.

This research is important because it demonstrates that high accuracy simulations can be performed with little computational effort on large geometries. Previously, high fidelity simulations based on conduction approximations where all that were available when heat-pipe performance needed to be accurately captured. With this research a large resistance network can be formed to get whole core temperatures and power through-puts quickly with confidence in the results. This is important because the operational limits of heat-pipes are estimated based on temperature and power of the individual heat-pipe. So, with this simulation tool, heat-pipes can be designed closer to the operating limits of their design without unreasonably conservative margins for the design.

Bibliography

[1] Amir Faghri and Charles Harley. Transient lumped heat pipe analyses. *Heat Recovery Systems and CHP*, 14(4):351–363, 1994.

[2] C. Ferrandi, F. Iorizzo, M. Mameli, S. Zinna, and M. Marengo. Lumped parameter model of sintered heat pipe: Transient numerical analysis and validation. *Applied Thermal Engineering*, 50(1):1280–1290, jan 2013. ISSN 1359-4311. doi: 10.1016/J.APPLTHERMALENG.2012.07.022. URL https://www.sciencedirect.com/science/article/pii/S1359431112005042.

[3] G Hu, R Hu, JM Kelly, and J Ortensi. Multi-physics simulations of heat pipe micro reactor. Technical report, Argonne National Lab.(ANL), Argonne, IL (United States), 2019.

[4] G Hu, R Hu, and L Zou. Development of heat pipe reactor modeling in sam. Technical report, Argonne National Lab.(ANL), Argonne, IL (United States), 2019.

[5] James W Sterbentz, James E Werner, Andrew J Hummel, John C Kennedy, Robert C O'Brien, Axel M Dion, Richard N Wright, and Krishnan P Ananth. Preliminary assessment of two alternative core design concepts for the special purpose reactor. Technical report, Idaho National Lab.(INL), Idaho Falls, ID (United States), 2017.

[6] R. Akbari, D. Rezaei Ochbelagh, A. Gharib, J.R. Maiorino, and F. D'Auria. Small modular reactor full scope core optimization using cuckoo optimization algorithm. *Progress in Nuclear Energy*, 122:103271, 2020. ISSN 0149-1970. doi: https://doi.org/10.1016/j.pnucene.2020.103271. URL https://www.sciencedirect.com/science/article/pii/S0149197020300305.

[7] J. G. Stevens, K. S. Smith, K. R. Rempe, and T. J. Downar. Optimization of pressurized water reactor shuffling by simulated annealing with heuristics. *Nuclear Science and Engineering*, 121(1):67–88, 1995. doi: 10.13182/NSE121-67. URL https://doi.org/10.13182/NSE121-67.

[8] Wagner F. Sacco, Cassiano R.E. de oliveira, and Cláudio M.N.A. Pereira. Two stochastic optimization algorithms applied to nuclear reactor core design. *Progress in Nuclear Energy*, 48(6):525–539, 2006. ISSN 0149-1970. doi: https://doi.org/10.1016/j.pnucene.2005.10.004. URL https://www.sciencedirect.com/science/article/pii/S0149197005002106.

[9] Anderson Alvarenga de Moura Meneses, Marcelo Dornellas Machado, and Roberto Schirru. Particle swarm optimization applied to the nuclear reload problem of a pressurized water reactor. *Progress in Nuclear Energy*, 51(2):319–326, 2009. ISSN 0149-1970. doi: https://doi.org/10.1016/j.pnucene.2008.07.002. URL https://www.sciencedirect.com/science/article/pii/S0149197008001078.

[10] Mingyang Ma, Wenfeng Liang, Shumiao Wang, Qilin Xie, Dazhi Qian, Zhongxiong Bai, Tao Zhang, and Rui Zhang. A pure-conduction transient model for heat pipes via derivation of a pseudo wick thermal conductivity. *International Journal of Heat and Mass Transfer*, 149: 119122, 2020.

[11] Z.J. Zuo and A. Faghri. A network thermodynamic analysis of the heat pipe. *International Journal of Heat and Mass Transfer*, 41(11):1473–1484, jun 1998. ISSN 0017-9310. doi: 10.1016/S0017-9310(97)00220-2. URL https://www.sciencedirect.com/science/article/pii/S0017931097002202.

[12] KH Sun and CL Tien. Simple conduction model for theoretical steady-state heat pipe performance. *AIAA Journal*, 10(8):1051–1057, 1972.

[13] Patrick Ray Mcclure, David Irvin Poston, Venkateswara Rao Dasari, and Robert Stowers Reid. Design of megawatt power level heat pipe reactors. *LANL*, 11 2015. doi: 10.2172/1226133.

[14] Cole Mueller and Pavel Tsvetkov. Novel design integration for advanced nuclear heat-pipe systems. *Annals of Nuclear Energy*, 141:107324, jun 2020. ISSN 0306-4549. doi: 10.1016/

J.ANUCENE.2020.107324. URL https://www.sciencedirect.com/science/article/pii/S0306454920300220?dgcid=author.

[15] Ehud Greenspan. Solid-core heat-pipe nuclear battery type reactor. Technical report, University of California, 2008.

[16] B.H. Yan, C. Wang, and L.G. Li. The technology of micro heat pipe cooled reactor: A review. *Annals of Nuclear Energy*, 135:106948, 2020. ISSN 0306-4549. doi: https://doi.org/10.1016/j.anucene.2019.106948. URL http://www.sciencedirect.com/science/article/pii/S0306454919304359.

5. CONCLUSION

Heat-pipe reactors are promising when it comes to advanced nuclear technology. They are passively cooled and can operate at moderately high temperatures giving nuclear the capabilities to serve more industries in a highly modular configuration. Combined with next generation micro-grids, these reactors could be excellent in serving niche markets power needs for long periods of time without risk of failure or fear of losing power. There are a lot of challenges that still need to be overcome.

Predicting operational behavior is the most essential part of the design process. If there is no confidence in the steady state behavior of the design there is no reason to consider manufacturing or operation. This is why it is important to develop modeling techniques that can give accurate information about the design being investigated. Many modeling and simulation techniques were developed for heat-pipe performance prediction when space programs were heavily investigating them for use in nuclear systems. In the early days of the investigations, these models were investigating limiting behavior of heat-pipes and were intended to guide operators in determining operational limits. These limits carried forward as an important design analysis in the prevailing limits. There are various limits that exist depending on the geometry and the configuration.

In the later years of analysis, computational power improved and highly detailed simulations were able to be done that were able to predict exact operational performance through a transient. These have been invaluable tools for heat-pipe analysis and most current concepts are developed with these as a strong foundation for the analysis and licensing work. But all of these concepts throughout history have limited themselves to simplified, and often, complex systems, because the tools were for limited geometric descriptions and in some cases singular descriptions.

This dissertation provided three important contributions to the nuclear industry. The first is a non-standard geometric configuration that is more unit-cell in style, but this lead to more general prevailing limit descriptions that allow designers to better investigate differing geometries with confidence that the limits are more appropriate. This provided several quantitative constraints

that can be used for design optimization. These can be evaluated rapidly and reduce the burden required by the higher fidelity simulation tools to capture detailed physical behaviors. This showed the potential advantages for exploring alternative designs outside the current capabilities of existing models and tools.

The second important contribution provided is a detailed review of modeling and simulation techniques and their motivations for development. Often, the motivations are overlooked in favor of specific criteria, but understanding why key decisions may have been made could allow analysts and future developers to build by including terms that were intentionally left out. The review directly compared the level of detail and the computational effort required to solve them which will help individuals make informed decisions on specific implementations. With this information, insight was gained for developing a procedure to get accurate operational behavior and the best way to determine limits on that behavior.

The final important contribution that was developed came directly from investigations in the review. Almost all the tools currently developed were for analyzing singular heat-pipes without concern for their interactions with each other. This is a useful conservative method for determining operational behavior but including the interactions with the neighbor will give better confidence on the operational performance but could give additional margins to the safety criteria allowing increased output. This method was primarily designed for optimization studies, but given the accuracy in certain geometries when comparing to high fidelity tools, specifically OpenFOAM, there are cases where this could be used in place of high fidelity tools at a fraction of the computational cost. This would give designers the ability to get high fidelity accuracy in their design iterations leading to highly optimized designs with great confidence in the final results.

With this, there now exists a set of tools that can accurately analyze the steady reactor behavior of a heat-pipe based system. With the characteristic limits there is a fast way to analyze constrained behavior for the whole system. With the network analysis method developed, a full core heat-pipe system can be accurately analyzed to give temperature information and power throughput information to compare with the constraints of the system. All this was born of the review which

should go on to assist others in developing accurate simulation and analysis tools. Throughout the work, a surrogate was used as representative replacement design for a LANL MegaPower unit-cell. This fully handles the first two objectives listed. The third objective is partially met as an optimization was never performed but the components were all there. This was not done because the desire would be to couple the fast thermal analysis to neutronic analysis and optimize the design in a true multiphysics configuration.

5.1 Novel Design Integration

The main motivation for this research was derived from the novel design integration proposed in Chapter 2. Heat-pipe reactors tend to be segregated between cooling components and fuel components which leads to lower fuel densities and large amounts of parasitic structural material. The novel design integration here has a central fuel element with a surrounding heat-pipe. This allows the heat-pipe to act as structure and a cooling device. This has the added effect of gaining a high conductivity pathway to neighboring elements. If a heat pipe fails the fuel remains the highest temperature portion of the geometry.

With this new geometry additional challenges are introduced. Specifically, prevailing limits do not exist to give performance bounds to the design. This needed to be accounted for to remain consistent with prior analysis of heat-pipes. This would allow the seamless integration into design iterations. Chapter 2 provides these prevailing limits for this design integration. These limits are more general and so should be easier to apply to complex heat-pipe geometries.

5.2 Review of Heat-pipe Modeling and Simulation

A review of heat-pipe modeling and simulation methods was performed in Chapter 3. Reviewing heat pipe modeling and simulation was an important step because it brought together a list of simulation approaches and classified them based on their constituent behaviors. This not only helps engineers and designers better select models for their needed application but it gives a quick reference for the potential issues and advantages in the model. This gives an immediate qualitative understanding of the model benefits to the design and what would need to be done to better capture

the information available.

This provided support and guidance to further analysis specifically for the full core heat-pipe analysis developed during this research. The review explored the performance and speed of models with various complexities and provided insight to models that could be appropriate for rapid iterative analysis and potential optimization scenarios. The review showed clear gaps in applications and study that is needed for reactor analysis currently.

5.3 Full Core Heat-Pipe Analysis

Chapter 4 provided a method for determining the full core thermal behavior quickly and inexpensively. This could easily be used for optimization as the accuracy's based on certain simulation criteria were within 7% of the result presented in OpenFOAM and for the Novel Design Integration provided results that were within 1%. This is with a simulation that took less than 1 second to run when the OpenFOAM simulation took almost 12 hours to converge. This benchmark gives excellent confidence in the model.

This could be used to get an initial guess for high-fidelity simulations as well, or it could be used to provide temperature information into neutronics analysis quickly. Most importantly, this method fills a gap in analysis that provides the information related to thermal communication between the neighboring elements. A typical reactor will not have a uniform power profile meaning the heat-pipe that is experiencing the highest thermal throughput will limit the performance of the reactor. It is possible to have heat-pipes vary geometrically to account for the reduced throughput elsewhere but this is not economical to produce. Knowing the thermal-throughput of each heat-pipe individually, the heat-pipe can be designed based on a more accurate thermal environment rather than an conservative adiabatic assumption.

With this dissertation, a substantial and important contribution has been made to a growing nuclear industry. New heat-pipe reactors need both these approaches to improve economics, accuracy, and speed of analysis. This is true whether a regulator needs to perform detailed safety calculations to determine margins of operation, or if a designer is performing iterations to optimize a previous concept. Knowing what model to run and where to run it is crucial. Having fast options

to iterate on steady state behavior is just as important as having highly accurate options to give confidence to all involved.

5.4 Accomplishments

This dissertation describes a substantial contribution to the subject area with several notable accomplishments. An important groundwork has been laid for several efforts that will advance next generation reactor technologies. This groundwork includes a more general analysis of performance limiting behaviors when it comes to novel geometries. Less assumptions are needed to determine these limits giving more confidence in their validity. This combined with a general full core thermal analysis method for heat-pipe reactors can lead to fast simulations of heat-pipes with confidence that the performance is accurate. This could be used in optimization tools to create an optimized design according to various objective functions in a low cost manner. From a high fidelity modeling perspective, a path forward was created for creating a simulation procedure that would efficiently and accurately capture the information needed without wasting resources. Employing the simplest forms of the equations that get the desired accuracy and only using more complex forms when there are indications that important physical phenomena are being missed in the simpler models.

5.5 Summary

During the course of this research, it was demonstrated that fast analysis of heat-pipe systems could be performed with little sacrifice in terms of accuracy. This analysis could be used on full core geometries and bounding performance metrics could be developed to ensure the heat-pipes do not exceed operational limits. This was demonstrated on an previous heat-pipe reactor design, specifically the LANL MegaPower design, to show that novel geometries could improve performance of these cores. This satisfies two of the three research objectives, with the final one not being completed. This final objective requires the development of coupled analysis methods between thermal and neutronic solvers to accurately optimize. The optimization method needs to be selected in conjunction with the neutronic solver to ensure optimization is not overly costly. Based on the work currently done with thermal analysis, the thermal solver could be easily and

quickly implemented with very small computational expense but coupling that to neutronic solvers, and enveloping that system into an optimization scheme is a large task.

5.6 Future Work

There are many pathways forward on this research both from a design perspective and a computational perspective. A major goal would be to perform optimization studies on the novel design integration as well as standard heat-pipe configurations using the developed method. This was mentioned as an objective but was determined to be a substantial additional effort and should be done in the future. Improvements can be made to the method as well, and additional capabilities and situations could be handled to account for more real world designs, or versatile designs.

Optimization studies of a heat-pipe reactor using both the novel design integration and a standard heat-pipe geometry is a clear future action. To do this, a neutronics code would need to be selected that can take temperature distribution information and provide power profiles at every position. Using the method developed the thermal analysis would be almost no cost to the simulation and more of the computational effort could be focused on neutronics where a substantial computational cost will be incurred.

The developed method could gain improvements for handling standard heat-pipe geometries. Specifically, a tangential relationship could be added to account for heat transfer that occurs tangential to the surface of the fuel. The high-conductivity regions result in additional heat transfer pathways that act to reduce the effective thermal resistance between the fuel and the heat-pipe. With this accounted for, we lose the nice property of being a conservative estimate, meaning calculated temperatures are higher than reality, but accuracy is gained with a method that is fairly accurate already.

A capability that could be investigated is the inclusion of non-condensable gases in the heat-pipe vapor region. The addition of non-condensable gases could change the thermal response of the heat-pipe, damping the temperature change over the same power throughput change for a heat-pipe without gases inserted. This can give a wider operating margin on each heat-pipe and potentially create interesting controllable parameters within the core. This is not uncommon in heat-pipe used

in other industries but has not been seen in any nuclear reactor designs at this point.